

Title	Studies on Unimer Nanoparticles Composed of Hydrophobized Poly( $\gamma$ - glutamic acid) as Drug Carriers for Cancer Therapeutics
Author(s)	Piyapakorn, Phassamon
Citation	大阪大学, 2014, 博士論文
Version Type	VoR
URL	<a href="https://doi.org/10.18910/34448">https://doi.org/10.18910/34448</a>
rights	
Note	

*Osaka University Knowledge Archive : OUKA*

<https://ir.library.osaka-u.ac.jp/>

Osaka University

Doctoral Dissertation

Studies on Unimer Nanoparticles

Composed of Hydrophobized Poly( $\gamma$ -glutamic acid)  
as Drug Carriers for Cancer Therapeutics

Phassamon Piyapakorn

January 2014

Graduate School of Engineering,  
Osaka University

# Contents

	Page
<b>General introduction</b>	1
References	5
<b><i>Chapter 1</i></b>	
<b>Preparation of <math>\gamma</math>-PGA-Phe unimer nanoparticles</b>	
1.1. Introduction	7
1.2. Experimental Section	10
1.3. Results and Discussion	15
1.4. Conclusion	42
References	43
<b><i>Chapter 2</i></b>	
<b>Structure analysis of <math>\gamma</math>-PGA-Phe unimer nanoparticles</b>	
2.1. Introduction	47
2.2. Experimental Section	49
2.3. Results and Discussion	54
2.4. Conclusion	69
References	70

## *Chapter 3*

### **Stimuli-responsive unimer nanoparticles and their potential applications for cancer therapy**

3.1. Introduction	73
3.2. Experimental Section	76
3.3. Results and Discussion	83
3.4. Conclusion	108
References	109
<b>Concluding Remarks</b>	111
<b>List of Publications</b>	114
<b>International Conferences</b>	115
<b>Acknowledgments</b>	116

## General introduction

Nowadays, cancer is one of the most severe diseases for humans. In cancer, cells divide and grow uncontrollably, forming tumors, and invade nearby parts of the body. Therefore, effective treatment for cancer therapeutics employing anti-cancer drugs is urgently required in order to kill and remove the cancer cells. However, there are some problems of anti-cancer drugs for example, low solubility in water, no targetable (resulting in side effect or toxicity to normal cells) as well as the short blood circulation which obstruct the transportation of drugs to tumor cells.<sup>1-2</sup> Hence, effective carrier used as anti-cancer agent is required to solve these problems. Various types of carriers such as micelles, nanoparticles, as well as biocompatible/biodegradable molecules such as proteins have been widely employed in cancer therapeutics.<sup>3-5</sup> In general, proteins such as human serum albumin have been used as carriers in order to improve the solubility of drugs, for example conjugation with paclitaxel (trade name Abraxane), an anti-cancer drug.<sup>6,7</sup> However, protein albumin does not possess the capability of controlled release such as stimuli-sensitive systems, which represent one of the most outstanding achievements in the drug delivery field. Therefore, it is important to continuously develop a biodegradable carrier having the ability to control drug release.

In cancer therapies, many researches have used the enhanced permeability and retention (EPR) effect<sup>8</sup> for drug targeting which can provide a great opportunity for more selective targeting to tumor cells. Recently, it is demonstrated that particle size is an important factor for not only EPR effect, but also tumor accumulation of drug-conjugated carriers.<sup>9</sup> Thereby, precise control of size of drug carrier is a challenging issue.

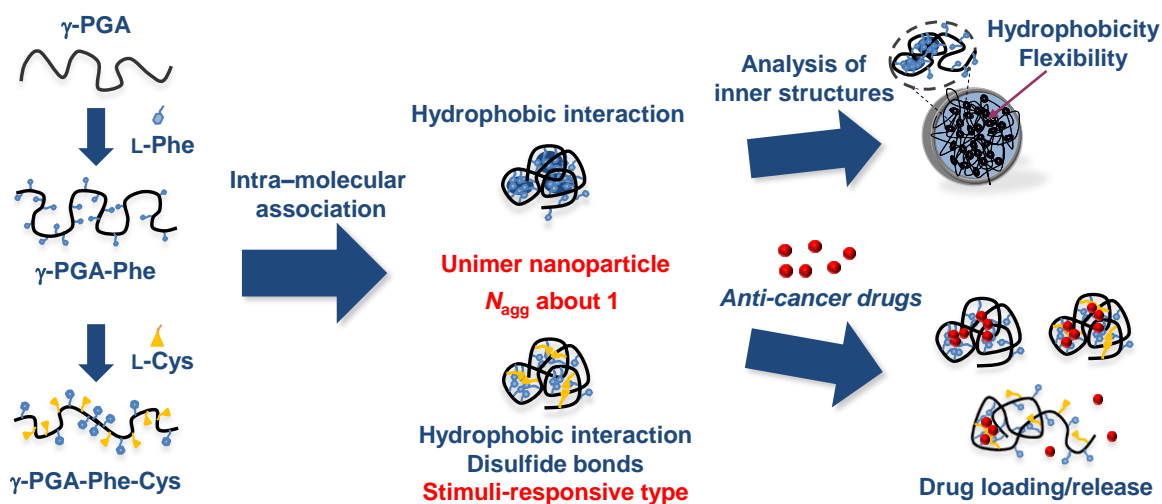
The synthesis of polymeric nanoparticles with controlled characteristics has become an appealing research topic lately. Polymeric amphiphiles such as amphiphilic diblock copolymers, and graft copolymers are able to spontaneously form micelles/nanoparticles through inter- or intra-molecular associations during which drug molecules are incorporated.<sup>10</sup> One of the unique properties of amphiphilic random copolymers is their ability to form unimolecular (unimer) nanoparticles with intra-polymer associations. Furthermore, there has been growing research on the methods to control the single chain state, which are mainly performed under dilute conditions, for example, the photo-induced folding of polymer chain<sup>11, 12</sup> as well as collapse via heating on thermo-responsive polymers.<sup>13</sup> In contrast, simpler methods to control the folding, for example via hydrophobic interactions, have been investigated over the past decade.<sup>14, 15</sup> However, a few studies have focused on their applications as single chain carriers for cancer therapy.

For targeted cancer therapy, only unimolecular micelles obtained from star-shaped polymers and hyper-branched polymer have been reported most recently. Such polymeric systems have their own hydrophobic domains formed by only intra-molecular associations, which are capable of encapsulating hydrophobic molecules, while not displaying any critical micelle concentration (CMC). However, these polymeric systems often require complicated synthesis and preparation. Their characterization cannot readily be carried out because of the highly branched structures with a large number of functional end groups, and this increases the possibility of structural defects of the polymer causing complexity and heterogeneity within its final structure.<sup>16</sup>

In a previous study, our research group prepared nanoparticles composed of hydrophobically modified poly( $\gamma$ -glutamic acid) ( $\gamma$ -PGA) by intra-/inter-molecular

association in aqueous solution.<sup>17</sup> By employing hydrophobic moieties of L-phenylalanine (L-Phe) grafted onto  $\gamma$ -PGA main chains, nanoparticles could be easily prepared, and the size of nanoparticles could be controlled by altering the preparative conditions. Recently, it has been demonstrated that the size of the nanoparticles plays a critical role in controlling immune responses.<sup>18</sup> Therefore, the fabrication of unimer nanoparticles consisting of the amphiphilic graft copolymer is one of the major challenges in polymer science and pharmaceuticals, and intra-molecularly associated single chain particles can be considered as the smallest polymeric nanoparticles. It is expected that biodegradable unimer nanoparticles will have several advantages associated with their specific size and structure: (i) due to their large surface to volume ratio relative to larger-sized particles, it is possible to more efficiently entrap target molecules; (ii) these nanoparticles would be capable of targeting specific tissues, cells or intracellular organelles for drug delivery system (DDS); and (iii) the degradation behaviors of the nanoparticles and the release rate of entrapped therapeutic drugs can be easily control.

The objective of the present studies is to fabricate “unimer nanoparticles” by controlling the association number of amphiphilic poly( $\gamma$ -glutamic acid) ( $\gamma$ -PGA) (**Scheme 1**).



**Scheme 1.** Illustration of the scope of the present studies.

This thesis includes the following 3 Chapters.

In **Chapter 1**, the physical factors that control the formation of  $\gamma$ -PGA-Phe unimer nanoparticles, such as the molecular weight of the initial polymers balanced against their hydrophobicity and microscopic structures of these nanoparticles, are investigated.

In **Chapter 2**, as the stability of drug incorporation, the drug loading efficiency as well as the release behaviors can be affected by the structure of inner particles. Thus, the morphologies and the inner structures of the obtained  $\gamma$ -PGA-Phe unimer nanoparticles are further investigated.

In **Chapter 3**, in order to enhance the abilities to control its intra-molecular associations for effective drug control release, unimer nanoparticles having stimuli-responsive properties are developed and studied their potential applications as drug carriers for cancer therapy.

Finally, it is expected that the obtained unimer nanoparticles can be an interesting candidate as a solubilizer and carrier for hydrophobic drugs, especially targeted cancer therapies.



## References

1. R. Duncan, *Nat. Rev. Cancer* **6**, 688 (2006).
2. J. W. Singer, S. Shaffer, B. Baker, A. Bernareggi, S. Stromatt, D. Nienstedt and M. Besman, *Anticancer Drugs* **16**, 243 (2005).
3. M. Oba, K. Aoyagi, K. Miyata, Y. Matsumoto, K. Itaka, N. Nishiyama, Y. Yamasaki, H. Koyama and K. Kataoka, *Mol. Pharmaceutics* **5**, 1080 (2008).
4. P. P. Lv, Y. F. Ma, R. Yu, H. Yue, D. Z. Ni, W. Wei and G. H. Ma, *Mol. Pharmaceutics* **9**, 1736 (2012).
5. Y. Xiao, H. Hong, A. Javadi, J. W. Engle, W. Xu, Y. Yang, Y. Zhang, T. E. Barnhart, W. Cai and S. Gong, *Biomaterials* **33**, 3071 (2012).
6. F. Dosio, S. Arpicco, P. Brusa, B. Stella and L. Cattel, *J. Control. Release* **76**, 107 (2001).
7. M. Skwarczynski, Y. Hayashi and Y. Kiso, *J. Med. Chem.* **49**, 7253 (2006).
8. H. Maeda, J. Wu, T. Sawa, Y. Matsumura and K. Hori, *J. Control. Release* **65**, 271 (2000).
9. H. Cabral, Y. Matsumoto, K. Mizuno, Q. Chen, M. Murakami, M. Kimura, Y. Terada, M. R. Kano, K. Miyazono, M. Uesaka, N. Nishiyama and K. Kataoka, *Nat. Nanotechnol.* **23**, 815 (2011).
10. W. Wang, X. Qu, A. I. Gray, L. Tetley and I. F. Uchegbu, *Macromolecules* **37**, 9114 (2004).
11. T. Mes, R. van der Weegen, A. R. A. Palmans and E. W. Meijer, *Angew. Chem. Int. Ed.* **50**, 5085 (2011).
12. J. He, L. Tremblay, S. Lacelle and Y. Zhao, *Soft Matter* **7**, 2380 (2011).

13. E. Harth, B. V. Horn, V. Y. Lee, D. S. Germack, C. P. Gonzales, R. D. Miller and C. J. Hawker, *J. Am. Chem. Soc.* **124**, 8653 (2002).
14. Y. Morishima, S. Nomura, T. Ikeda, M. Seki and M. Kamachi, *Macromolecules* **28**, 2874 (1995).
15. S. Yusa, A. Sakakibara, T. Yamamoto and Y. Morishima, *Macromolecules*, **35**, 5243 (2002).
16. Karak, Niranjana. *Fundamentals of Polymers: Raw Materials to Finish Products*, PHI Learning Pvt. Ltd., 2009.
17. H. Kim, T. Akagi and M. Akashi, *Macromol. Biosci.* **9**, 842 (2009).
18. H. Kim, T. Uto, T. Akagi, M. Baba and M. Akashi, *Adv. Funct. Mater.* **20**, 3925 (2010).

## Chapter 1

### Preparation of $\gamma$ -PGA-Phe unimer nanoparticles

#### 1.1. Introduction

Amphiphilic block or graft copolymers can organize into many morphologies, such as spheres, rods, and vesicles, in aqueous solution. The morphology of these nanostructured materials can be varied by changing the composition of the hydrophobic and hydrophilic segments on the polymer chains.<sup>1-3</sup> In general, self-assembled amphiphilic nanoparticles are composed of an inner hydrophobic core and an outer shell of hydrophilic groups. Hydrophobic blocks form the inner core of the structure, which acts as a drug incorporation site, especially for hydrophobic drugs. Hydrophobic drugs can thus be easily entrapped within the inner core by hydrophobic interactions. These self-assembling characteristics of amphiphilic copolymers have attracted considerable attention as effective and targetable drug carriers.<sup>4-6</sup>

One of the unique properties of amphiphilic random copolymers is their ability to form unimolecular (unimer) nanoparticles with intrapolymer associations.<sup>7-10</sup> The random distribution of hydrophobic segments in a polymer chain shows a tendency for intrapolymer association in aqueous solution, whereas blocky distributions show a trend for interpolymer associations.<sup>11, 12</sup> Moreover, these intrapolymer associations occur preferentially when the content of hydrophobic segments (hydrophobicity) of the polymer chain is high, whereas interpolymer associations occur favorably when the hydrophobicity is decreased.<sup>13</sup> Yusa *et al.* reported that random copolymers composed of sodium 2-(acrylamido)-2-methylpropanesulfonate (NaAMPS) and 11-acrylamidoundecanoic acid (AmU) can form unimer micelles in response to the pH.<sup>14, 15</sup>

It has also been reported that amphiphilic graft copolymers composed of poly(methyl metacrylate) (PMMA) and poly(styrene) (PS) are able to form unimolecular rod-like chains of micelles, depending on the quality of the solvent, with respect to the backbone and the grafts.<sup>16, 17</sup> However, the majority of the research on the formation of unimer nanoparticles in aqueous media has been performed on non-biocompatible and non-biodegradable systems. In addition, the preparation of unimer nanoparticles using biodegradable, hydrophobically-modified polymers and their applications as drug delivery system (DDS) has been reported only by a few researchers. It is expected that biodegradable unimer nanoparticles will have several advantages associated with their specific size and structure: (i) due to their large surface to volume ratio relative to larger-sized particles, it is possible to more efficiently entrap target molecules; (ii) these nanoparticles would be capable of targeting specific tissues, cells or intracellular organelles for DDS; and (iii) the degradation behaviors of the nanoparticles and the release rate of entrapped therapeutic drugs can be easily control.

Poly( $\gamma$ -glutamic acid) ( $\gamma$ -PGA) is a naturally occurring, water-soluble, biodegradable, edible, and non-toxic polyamide which is synthesized by certain strains of *Bacillus*.<sup>26</sup> It is a high-molecular-weight polypeptide composed of  $\gamma$ -linked glutamic acid units, and its  $\alpha$ -carboxylate side chains can be chemically modified. Thus,  $\gamma$ -PGA has been selected as the biodegradable anionic polymer. In a previous study, nanoparticles composed of hydrophobically-modified  $\gamma$ -PGA for the development of vaccine and drug carriers was prepared. Amphiphilic graft copolymers composed of  $\gamma$ -PGA as the hydrophilic backbone and L-phenylalanine (L-Phe) as the hydrophobic segment formed monodispersed nanoparticles in water due to their amphiphilic characteristics.<sup>18-21</sup> The size of the nanoparticles could be easily controlled from 30 to 200 nm by changing the

preparation conditions.<sup>22</sup> The main driving force for particle formation is the intra- or intermolecular associations of Phe attached to  $\gamma$ -PGA in the core of the nanoparticles. Moreover, it is demonstrated that the size of the nanoparticles plays a critical role in controlling immune responses.<sup>23</sup> The surface interactions between the small-sized nanoparticles with high-specific surface areas and immune cells is important for the induction of immune responses.<sup>24, 25</sup> Therefore, the fabrication of unimer nanoparticles consisting of the amphiphilic graft copolymer is one of the major challenges in polymer science and pharmaceuticals, and intramolecularly associated single chain particles can be considered the smallest polymeric nanoparticles.

In this Chapter, the fabrication of unimer nanoparticles via controlling the association number of  $\gamma$ -PGA-*graft*-Phe ( $\gamma$ -PGA-Phe) copolymers was studied by focusing on the physical factors that control the intrapolymer hydrophobic interactions of L-Phe for single chain state, such as the molecular weight of the initial polymers balanced against their hydrophobicity of side chain. For this purpose, three different molecular weights of  $\gamma$ -PGA (70, 140 and 220 kDa) were employed to synthesize and prepare  $\gamma$ -PGA-Phe unimer nanoparticles (**Figure 1.1**). Besides, the effects of the grafting degree of L-Phe on their self-association behaviors were also characterized by dynamic light scattering (DLS), static light scattering (SLS) and fluorescence spectroscopy.

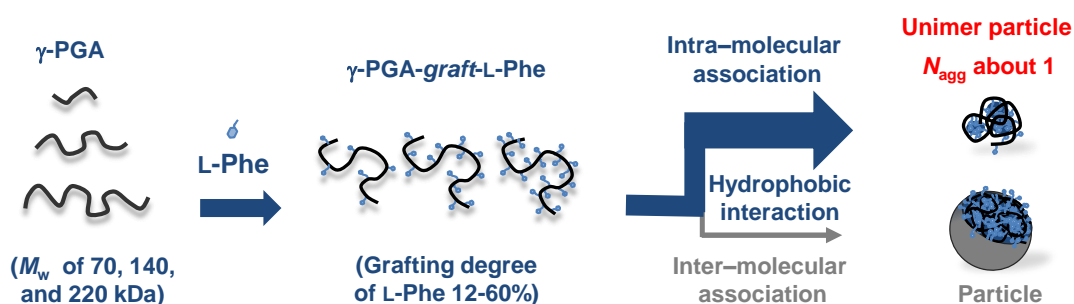


**Figure 1.1.** Illustration of the formation of  $\gamma$ -PGA-Phe unimer nanoparticles by intra-molecular association.

## 1.2. Experimental Section

### *Materials*

$\gamma$ -PGA with molecular weights ( $M_w$ ) of 140 and 220 kDa (D-Glu/ L-Glu = 70/30) as determined by static light scattering (SLS) were purchased from Wako Pure Chemical, Ltd. (Japan). Low  $M_w$  of  $\gamma$ -PGA (70 kDa) was prepared by alkaline hydrolysis from  $\gamma$ -PGA with a  $M_w$  of 140 kDa using 0.1 M NaOH incubation at 4°C for 4 h.<sup>27</sup> The size and PDI of the three used  $\gamma$ -PGA determined by dynamic light scattering (DLS) were summarized in **Table 1.1**. The results are presented as means  $\pm$  SD (n=3). L-phenylalanine ethyl ester (L-Phe) was purchased from Sigma-Aldrich Chem. Co., and 1-ethyl-3-[3-dimethylaminopropyl]carbodiimide hydrochloride (EDC) was from Dojindo Laboratories (Japan). Pyrene served as a fluorescence probe was from Wako Pure Chemical, Ltd. (Japan). Water was purified with a Direct-Q system (Millipore, Co.). All other chemicals used were of analytical grade.

### *Synthesis of $\gamma$ -PGA-graft-L-Phe copolymers*

To study the effects of different  $M_w$  of main chains on the formation of unimer nanoparticles, three different  $M_w$  of  $\gamma$ -PGA (70, 140 and 220 kDa, hereafter abbreviated as  $\gamma$ -PGA 70k,  $\gamma$ -PGA140k and  $\gamma$ -PGA220k, respectively) were employed for the synthesis and preparation of nanoparticles. Briefly,  $\gamma$ -PGA (4.7 unit mmol) was dissolved into 100 mM NaHCO<sub>3</sub> (pH 8.3). Subsequently, a specific amount of coupling agent (EDC) (from 1.2 to 7.0 mmol) and L-Phe (4.7 mmol) were added into the solution. After incubation for 24 h, the mixtures were dialyzed against distilled water and freeze-

dried for several days. The chemical structures of the obtained copolymers were confirmed by  $^1\text{H}$  NMR and FT-IR. The purified  $\gamma$ -PGA-Phe was then characterized in DMSO- $d_6$  and in D $_2$ O by  $^1\text{H}$  NMR spectroscopy. The grafting degree of L-Phe was determined from the integral intensity ratio of the methylene peaks of  $\gamma$ -PGA to the phenyl group peaks of L-Phe.

### ***Preparation of $\gamma$ -PGA-Phe unimer nanoparticles***

The synthesized copolymers with grafting degrees ranging from 12 to 65% were employed for the preparation of the nanoparticles.  $\gamma$ -PGA-Phe copolymers with a grafting degree of over 42% was soluble in phosphate buffered saline (PBS, pH 7.4), but became insoluble over a grafting degree of 50%. Thereby, depending on the solubility of the hydrophobized  $\gamma$ -PGA and the grafting degree of L-Phe, there are two different methods to prepare nanoparticles: (1) ***direct dispersion*** and (2) ***dialysis methods***. In the case of a copolymer with a grafting degree lower than 42%, the copolymer was dispersed in PBS or pure water with stirring at the desired concentration before characterization. On the other hand, modified  $\gamma$ -PGA with high grafting degrees of L-Phe over 42% could not be dissolved well in water, and thus the dialysis method was employed for the preparation of nanoparticles by dissolving the copolymers at 10 mg/mL in dimethyl sulfoxide (DMSO). Next, the prepared copolymers in DMSO were mixed with a NaCl solution (varying concentrations from 0 to 0.5 M) of the same volume, and the mixtures were then dialyzed against distilled water using cellulose membrane tubing (50,000 molecular weight cut-off), and subsequently lyophilized for several days. The obtained powders were dispersed in PBS or pure water before characterization. The

sample solutions obtained from both methods were further sonicated (AS ONE corporation, VS-150) at 150 W for 1 min before measurement.

Samples were coded according to the following convention. Thus,  $\gamma$ -PGA140k-Phe-42(10-0.1) indicates that the  $M_w$  of the  $\gamma$ -PGA is 140 kDa, Phe-42 is 42% L-Phe grafting, and (10-0.1) means 10 mg/mL  $\gamma$ -PGA-Phe dissolved in DMSO was added to 0.1 M NaCl solution at the same volume.

### ***Characterization of particle size, molecular weight and zeta potential***

The  $\gamma$ -PGA-Phe nanoparticles were characterized in terms of their particle size,  $M_w$  and zeta potential by DLS and SLS methods, respectively. The mean particle size of the prepared nanoparticles (1 mg/mL in PBS) was measured by DLS (Zetasizer Nano ZS, Malvern, UK) at a wavelength of 633 nm and a detection angle of  $173^\circ$ , by taking the average of at least 3 measurements, and represented the hydrodynamic diameter of the particle. The mean size was derived from a Cumulants analysis of the measured correlation curve, wherein a single particle size is assumed and a single exponential fit was applied to the autocorrelation function. In addition to the mean particle size, the instrument reports the polydispersity index (PDI) between 0 (monodispersed particles) and 1 (polydispersed particles).

The  $M_w$  of the nanoparticles was determined by measuring the sample at different concentrations (a series of two-fold dilutions was used for nanoparticles dispersed in PBS whose concentrations starting from 5 mg/mL) and applying the Rayleigh equation. The refractive index increment ( $dn/dc$ ) was determined by a differential refractometer



(Otsuka electronics Co. LTD., DRM-3000, wavelength: 633 nm). The value of  $dn/dc$  for all of polymers used in this study was ranged from 0.155 to 0.157 mL/g. Toluene was used to determine Rayleigh ratio as a standard (Rayleigh ratio:  $1.352 \times 10^{-5} \text{ cm}^{-1}$ , Refractive index: 1.496). The sample scattering in PBS was then measured, followed by measurement of various concentrations of sample. It is known that the intensity of scattered light that a particle produces is proportional to the product of the weight-average molecular weight and the concentration of the particle. The Intensity of scattered light of various particle concentrations at one angle was measured, and then, the value was compared with the scattering produced from a standard (toluene). In this measurement method, the scattering is assumed as Rayleigh scattering and the Rayleigh approximation is used for  $M_w$  determination. The representative example data of DLS and SLS were shown in **Figure 1.2**. The  $M_w$  of  $\gamma$ -PGA-Phe was determined by a Debye plot obtained from the intensity of the scattered light.

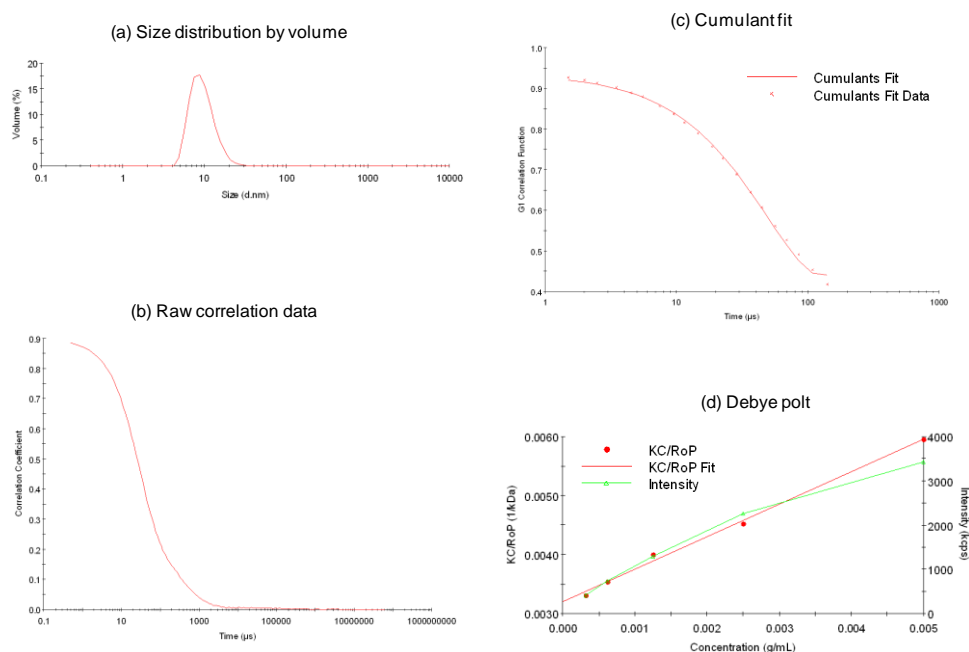


**Figure 1.2.** DLS (a) size distribution, (b) raw correlation data, (c) cumulant fit and SLS (d) Debye plot data of  $\gamma$ -PGA140k-Phe-42 (10-0).

Furthermore, the surface charge of the nanoparticles in PBS was determined by zeta potential measurements using a Zetasizer Nano ZS. The zeta potential was estimated on the basis of the electrophoretic mobility under an electric field as an average of at least 3 measurements. The frequency shift of an incident laser beam caused by these moving particles is converted to the zeta potential by the application of the Smoluchowski equation. The temperature was kept constant at 25°C during DLS, SLS and zeta potential measurements.

In addition, the structure of unimer nanoparticles was analyzed by  $^1\text{H}$  NMR spectroscopy. The  $^1\text{H}$  NMR spectra of unimer nanoparticles dispersed in  $\text{D}_2\text{O}$  (7 mg/mL) or dissolved in  $\text{DMSO-}d_6$  (7 mg/mL) were obtained.

### ***Steady-state fluorescence measurements***

The formation of the hydrophobic domains of the  $\gamma$ -PGA-Phe samples were further characterized by steady-state fluorescence measurements using pyrene as a fluorescence probe.<sup>28</sup> Steady-state fluorescence spectra were recorded on a JASCO FP-6500 spectrofluorometer. A stock solution of pyrene in ethanol ( $1 \times 10^{-4}$  M) was added to a glass vial, and the ethanol was evaporated by flushing gaseous nitrogen to form a pyrene thin film. The  $\gamma$ -PGA-Phe samples dissolved or dispersed in PBS were then added to the thin film, and the resulting mixture was incubated for 24 h at room temperature before measurement. The final concentration of pyrene in the mixture was  $1 \times 10^{-6}$  M. The fluorescence emission spectra of pyrene were measured at an excitation wavelength of 339 nm at room temperature. The excitation spectra were monitored at 372 nm. By varying the concentration of polymer in the PBS, the formation of hydrophobic domains could be detected.

### ***Stability of unimer nanoparticles***

The stability of unimer nanoparticles in PBS was examined by changing the particle size with respect to the concentration, and incubation time. To study the effects of the polymer concentration on particle size,  $\gamma$ -PGA-Phe of various grafting degrees was dispersed into PBS at the desired concentration (from 0.01 to 10 mg/mL). Their particle sizes were measured by DLS for each polymer concentration.

In addition,  $\gamma$ -PGA-Phe of various grafting degrees was dispersed in PBS at 1 mg/mL in order to study the effect of the incubation time at 4°C on the stability of the particle size. At different time intervals, the size of the nanoparticles was measured by DLS.

## **1.3. Results and Discussion**

### ***Synthesis of $\gamma$ -PGA-graft-L-Phe copolymers***

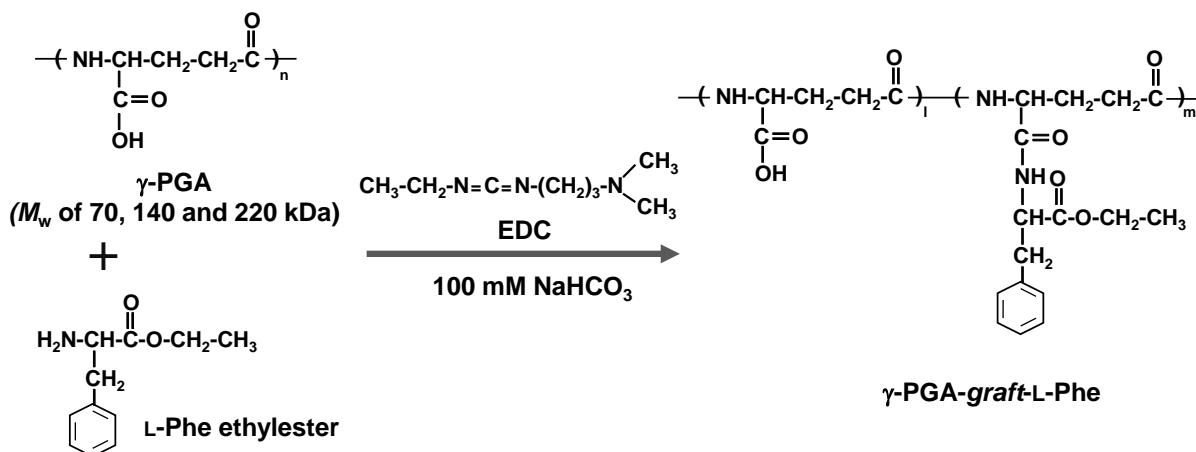
The size and PDI of the three used  $\gamma$ -PGA determined by DLS were shown in **Table 1.1**. For the synthesis of the  $\gamma$ -PGA-Phe copolymers, L-Phe was conjugated to the carboxylic groups of  $\gamma$ -PGA by carbodiimide-catalyzed coupling. The amide bond formation between the carboxyl groups on  $\gamma$ -PGA and the amine groups of L-Phe was catalyzed by EDC (**Scheme 1.1**). The grafting degree of L-Phe on the  $\gamma$ -PGA main chains could be controlled by changing the amount of coupling agent during the synthesis step, which was further verified by  $^1\text{H}$  NMR to confirm the modified structure and to determine the grafting degree of L-Phe (%) using integral intensity ratio of the methylene peaks of  $\gamma$ -PGA to the phenyl group peaks of Phe as shown in **Figure 1.3** (sample was dissolved in DMSO- $d_6$ ). In this experiment,  $\gamma$ -PGA-Phe with Phe groups ranging from 12 to 60 Phe per 100 glutamic acid units of  $\gamma$ -PGA were prepared for all

$M_w$  of  $\gamma$ -PGA (Table 1.2). The resulting copolymers were also measured by FT-IR, which confirmed the formation of the amide bond C=O stretch at around  $1650\text{ cm}^{-1}$  and the presence of a phenyl group on the structure at  $700\text{ cm}^{-1}$  (Figure 1.4).

**Table 1.1. Size and PDI of different  $M_w$  of  $\gamma$ -PGA**

$\gamma$ -PGA	Size (nm) <sup>a</sup>	PDI <sup>b</sup>
$\gamma$ -PGA70k	$5.3 \pm 0.3$	$0.32 \pm 0.05$
$\gamma$ -PGA140k	$12.0 \pm 0.4$	$0.22 \pm 0.02$
$\gamma$ -PGA220k	$13.9 \pm 5.0$	$0.41 \pm 0.05$

<sup>a</sup>The diameter was measured in PBS (1 mg/mL) by dynamic light scattering (DLS) using a Zetasizer nano ZS. <sup>b</sup> PDI represents polydispersity index. The results are presented as means  $\pm$  SD (n=3).



**Scheme 1.1.** Synthesis scheme of  $\gamma$ -PGA-graft-L-Phe copolymers.

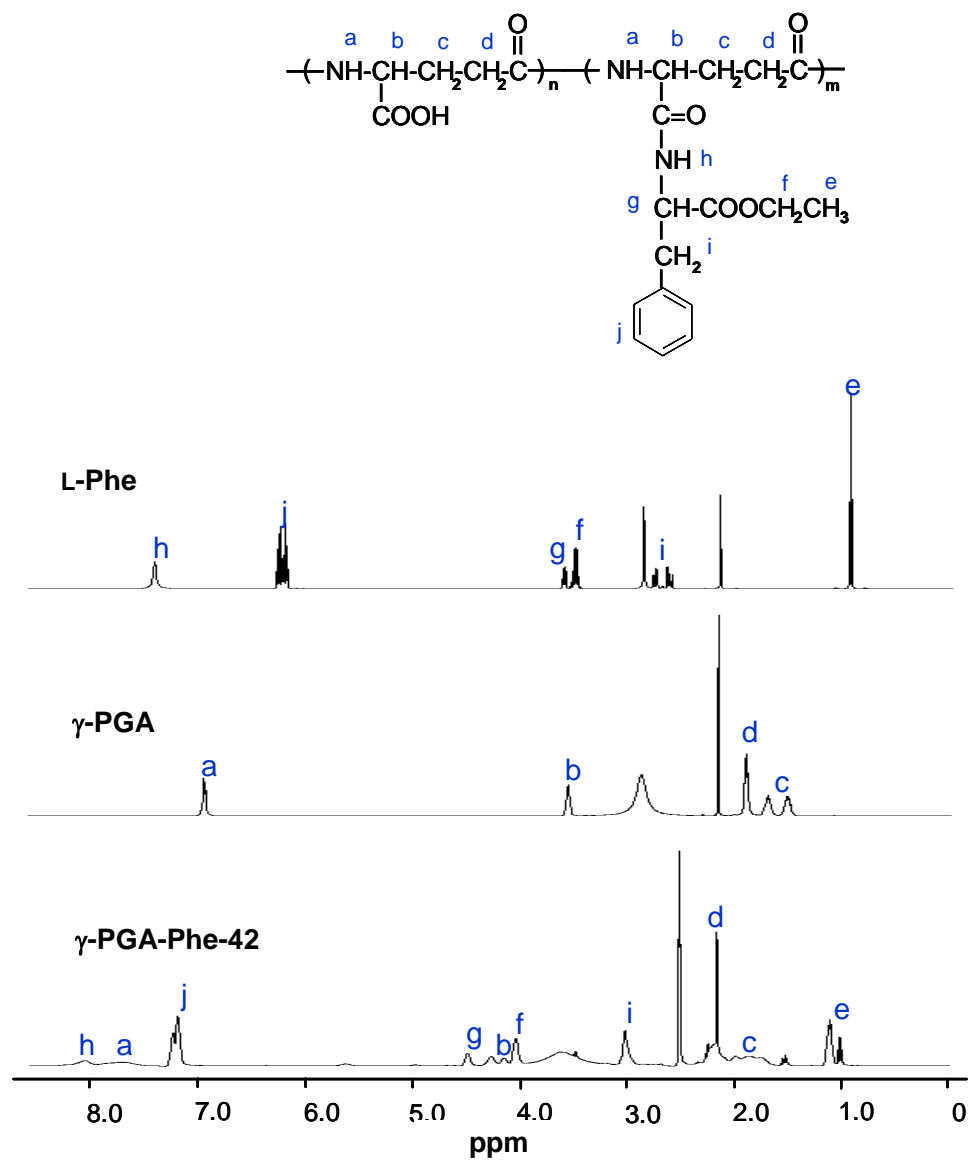


**Figure 1.3.** <sup>1</sup>H NMR was performed to confirm the modified structure and to determine the grafting degree of L-Phe (%) in DMSO-d<sub>6</sub>.

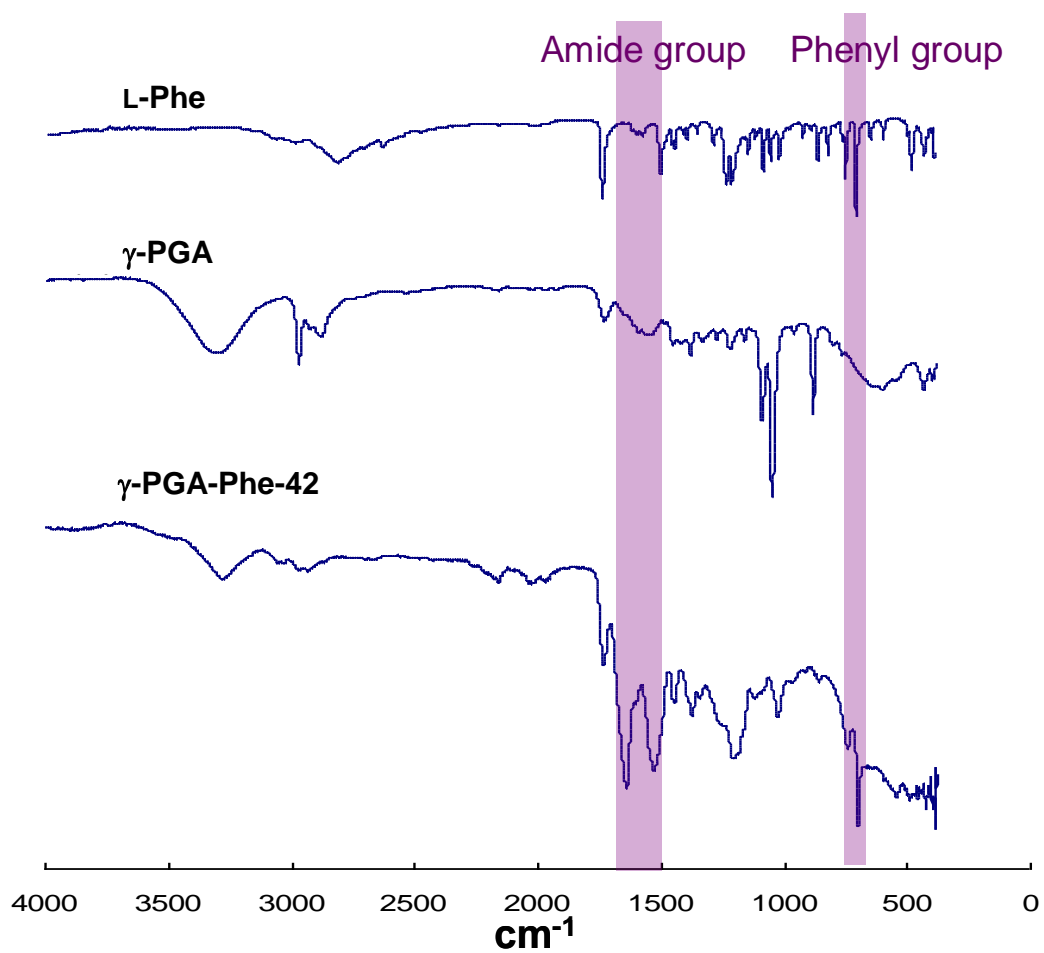


**Figure 1.4.** FT-IR was performed to confirm the chemical structures of the synthesized  $\gamma$ -PGA-Phe graft copolymers.

**Table 1.2.** Synthesis of  $\gamma$ -PGA-*graft*-Phe copolymers.

Sample	$\gamma$ -PGA (unit mmol)	L-Phe (mmol)	EDC (mmol)	Yield (%)	Grafting degree <sup>a</sup> (%)
$\gamma$ -PGA70k-Phe-12	4.7	4.7	1.2	45	12
$\gamma$ -PGA70k-Phe-27	4.7	4.7	2.3	48	27
$\gamma$ -PGA70k-Phe-35	4.7	4.7	3.5	28	35
$\gamma$ -PGA70k-Phe-42	4.7	4.7	4.1	27	42
$\gamma$ -PGA70k-Phe-50	4.7	4.7	4.7	35	50
$\gamma$ -PGA140k-Phe-12	4.7	4.7	1.2	56	12
$\gamma$ -PGA140k-Phe-27	4.7	4.7	2.3	46	27
$\gamma$ -PGA140k-Phe-35	4.7	4.7	3.5	58	35
$\gamma$ -PGA140k-Phe-42	4.7	4.7	4.7	45	42
$\gamma$ -PGA140k-Phe-58	4.7	4.7	6.5	68	58
$\gamma$ -PGA220k-Phe-12	4.7	4.7	1.2	47	12
$\gamma$ -PGA220k-Phe-27	4.7	4.7	2.3	54	27
$\gamma$ -PGA220k-Phe-35	4.7	4.7	4.1	66	35
$\gamma$ -PGA220k-Phe-42	4.7	4.7	4.7	42	42
$\gamma$ -PGA220k-Phe-55	4.7	4.7	6.5	62	55

<sup>a</sup> The grafting degree of L-Phe was measured by <sup>1</sup>H NMR.

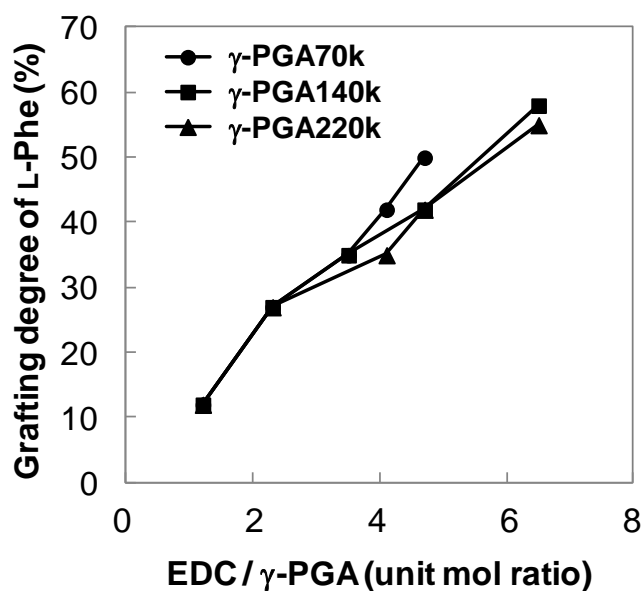


**Figure 1.5.** Synthesis of  $\gamma$ -PGA-Phe copolymers with different grafting degrees of L-Phe.  $\gamma$ -PGA different in  $M_w$  were employed to synthesize the  $\gamma$ -PGA-Phe copolymers. The grafting degrees of L-Phe were measured by  $^1\text{H}$  NMR.

### *Preparation and characterization of unimer nanoparticles*

By controlling the amount of coupling agent during the synthesis,  $\gamma$ -PGA-Phe with grafting degrees ranging from 12 to 60% evaluated by  $^1\text{H}$  NMR could be readily obtained for all  $M_w$  of  $\gamma$ -PGA (**Figure 1.5**). The aqueous solubility of the copolymers depends on the substitution degree of the Phe moieties. Therefore, when using copolymers with grafting degrees of L-Phe lower than 42%, the nanoparticles were prepared by directly dissolving the copolymers in an aqueous solution, which allowed the self-assembly to occur spontaneously. The particle sizes,  $M_w$  and number of polymer aggregates in one particle ( $N_{\text{agg}}$ ) of the nanoparticles were determined by DLS and SLS respectively. Thus, the  $N_{\text{agg}}$  could be calculated from the measured  $M_w$  of  $\gamma$ -PGA-Phe. As shown in **Table 1.3**, the particle sizes were around 9-13 nm for all samples. However, decreasing the  $M_w$  of  $\gamma$ -PGA to 70 kDa resulted in samples with a high PDI at all



polymer concentrations (data not shown). This is probably due to the modified  $\gamma$ -PGA (70 kDa) has a large number of end groups both COOH groups and NH<sub>2</sub> groups much more than the modified  $\gamma$ -PGA (140 kDa and 220 kDa), resulting in strong inter-molecular association, and thus aggregates favorably occurred. Therefore, the  $N_{\text{agg}}$  of the samples prepared using  $\gamma$ -PGA low  $M_w$  70k could not be determined. However, a  $N_{\text{agg}}$  of about 1 was obtained from the sample with  $M_w$  values of 140 and 220 kDa.

**Table 1.3. Characterization of  $\gamma$ -PGA-Phe nanoparticles prepared by direct dispersion method**

Sample	Calculated $M_w$ (kDa) <sup>a</sup>	Size (nm) <sup>b</sup>	PDI <sup>c</sup>	Zeta potential (mV) <sup>b</sup>	Measured $M_w$ (kDa) <sup>d</sup>	$N_{\text{agg}}$ <sup>e</sup>	Domain formation <sup>f</sup>
$\gamma$ -PGA140k-Phe-12	168	13.6 ± 2.4	0.32 ± 0.06	- 23.0 ± 2.2	246	1.5	X
$\gamma$ -PGA140k-Phe-27	202	11.0 ± 1.6	0.31 ± 0.03	- 23.1 ± 1.3	276	1.4	X
$\gamma$ -PGA140k-Phe-35	220	7.9 ± 1.3	0.33 ± 0.06	- 26.7 ± 3.5	296	1.3	○
$\gamma$ -PGA140k-Phe-42	236	9.7 ± 0.5	0.29 ± 0.02	- 22.6 ± 0.9	313	1.3	○
$\gamma$ -PGA140k-Phe-58	273	Aggregation	n.d. <sup>g</sup>	n.d.	n.d.	n.d.	n.d.
$\gamma$ -PGA220k-Phe-12	263	n.d.	n.d.	n.d.	n.d.	n.d.	n.d.
$\gamma$ -PGA220k-Phe-27	317	10.2 ± 1.0	0.45 ± 0.02	-33.3 ± 1.9	425	1.3	○
$\gamma$ -PGA220k-Phe-35	345	10.0 ± 2.2	0.39 ± 0.06	-28.8 ± 0.8	391	1.1	○
$\gamma$ -PGA220k-Phe-42	370	9.5 ± 0.2	0.38 ± 0.02	-27.6 ± 0.8	420	1.1	○
$\gamma$ -PGA220k-Phe-55	417	Aggregation	n.d.	n.d.	n.d.	n.d.	n.d.

<sup>a</sup> The  $M_w$  of  $\gamma$ -PGA-Phe was calculated from the  $M_w$  of  $\gamma$ -PGA measured by static light scattering (SLS), and the grafting degree of L-Phe (%) measured by <sup>1</sup>H NMR. <sup>b</sup> The particle diameter and zeta potential were measured in PBS (1 mg/mL) by dynamic light scattering (DLS) and laser doppler velocimetry using a Zetasizer nano ZS. <sup>c</sup> PDI represents polydispersity index. The results are presented as means ± SD (n =3). <sup>d</sup> The  $M_w$  of  $\gamma$ -PGA-Phe in PBS was measured by SLS. <sup>e</sup> The number of  $\gamma$ -PGA-Phe aggregates ( $N_{\text{agg}}$ ) was calculated by the Measured  $M_w$  / Calculated  $M_w$ . <sup>f</sup> The formation of hydrophobic domains was detected by steady-state fluorescence measurement using pyrene as a probe. <sup>g</sup> n. d. means not determined.

### ***Control of the number of polymer aggregation and particle size by dialysis method***

The physical properties and self-association behaviors of amphiphilic copolymers are governed by the balance between the hydrophobicity and hydrophilicity of the polymer chain, which itself is controlled by its chemical composition and microstructure.<sup>29, 30</sup> In a previous study, our research group prepared size-controlled nanoparticles using  $\gamma$ -PGA-Phe with a 50% Phe grafting degree. The size of the nanoparticles could be easily controlled from 30 to 200 nm by changing the NaCl concentration during the formation of the particles.<sup>22</sup> In order to clearly observe the effect of the Phe grafting degrees (%) on the formation of  $\gamma$ -PGA-Phe nanoparticles by intra- or inter-polymer associations,  $\gamma$ -PGA140k-Phe was employed as the main example. To prepare  $\gamma$ -PGA140k-Phe nanoparticles,  $\gamma$ -PGA140k-Phe-42, 46, 58 or 65 dissolved in DMSO was added to pure water or various concentrations of NaCl solution, and the resulting mixture were dialyzed and freeze-dried. **Table 1.4** summarizes the properties of nanoparticles composed of  $\gamma$ -PGA140k-Phe with different grafting degrees. The formation and size of the nanoparticles depended on the NaCl concentration and Phe grafting degree. When  $\gamma$ -PGA140k-Phe-42 dissolved in DMSO was added to water, the particle size increased with increasing NaCl concentration (**Figure 1.6**). The increased particle size was correlated with the  $N_{\text{agg}}$ . In the case of  $\gamma$ -PGA140k-Phe-42, the  $N_{\text{agg}}$  (from 1 to 12 chains) in one particle could be easily controlled by changing the NaCl concentration during the formation of the particles. The increased NaCl concentration reduced the electrostatic repulsion of the carboxyl groups of  $\gamma$ -PGA-Phe. The addition of salt results in an increased interpolymer association of  $\gamma$ -PGA-Phe. The difference in particle size can be attributed to the difference in the association number of  $\gamma$ -PGA140k-Phe. At the higher grafting degree of  $\gamma$ -PGA140k-Phe-58 and 65, the increased polymer

hydrophobicity resulted in an increased  $N_{agg}$ . The  $\gamma$ -PGA140k-Phe-58 (10-0) showed a higher  $N_{agg}$  as compared to  $\gamma$ -PGA140k-Phe-42 (10-0). These results indicated that the Phe grafting degree is one of important factors for the self-association behavior of  $\gamma$ -PGA-Phe.

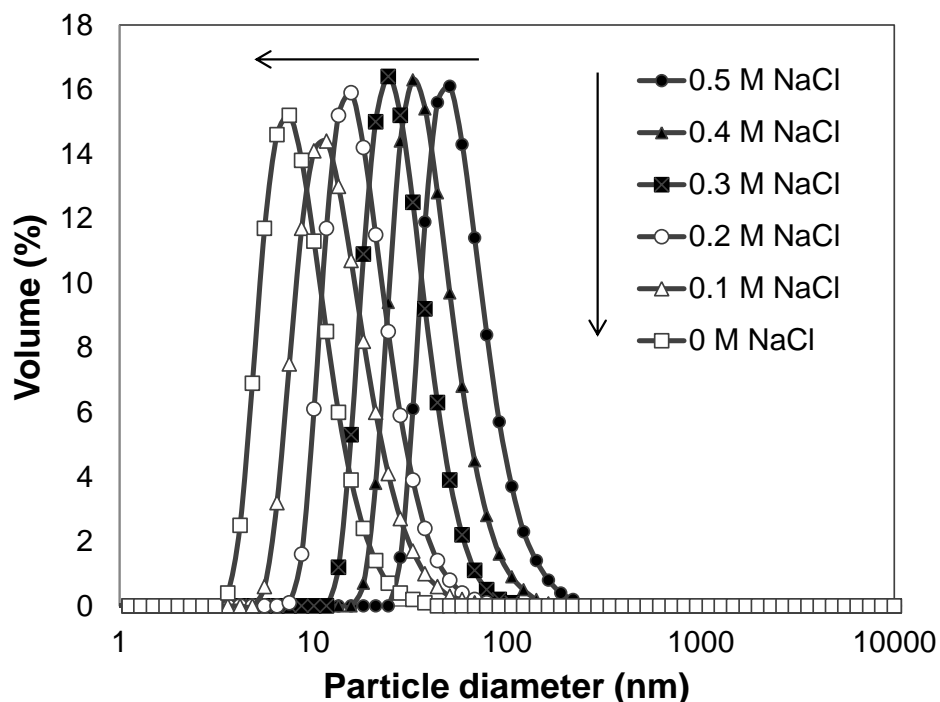


**Figure 1.6.** Size changes of  $\gamma$ -PGA140k-Phe-42 nanoparticles prepared at various NaCl concentrations.  $\gamma$ -PGA140k-Phe-42 (10 mg/mL in DMSO) was added to the same volume of NaCl aqueous solution. To regulate the size of the nanoparticles, the NaCl concentration was varied from 0 to 0.5 M. The size of the nanoparticles was measured in PBS by DLS.

**Table 1.4.** Characterization of  $\gamma$ -PGA140k-Phe nanoparticles prepared by the dialysis method.

Sample	Polymer conc. in DMSO <sup>a</sup> (mg/mL) <sup>a</sup>	NaCl (M) <sup>a</sup>	Size (nm) <sup>b</sup>	PDI <sup>c</sup>	Zeta potential (mV) <sup>b</sup>	Measured $M_w$ (kDa) <sup>d</sup>	$N_{agg}$ <sup>e</sup>	Domain formation <sup>f</sup>
$\gamma$ -PGA140k-Phe-42 (10-0)	10	0	9.8 $\pm$ 1.0	0.29 $\pm$ 0.02	-23.0 $\pm$ 1.8	343	1.5	○
$\gamma$ -PGA140k-Phe-42 (10-0.1)	10	0.1	16.3 $\pm$ 0.8	0.21 $\pm$ 0.04	-27.1 $\pm$ 1.8	608	3	○
$\gamma$ -PGA140k-Phe-42 (10-0.2)	10	0.2	21.4 $\pm$ 0.4	0.30 $\pm$ 0.06	-27.5 $\pm$ 0.2	1060	4	○
$\gamma$ -PGA140k-Phe-42 (10-0.3)	10	0.3	30.3 $\pm$ 0.8	0.19 $\pm$ 0.03	-27.6 $\pm$ 0.6	1850	8	○
$\gamma$ -PGA140k-Phe-42 (10-0.4)	10	0.4	46.3 $\pm$ 2.3	0.20 $\pm$ 0.01	-27.0 $\pm$ 1.2	2730	12	○
$\gamma$ -PGA140k-Phe-42 (10-0.5)	10	0.5	61.4 $\pm$ 2.8	0.19 $\pm$ 0.03	-28.1 $\pm$ 1.5	<sup>g</sup> n.d.	n.d.	○.
$\gamma$ -PGA140k-Phe-46 (10-0)	10	0	9.8 $\pm$ 0.9	0.29 $\pm$ 0.06	-28.9 $\pm$ 1.9	297	1.2	○
$\gamma$ -PGA140k-Phe-58 (10-0)	10	0	18.7 $\pm$ 0.2	0.34 $\pm$ 0.01	-27.3 $\pm$ 2.9	4060	15	○
$\gamma$ -PGA140k-Phe-65 (10-0)	10	0	Aggregation	–	–	–	–	○

<sup>a</sup>  $\gamma$ -PGA140k-Phe dissolved in DMSO was mixed with NaCl aq. at the same volume. <sup>b</sup> The particle diameter and zeta potential was measured in PBS (1 mg/mL) by DLS and laser doppler velocimetry using a Zetasizer nano ZS. <sup>c</sup> PDI represents polydispersity index. <sup>d</sup> The  $M_w$  of  $\gamma$ -PGA-Phe in PBS was measured by SLS. <sup>e</sup> The number of  $\gamma$ -PGA-Phe aggregates ( $N_{agg}$ ) was calculated by the Measured  $M_w$  / Calculated  $M_w$ . <sup>f</sup> The formation of hydrophobic domains was detected by steady-state fluorescence measurement using pyrene as a probe. <sup>g</sup> n. d. means not determined.

In the case of  $\gamma$ -PGA140k-Phe-58 (10-0), the particle formation is attributed to inter-polymer rather than intra-polymer associations. In contrast, when  $\gamma$ -PGA140k-Phe-65 was mixed with pure water, large-sized aggregates were observed, and  $\gamma$ -PGA140k-Phe-65 (10-0) led to the formation of water-insoluble aggregates. In addition, the increase of temperature and the decrease of starting polymer concentration during synthesized process of high grafting degree  $\gamma$ -PGA140k-Phe-58 were also performed in order to achieve single chain state for sample having higher grafting degree of L-Phe. However,

it was observed that the particle size and the  $N_{agg}$  of samples did not show any big change when altering temperature as well as starting polymer concentration (**Table 1.5**). This is probably due to the sample having high grafting degree of L-Phe has a very strong hydrophobic interaction, thus inter-molecular associations favorably occurs, thereby single chain state could not be obtained for  $\gamma$ -PGA140k-Phe-58 even inducing by temperature or using low concentration.

**Table 1.5. Preparation of nanoparticles composed of  $\gamma$ -PGA140k-Phe-58 (calculated  $M_w = 273$  kDa) with the help of preparative conditions.**

Temperature (°C)	Polymer conc. in DMSO (mg/mL)	NaCl <sup>a</sup> (M)	Size (nm) <sup>b</sup>	PDI <sup>c</sup>	Measured $M_w$ (kDa) <sup>d</sup>	$N_{agg}$ <sup>e</sup>	Domain formation <sup>f</sup>
25	10	0.5	736±127	0.264	n.d. <sup>g</sup>	n.d.	n.d.
25	10	0.3	100±0.6	0.101	n.d.	n.d.	n.d.
25	10	0.1	38.6±0.1	0.211	n.d.	n.d.	n.d.
0	10	0	12.3±0.1	0.506	2890	11	○
25	10	0	14.3±0.2	0.319	3140	12	○
75	10	0	15.4±0.2	0.508	3600	13	○
0	5	0	11.0±0.8	0.816	3310	12	○
25	5	0	11.7±0.1	0.504	2990	11	○
75	5	0	14.4±0.5	0.288	2940	11	○
0	2.5	0	10.3±0.6	0.534	2780	10	○
25	2.5	0	10.4±0.4	0.625	2660	10	○
75	2.5	0	11.8±0.2	0.455	2640	10	○

<sup>a</sup>  $\gamma$ -PGA-Phe dissolved in DMSO (10 mg/mL) was mixed with indicated NaCl (aq) at the same volume. <sup>b</sup> The particle diameter and zeta potential were measured in PBS (1 mg/mL) by dynamic light scattering (DLS) and laser doppler velocimetry using a Zetasizer nano ZS. <sup>c</sup> PDI represents polydispersity index. <sup>d</sup> The  $M_w$  of  $\gamma$ -PGA-Phe in PBS was measured by SLS. <sup>e</sup> The number of  $\gamma$ -PGA-Phe aggregates ( $N_{agg}$ ) was calculated by the Measured  $M_w$  / Calculated  $M_w$ . <sup>f</sup> The formation of hydrophobic domains was detected by steady-state fluorescence measurement using pyrene as a probe. <sup>g</sup> n. d. means not determined.

Various types of amphiphilic copolymers have been synthesized, and their intra- and/or interpolymer associating behaviors have been widely investigated. However, there are few reports on self-assemblies of naturally occurring polymers and their derivatives. Akiyoshi *et al.* have intensively studied cholesterol bearing pullulans (CHP), which formed a monodispersed nanogel via intra- and/or interpolymer associations in aqueous solution.<sup>31</sup> CHP nanogels are self-assembled physical gels in which the association of hydrophobic cholesteryl groups provides physical cross-linking points. They reported that the size and polymer density of these nanogels can be controlled by changing the grafting degree of the cholesteryl groups.<sup>32</sup> However, the number of CHP aggregates in one particle was almost constant (about 10). Conventional self-assembly of amphiphilic copolymers in selective solvents occurs spontaneously. Thus, it is difficult to quantitatively control the  $N_{\text{agg}}$  of the resulting structures. Some groups have reported that the structure of polymer aggregates or the  $N_{\text{agg}}$  of micelles can be regulated by the self-assembly of block copolymers in a two or three dimensional confined space. Li *et al.* reported that the  $N_{\text{agg}}$  of micelles composed of poly(ethylene glycol)-*block*-poly(4-vinylpyridine) (PEG-*b*-P4VP) can be controlled by using a W/O inverse emulsion as an excellent isolated domain for the self-assembly of the polymer.<sup>33</sup> By tuning the size of the inverse emulsion droplet and the concentration of the block copolymer solution, the  $N_{\text{agg}}$  of micelles formed in water pools can be controlled. In the case of  $\gamma$ -PGA-Phe-42 (**Table 1.6, Figure 1.7**), the precise assembly of amphiphilic graft copolymers was effectively achieved without the use of any templates or closed spaces.

**Table 1.6. Characterization of  $\gamma$ -PGA-Phe nanoparticles prepared by dialysis method for  $\gamma$ -PGA-Phe-42**

Sample	NaCl <sup>a</sup> (M)	Size (nm) <sup>b</sup>	PDI <sup>c</sup>	Zeta potential (mV) <sup>b</sup>	Measured $M_w$ (kDa) <sup>d</sup>	$N_{agg}$ <sup>e</sup>	Domain formation <sup>f</sup>
$\gamma$ -PGA70k-Phe-42 (10-0)	0	12.7 ± 0.2	0.38 ± 0.06	-24.7 ± 0.3	381	3	○
$\gamma$ -PGA70k-Phe-42 (10-0.1)	0.1	30.3 ± 0.9	0.20 ± 0.01	-25.0 ± 1.8	4910	42	○
$\gamma$ -PGA70k-Phe-42 (10-0.3)	0.3	85.6 ± 0.7	0.18 ± 0.02	-29.8 ± 0.2	n.d. <sup>g</sup>	n.d.	○
$\gamma$ -PGA140k-Phe-42 (10-0)	0	9.8 ± 1.0	0.29 ± 0.02	-23.0 ± 1.8	343	1.5	○
$\gamma$ -PGA140k-Phe-42 (10-0.1)	0.1	16.3 ± 0.8	0.21 ± 0.04	-27.1 ± 1.8	608	3	○
$\gamma$ -PGA140k-Phe-42 (10-0.3)	0.3	30.3 ± 0.8	0.19 ± 0.03	-27.6 ± 0.6	1850	8	○
$\gamma$ -PGA140k-Phe-42 (10-0.5)	0.5	61.4 ± 2.8	0.19 ± 0.03	-28.1 ± 1.5	n.d.	n.d.	○
$\gamma$ -PGA220k-Phe-42 (10-0)	0	11.2 ± 0.7	0.31 ± 0.07	-27.2 ± 0.6	325	1	○
$\gamma$ -PGA220k-Phe-42 (10-0.1)	0.1	13.8 ± 2.2	0.35 ± 0.08	-27.3 ± 0.7	433	1.2	○
$\gamma$ -PGA220k-Phe-42 (10-0.3)	0.3	22.1 ± 1.1	0.37 ± 0.02	-27.5 ± 0.7	943	3	○

<sup>a</sup>  $\gamma$ -PGA-Phe dissolved in DMSO (10 mg/mL) was mixed with indicated NaCl (aq) at the same volume. <sup>b</sup> The particle diameter and zeta potential were measured in PBS (1 mg/mL) by dynamic light scattering (DLS) and laser doppler velocimetry using a Zetasizer nano ZS. <sup>c</sup> PDI represents polydispersity index. The results are presented as means ± SD (n=3). <sup>d</sup> The  $M_w$  of  $\gamma$ -PGA-Phe in PBS was measured by SLS. <sup>e</sup> The number of  $\gamma$ -PGA-Phe aggregates ( $N_{agg}$ ) was calculated by the Measured  $M_w$  / Calculated  $M_w$ . <sup>f</sup> The formation of hydrophobic domains was detected by steady-state fluorescence measurement using pyrene as a probe. <sup>g</sup> n. d. means not determined.

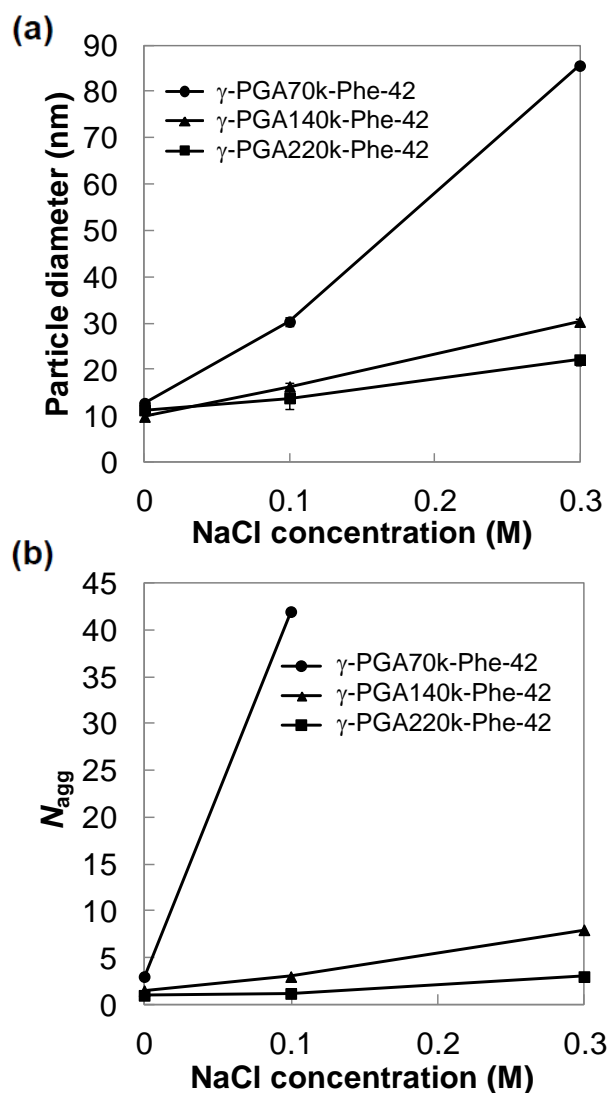


**Figure 1.7.**  $\gamma$ -PGA-Phe-42 nanoparticles using different  $M_w$  of  $\gamma$ -PGA prepared under various NaCl concentrations.  $\gamma$ -PGA-Phe-42 (10 mg/mL in DMSO) was added to the same volume of NaCl aqueous solution. The size of the nanoparticles was measured in PBS by DLS (a). And, the aggregation number ( $N_{agg}$ ) calculated from SLS was plotted against the NaCl concentration (b).

### *Detection of hydrophobic domains by Steady-State Fluorescence Measurements*

The obtained single chain state showing a  $N_{agg}$  of about 1 was then detected by the formation of hydrophobic associations using steady-state fluorescence measurements and pyrene as the probe in order to confirm whether the unimolecular  $\gamma$ -PGA-Phe had hydrophobic domains formed by the Phe attached to  $\gamma$ -PGA. It is well-established that in



aqueous solutions of amphiphilic polymers, pyrene is solubilized into hydrophobic domains, showing an increase in the ratio of the intensities of the third to first vibronic bands ( $I_3/I_1$ ) in the pyrene fluorescence spectra.<sup>34</sup> Thus, pyrene is a useful fluorescence probe for the characterization of molecular assemblies of associating polymers, and for the evaluation of the micropolarity of the local environment.<sup>35</sup> The example of the detection of hydrophobic domains using pyrene is shown in **Figure 1.8 and 1.9, left** which shows the steady-state fluorescence emission spectra of pyrene dissolved in PBS in the presence of  $\gamma$ -PGA140k-Phe at varying concentrations. In all fluorescent measurements, the concentration of pyrene was fixed at  $1 \times 10^{-6}$  M. Because the content of pyrene labels in these samples is very low, each pyrene label is isolated from others, thus exhibiting only monomeric fluorescence. As a result, the fluorescence intensity depended on the Phe grafting degree and the polymer concentration, indicating that the pyrene probes were solubilized in the polymer phases. In the case of low grafting degrees ( $\gamma$ -PGA140k,  $\gamma$ -PGA140k-Phe-12 and 27) in **Figure 1.8, left**, the fluorescence intensity was practically the same over the whole range of polymer concentrations studied. This may be attributed to weak interactions between the Phe groups attached to the  $\gamma$ -PGA backbone. In contrast, for  $\gamma$ -PGA140k-Phe-35 and 42 prepared by direct dispersion method as well as  $\gamma$ -PGA140k-Phe-42 prepared by dialysis method (**Figure 1.9, left**), the fluorescence intensity increased with increasing polymer concentration. This tendency was more significant for the higher grafting degrees.

The excitation spectra of pyrene were also measured in the presence of  $\gamma$ -PGA140k-Phe at varying concentrations. The excitation spectra showed peaks associated with the (0-0) band of pyrene at 335 nm in a low polymer concentration and the peak shifted to

338 nm at higher concentrations (**Figure 1.8 and 1.9, right**). It is known that the (0-0) band of the pyrene excitation spectra in water shifts to longer wavelengths when pyrene is solubilized in hydrophobic domains in a micelle.<sup>36,37</sup> Thus, the ratio of the intensity at 338 nm relative to that at 335 nm ( $I_{338}/I_{335}$ ) obtained from the excitation spectra of  $\gamma$ -PGA140k-Phe at various grafting degrees was plotted against the polymer concentration in **Figure 1.10** for nanoparticles prepared by direct dispersion method, and in **Figure 1.11** for nanoparticles prepared by dialysis method different in particle size. The  $I_{338}/I_{335}$  ratio exhibited a tendency to increase with the polymer concentration in the case of  $\gamma$ -PGA140k-Phe-35 and 42 prepared by direct dispersion method as well as  $\gamma$ -PGA140k-Phe-42 (10-0), (10-0.3) and (10-0.5) prepared by dialysis method. These results showed the same tendency as that obtained from emission spectra data. The results obtained from emission and the excitation spectra of pyrene indicate that  $\gamma$ -PGA140k-Phe-35 and 42 both preparative methods have hydrophobic nanodomains in aqueous solution, and that pyrene is solubilized into the domains of the associated Phe groups. These observations also suggest that the Phe grafting degree is critical to the association behavior of  $\gamma$ -PGA-Phe, and that  $\gamma$ -PGA140k-Phe-35, 42 and 42(10-0) can form unimer nanoparticles by the intrapolymer association of  $\gamma$ -PGA140k-Phe. By using this method, therefore, the formation of hydrophobic domains for all  $\gamma$ -PGA-Phe samples could be detected as summarized in **Table 1.3-1.5**. In addition, we also attempted to estimate an apparent critical aggregation concentration (CAC) of  $\gamma$ -PGA140k-Phe. Noda *et al.* reported that CAC value of a polymer aggregate, consisting of hydrophobic domains surrounded by charged segments, can be calculated from the steady-state fluorescence excitation spectra (**Figure 1.10 and 1.11**) for pyrene probes.<sup>35</sup> The CAC values of  $\gamma$ -PGA140k-Phe depended on the Phe grafting degree; for unimer nanoparticles  $\gamma$ -PGA140k-Phe-35, an

apparent CAC was 0.2 mg/mL, whereas for  $\gamma$ -PGA140k-Phe-42 and  $\gamma$ -PGA140k-Phe-42(10-0), it decreased to 0.09 mg/mL and 0.06 mg/mL, respectively.

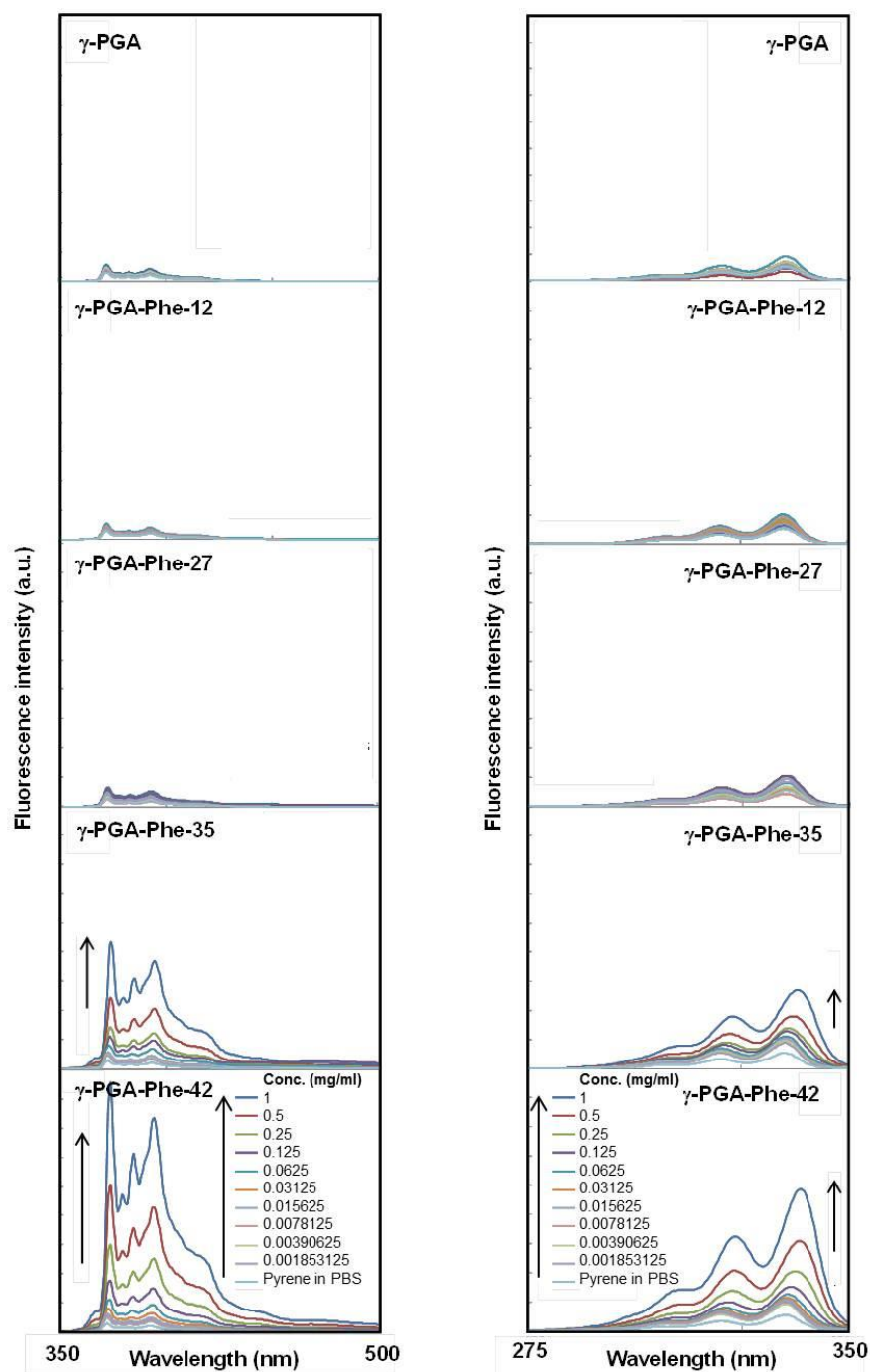


**Figure 1.8.** Steady-state fluorescence emission spectra (left) and excitation spectra (right) of pyrene ( $1 \times 10^{-6}$  M) of  $\gamma$ -PGA140k-Phe at various grafting degree of L-Phe in PBS in the presence of varying concentrations (0-1 mg/mL). The emission spectra and excitation spectra were monitored at 339 and 372 nm, respectively.

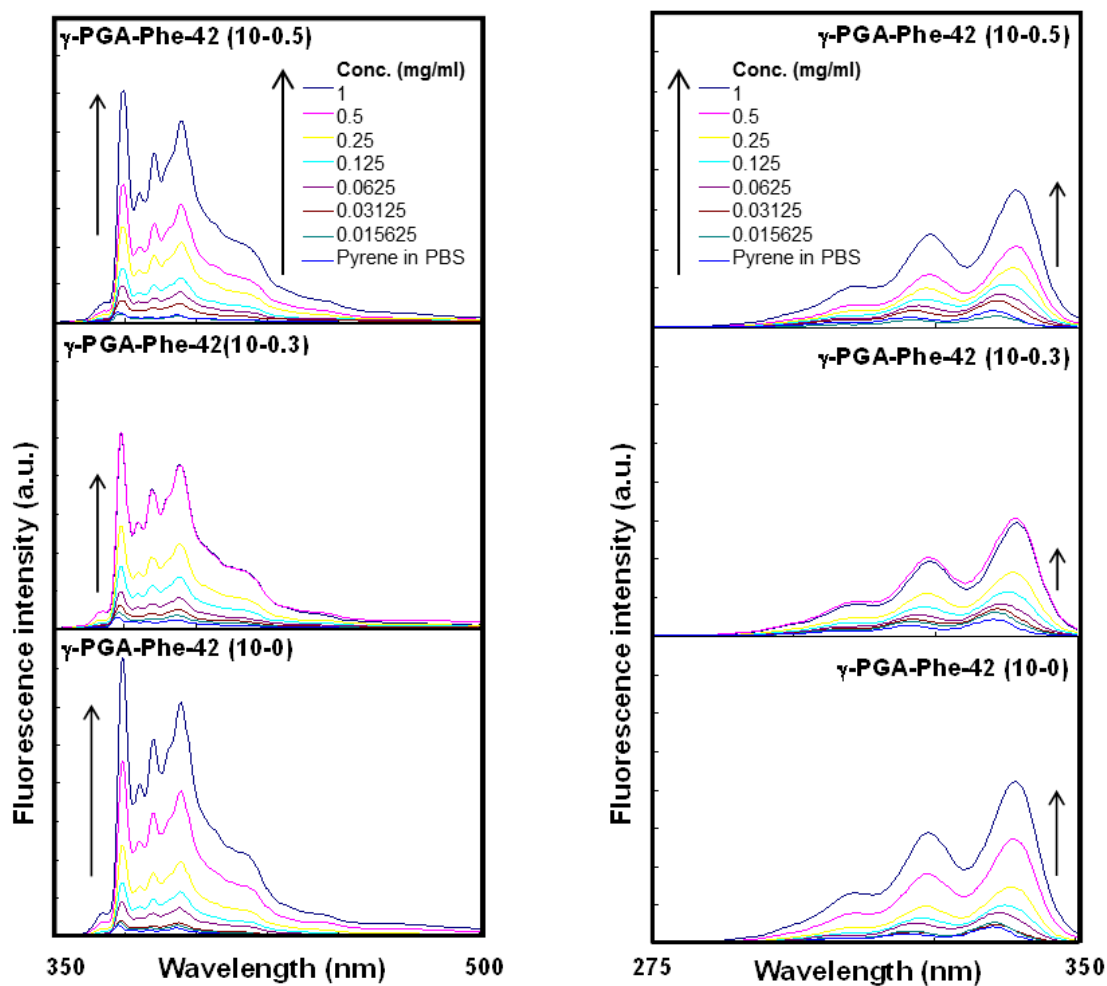


**Figure 1.9.** Steady-state fluorescence emission spectra (left) and excitation spectra (right) of pyrene ( $1 \times 10^{-6}$  M) of  $\gamma$ -PGA140k-Phe42 prepared by dialysis method dispersed in PBS in the presence of varying concentrations (0-1 mg/mL).

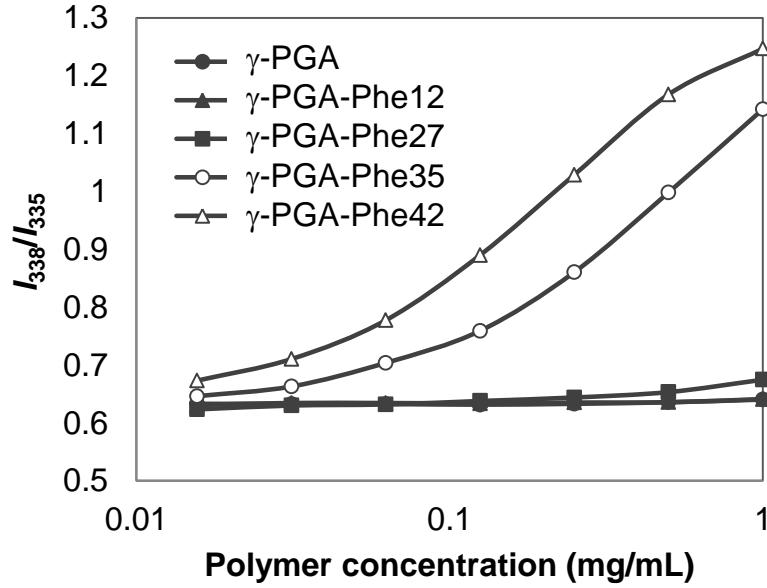


**Figure 1.10.** Intensity ratio  $I_{338}/I_{335}$  obtained from the fluorescence excitation spectra of pyrene plotted versus the  $\gamma$ -PGA140k-Phe concentration (0.015–1 mg/mL) for samples prepared by direct dispersion method showing the  $N_{agg}$  about 1.

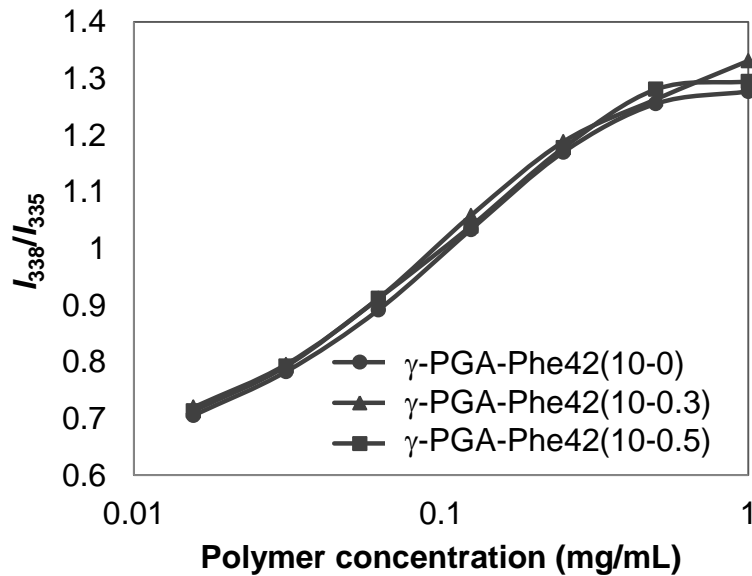


**Figure 1.11.** Intensity ratio  $I_{338}/I_{335}$  obtained from the fluorescence excitation spectra of pyrene plotted versus the  $\gamma$ -PGA140k-Phe concentration (0.015–1 mg/mL) for samples different particle sizes prepared by dialysis method.

### ***Formation of unimer nanoparticles***

For the effect of grafting degree of L-Phe and polymer chain length (or  $M_w$  of  $\gamma$ -PGA) prepared by both direct dispersion and dialysis methods, unimer nanoparticles could be formed by the hydrophobic association of L-Phe moieties intramolecularly when employing copolymers at grafting degrees higher than 27%, which was observed for concentrations at or below 1 mg/mL of polymer in PBS. With respect to the effect of the polymer chain length, it has been reported for some amphiphilic block/graft copolymers that inter-molecular associations occur preferentially for short polymer chains (low  $M_w$ ), whereas long polymer chains tend to self-assemble via intra-molecular associations.<sup>38</sup> Our results support these observations, suggesting that chain length is one of the important factors controlling the balance of molecular associations. Therefore, unimer nanoparticles formed by the intra-molecular association of the hydrophobic moieties of L-Phe could be obtained by the direct dispersion method when copolymers having long polymer chains (over 140 kDa) were modified with L-Phe grafting degree of 27-42%.

Moreover, as particle sizes were shown to be easily tailored by controlling the concentration of NaCl, in which the salinity of the solution can trigger polymer structures resulting in copolymer aggregates upon increasing the salt concentration. Thus, the synthesized copolymers with grafting degrees higher than 42, which could not be dissolved directly in PBS, were prepared using the dialysis method by altering the NaCl concentration during preparation. In the case of samples at a grafting degree of 42% ( $\gamma$ -PGA-Phe-42) using different  $M_w$  of  $\gamma$ -PGA as shown in **Table 1.6** and plotted in **Figure 1.7a**, the sizes of the  $\gamma$ -PGA-Phe nanoparticles could be efficiently controlled by employing this preparative method. However, in **Figure 1.7a and 1.7b**, it is clear that when employing high  $M_w$   $\gamma$ -PGA as a main chain, the particle size as well as the  $N_{agg}$

tended to increase slightly upon increasing the NaCl concentration, while those values obtained from low  $M_w$   $\gamma$ -PGA were significantly higher. This might be due to the fact that the NaCl solutions strongly affected the short polymer chain, resulting in the formation of nanoparticles by inter-molecular associations upon increasing the NaCl concentration. The addition of salt led to enhanced screening of the Coulomb interactions between the  $\gamma$ -PGA-Phe, resulting in an increased inter-molecular association of  $\gamma$ -PGA-Phe. Furthermore, in our study, unimer nanoparticles (a single chain state showing a  $N_{agg}$  of about 1) were easily obtained from samples prepared by mixing the polymer solution (10 mg/mL in DMSO) with low concentrations of NaCl (0 and/or 0.1 M). However, in copolymers with high grafting degrees of L-Phe (higher than 42%), the single chain state could not be obtained, even with mixing at very low concentrations of NaCl. This is probably due to the fact that the self-assembly of water-based copolymer systems is governed by a balance of ionic, steric and hydrophobic interactions, as well as the balance of intra- and inter-molecular associations as described by some researchers.<sup>14, 39</sup> Therefore, this suggests that the effect of the substitution degree is an important factor for balancing the hydrophilicity/hydrophobicity along the polymer chain, which can enable the formation of unimer nanoparticles composed of hydrophobically modified poly(amino acid)s. In addition, a higher  $M_w$   $\gamma$ -PGA (510 kDa) was also employed to study the formation of unimer nanoparticles, but a single chain state could not be obtained from either the direct dispersion or the dialysis method due to the poor solubility in aqueous solution as well as in PBS even at the low concentration (data not shown). This finding suggests that the optimal range for the  $M_w$   $\gamma$ -PGA main chain, which is also one of the critical factors for balancing intra- and inter-molecular

associations in order to readily obtain unimer nanoparticles, should be in a range of 140-220 kDa.

In general, an amphiphilic copolymer consisting of hydrophilic and hydrophobic segments is capable of forming polymeric structures in aqueous solutions via hydrophobic interactions. For the association of amphiphilic block copolymer in a selective solvent, a micelle is formed through interpolymer associations, because the single chain only has one associative segment. In contrast, a graft polymer has many side chains, and it can form a micelle with fewer chains or even a single polymer chain. Moreover, the intra- and interpolymer association of amphiphilic copolymers by self-assembly is affected by the nature of hydrophilic and hydrophobic segments, copolymer composition, and distribution sequence of the hydrophobic segments.<sup>40, 41</sup> Yamamoto *et al.* studied the intra- and interpolymer association of poly (sodium 2-(acrylamido)-2-methylpropanesulfonate-co-dodecylmethacrylamide) (AMPS-co-DodMAM), and found that the DodMAM content is critical to the association behavior of these copolymers.<sup>13</sup> Liu *et al.* also demonstrated that the self-association of poly(methacrylic acid) (PMAA)-*graft-n*-octylamine copolymer in water depended on the hydrophobe distribution sequences. In the case of a random amphiphilic graft copolymer, the polymer self-assembles and predominantly forms small aggregates of 1-2 polymer chains. In contrast, in the case of a multi-blocky type copolymer, the polymer associates intermolecularly as multiple well-defined polymer chain aggregates.<sup>42</sup> In this study, amphiphilic graft copolymers consisting of  $\gamma$ -PGA and Phe were employed. It is thought that the hydrophobic segments of L-Phe are randomly or blocky grafted to  $\gamma$ -PGA, but based on the results of the unimer nanoparticles formation, it is hypothesized that L-Phe is randomly introduced into a carboxylic group of  $\gamma$ -PGA. Thus, unimer nanoparticles



could be formed by the association of single polymer chains. According to the overall results (summarized in **Table 1.7**), by balance the hydrophobic–hydrophilic moieties in the polymer chain of amphiphilic graft copolymers, biodegradable  $\gamma$ -PGA-Phe unimer nanoparticles could be obtained when employing  $M_w$  of  $\gamma$ -PGA  $\geq 140$ kDa, and grafting degree of L-Phe about 27-42%.

**Table 1.7. Formation of  $\gamma$ -PGA-Phe unimer nanoparticles**

Sample	Grafting degree (%)	Formation of unimer NPs <sup>a</sup> by	
		Direct dispersion method	Dialysis method
$\gamma$ -PGA70k-Phe-12	12	X	n.d. <sup>b</sup>
$\gamma$ -PGA70k-Phe-27	27	X	n.d.
$\gamma$ -PGA70k-Phe-35	35	X	n.d.
$\gamma$ -PGA70k-Phe-42	42	X	X
$\gamma$ -PGA70k-Phe-50	50	X	X
$\gamma$ -PGA140k-Phe-12	12	X	n.d.
$\gamma$ -PGA140k-Phe-27	27	X	n.d.
$\gamma$ -PGA140k-Phe-35	35	○	n.d.
$\gamma$ -PGA140k-Phe-42	42	○	○
$\gamma$ -PGA140k-Phe-58	58	X	X
$\gamma$ -PGA220k-Phe-12	12	X	n.d.
$\gamma$ -PGA220k-Phe-27	27	○	n.d.
$\gamma$ -PGA220k-Phe-35	35	○	n.d.
$\gamma$ -PGA220k-Phe-42	42	○	○
$\gamma$ -PGA220k-Phe-55	55	X	X

<sup>a</sup> ○ = formation of unimer nanoparticles, X = Not formed unimer nanoparticles, <sup>b</sup> n. d. means not determined.

### ***Structure of unimer nanoparticles***

Further evidence for unimer nanoparticles formation of  $\gamma$ -PGA140k-Phe was obtained with  $^1\text{H}$  NMR spectroscopy using  $\text{DMSO-}d_6$  and  $\text{D}_2\text{O}$ , as shown in **Figure 1.12**. NMR can be employed to study the structure of polymeric nanoparticles, especially for core-shell type particles.<sup>43, 44</sup> Since both  $\gamma$ -PGA and L-Phe are easily dissolved in  $\text{DMSO-}d_6$  and exist in a liquid state, particle formation is not expected. The characteristic peaks of  $\gamma$ -PGA and L-Phe was shown in  $\text{DMSO-}d_6$  (**Figure 1.12b**). However, as shown in **Figure 1.12a**, the characteristic NMR peaks of  $\gamma$ -PGA-Phe disappeared completely using  $\text{D}_2\text{O}$ . These results indicate that the protons of  $\gamma$ -PGA-Phe displayed restricted motions, and have a solid-like structure. In general, in the case of core-shell type micelles composed of amphiphilic block copolymers, the signal of the hydrophilic outer shell is detected in the spectra of the micelles, which indicates that the hydrophilic segment is in an extended solvated state. In contrast, the signal of the hydrophobic inner core is not seen due to the rigid solid structure of the hydrophobic core. In this experiment, the NMR peaks of the hydrophilic  $\gamma$ -PGA segments were not detected using  $\text{D}_2\text{O}$ , implying that the structure of unimer nanoparticles consisting of  $\gamma$ -PGA-Phe is not a definite core-shell type. Unlike amphiphilic block copolymers, these  $\gamma$ -PGA-Phe graft copolymers have a very short hydrophobic segment. Therefore, it implied that the core of the nanoparticles might be formed not only by L-Phe, but also by the  $\gamma$ -PGA of the main chain. The unimer nanoparticles also showed a negative zeta potential in PBS (**Table 1.3**). This could be attributed to the presence of ionized carboxyl groups from the  $\gamma$ -PGA on the nanoparticle surfaces. The zeta potential can influence the particle stability and

dispersibility. Electrostatic repulsion between particles with the same electric charge prevents any aggregation of these particles.

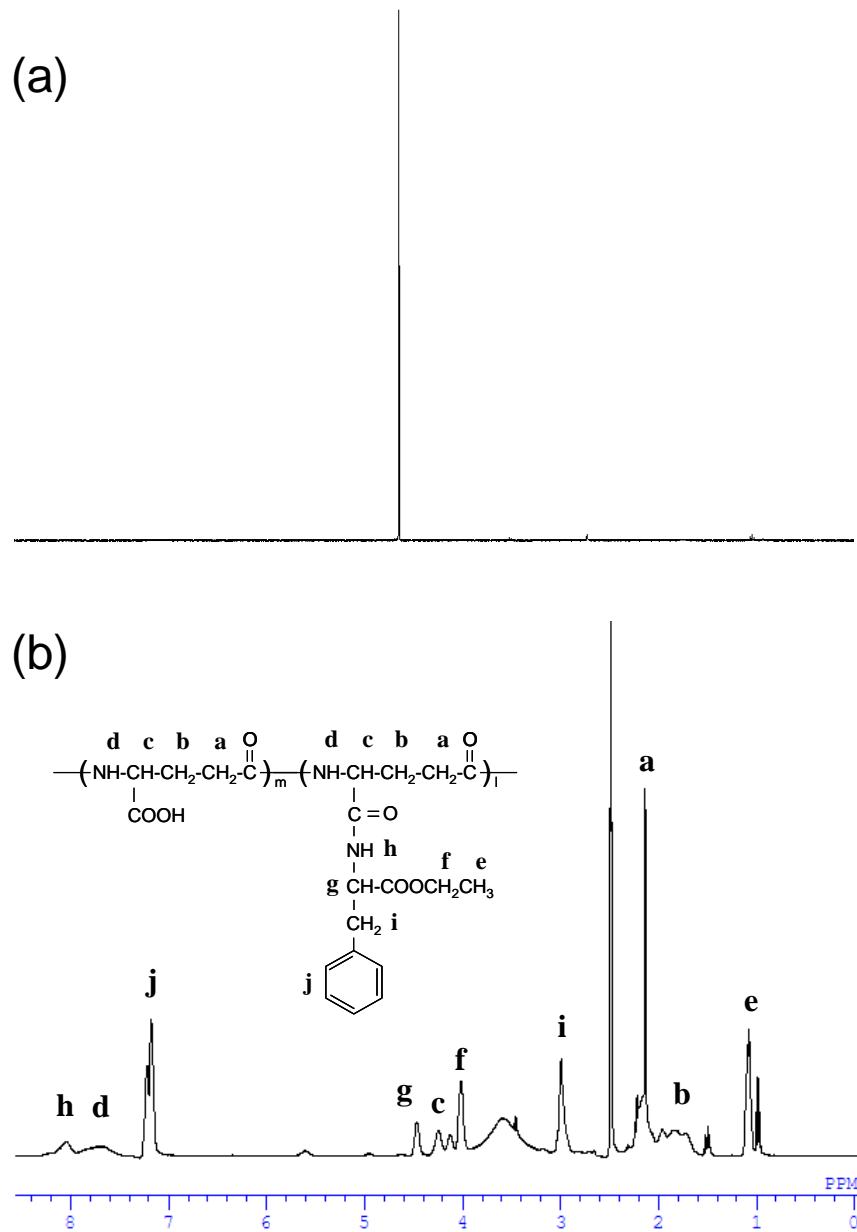


**Figure 1.12.**  $^1\text{H}$  NMR spectra of  $\gamma$ -PGA140k-Phe-35 dissolved in  $\text{D}_2\text{O}$  (a) and dispersed in  $\text{DMSO-}d_6$  (b).

### ***Stability of unimer nanoparticles***

The influence of the polymer concentration on the size of the  $\gamma$ -PGA140k-Phe nanoparticles is shown in **Figure 1.13**. It was observed that the size of unimer nanoparticles ( $\gamma$ -PGA-Phe-35, 42, 42 (10-0)) and nanoparticles ( $\gamma$ -PGA-Phe-42 (10-0.1), (10-0.3)) in PBS was constant over a concentration of 0.01-10 mg/mL. In contrast,  $\gamma$ -PGA-Phe-12 and 27 showed that the samples tended to aggregate at high polymer concentrations (data not shown).  $\gamma$ -PGA-Phe of a low grafting degree showed concentration-dependent aggregation behavior. These results suggest that the stability of the nanoparticles is affected by the hydrophobicity of the  $\gamma$ -PGA-Phe and by the formation of hydrophobic domains. Furthermore, a change in the size of unimer nanoparticles ( $\gamma$ -PGA-Phe-42, 42(10-0) and 46(10-0)) in PBS as a function of time was not observed for 30 days (**Figure 1.14**). These nanoparticles showed high stability over a wide range of polymer concentrations and times of incubation. The formation of hydrophobic domains by the intra- or interpolymer associations of  $\gamma$ -PGA-Phe was important for the stability of these nanoparticles.

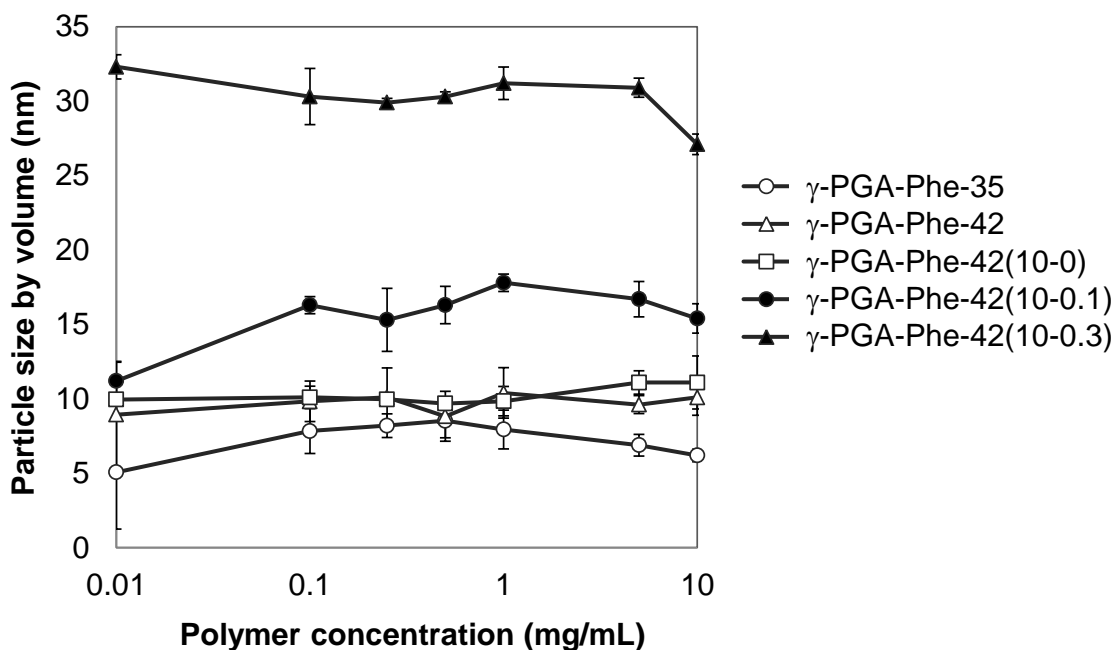


**Figure 1.13.** Changes in the size of the unimer nanoparticles as a function of the polymer concentration.  $\gamma$ -PGA140k-Phe of various grafting degrees was dispersed in PBS at the desired concentration (from 0.01 to 10 mg/mL). The particle sizes were measured by DLS for each polymer concentration.

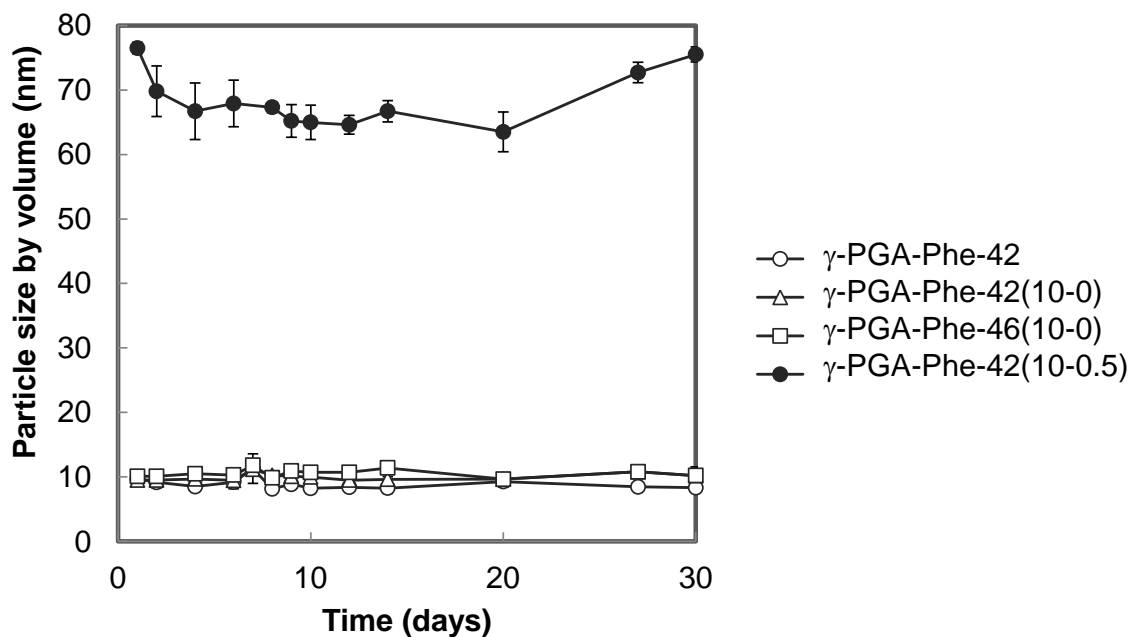


**Figure 1.14.** Changes in the size of the unimer nanoparticles as a function of the incubation time.  $\gamma$ -PGA140k-Phe of various grafting degrees was dispersed in PBS at 1 mg/mL, and then stored at 4°C. At different time intervals, the size of the nanoparticles was measured by DLS.

#### 1.4. Conclusion

Amphiphilic copolymers are capable of self-assembly into nanoscale structures in selective solvents. It is found that the self-association of amphiphilic copolymers can occur within a single polymer chain, among many polymer chains, or through both mechanisms. These nano/microstructures have been widely studied from both fundamental and technological aspects, because they can be used in the field of drug delivery. The present study focused on the preparation and characterization of unimer nanoparticles composed of biodegradable  $\gamma$ -PGA-Phe. We prepared  $\gamma$ -PGA-Phe unimer nanoparticles by tuning the hydrophilic-hydrophobic balance of the graft copolymers. As the effects of the  $M_w$  of the initial polymers ( $M_w$  of  $\gamma$ -PGA 70, 140 and 220 kDa) and the grafting degree of the hydrophobic parts along the polymer chains were investigated for the formation of unimer nanoparticles in aqueous solutions. A key step in controlling the aggregation number for the formation of unimer nanoparticles is to balance the hydrophobic-hydrophilic moieties in the polymer chain with the help of preparative methods in dilute conditions, in which salinity is one factor that can induce self-assembly. It has been reported that intra-molecular associations occur more favorably for high  $M_w$  main chains. Therefore, when employing  $M_w$  of  $\gamma$ -PGA higher than 140 kDa with grafting degrees of L-Phe ranging 27-42%, the unimer state (a single chain with an aggregation number of about 1) with hydrophobic domains detected by steady-state fluorescence measurements could be obtained. In addition, the  $N_{agg}$  of  $\gamma$ -PGA-Phe-42, including its unimolecular state, could be controlled by changing the salt concentration added to the  $\gamma$ -PGA-Phe-42 dissolved in DMSO. An increased salt concentration induced interpolymer associations of  $\gamma$ -PGA-Phe, resulting in an increased particle size. The dispersibility and stability of the  $\gamma$ -PGA-Phe were significantly enhanced by the

formation of a hydrophobic domain via intra- and interpolymer associations. This study revealed that  $\gamma$ -PGA-Phe has the unique characteristic to form unimer nanoparticles with a hydrophobic domain at their core. Unimer nanoparticles have a large surface area as compared to larger-sized particles. These particles will provide a new medium for particle design in drug delivery systems. Further studies include the structural analysis of the hydrophobic domains in detail and its application as a drug carrier for cancer therapy.

## References

1. A. Choucair and A. Eisenberga, *Eur. Phys. J. E* **10**, 37 (2003).
2. C. Cai, J. Lin, T. Chen and X. Tian, *Langmuir* **26**, 2791 (2010).
3. S. J. Holder, N. A. J. M. Sommerdijk, *Polym. Chem.* **2**, 1018 (2011).
4. G. Gaucher, M. H. Dufresne, V. P. Sant, N. Kang, D. Maysinger and J. C. Leroux, *J. Control. Release* **109**, 169 (2005).
5. K. Letchford and H. Burt, *Eur. J. Pharm. Biopharm.* **65**, 259 (2007).
6. N. Nishiyama and K. Kataoka, *Adv. Polym. Sci.* **193**, 67 (2006).
7. Y. Morishima, S. Nomura, T. Ikeda, M. Seki and M. Kamachi, *Macromolecules* **28**, 2874 (1995).
8. W. Liu, R. Liu, Y. Li, H. Kang, D. Shen, M. Wu and Y. Huang, *Polymer* **50**, 211 (2009).
9. J. Hao, Z. Li, H. Cheng, C. Wu and C. C. Han, *Macromolecules* **43**, 9534 (2010).

10. Q. Qiu, A. Lou, P. Somasundaran and B. A. Pethica, *Langmuir* **18**, 5921 (2002).
11. Y. Chang and C. L. McCormick, *Macromolecules* **26**, 6121 (1993).
12. M. H. Siu, C. He and C. Wu, *Macromolecules* **36**, 6588 (2003).
13. H. Yamamoto and Y. Morishima, *Macromolecules* **32**, 7469 (1999).
14. S. Yusa, A. Sakakibara, T. Yamamoto and Y. Morishima, *Macromolecules* **35**, 5243 (2002).
15. S. Yusa, A. Sakakibara, T. Yamamoto and Y. Morishima, *Macromolecules* **35**, 10182 (2002).
16. A. Kikuchi and T. Nose, *Macromolecules* **29**, 6770 (1996).
17. A. Kikuchi and T. Nose, *Polymer* **37**, 5889 (1996).
18. M. Matsusaki, K. Hiwatari, M. Higashi, T. Kaneko and M. Akashi, *Chem. Lett.* **33**, 398 (2004).
19. T. Akagi, T. Kaneko, T. Kida and M. Akashi, *J. Controlled Release* **108**, 226 (2005).
20. T. Akagi, X. Wang, T. Uto, M. Baba and M. Akashi, *Biomaterials* **28**, 3427 (2007).
21. T. Akagi, M. Baba and M. Akashi, *Polymer* **48**, 6729 (2007).
22. H. Kim, T. Akagi and M. Akashi, *Macromol. Biosci.* **9**, 842 (2009).
23. H. Kim, T. Uto, T. Akagi, M. Baba and M. Akashi, *Adv. Funct. Mater.* **20**, 3925 (2010).
24. T. Akagi, F. Shima and M. Akashi, *Biomaterials* **32**, 4959 (2011).



25. T. Uto, T. Akagi, K. Yoshinaga, M. Toyama, M. Akashi and M. Baba, *Biomaterials* **32**, 5206 (2011).
26. I. L. Shih and Y. T. Van, *Bioresour. Technol.* **79**, 207 (2001).
27. T. Akagi, M. Higashi, T. Kaneko, T. Kida and M. Akashi, *Biomacromolecules* **7**, 297 (2006).
28. H. Morinaga, H. Morikawa, Y. Wang, A. Sudo and T. Endo, *Macromolecules* **42**, 2229 (2009).
29. A. Choucair, C. Lavigueur and A. Eisenberg, *Langmuir* **20**, 3894 (2004).
30. C. Giacomelli, V. Schmidt, K. Aissou and R. Borsali, *Langmuir* **26**, 15734 (2010).
31. K. Akiyoshi, S. Deguchi, N. Moriguchi, S. Yamaguchi and J. Sunamoto, *Macromolecules* **26**, 3062 (1993).
32. K. Akiyoshi, S. Deguchi, H. Tajima, T. Nishikawa and J. Sunamoto, *Macromolecules* **30**, 857 (1997).
33. Y. Li, R. Ma, L. Zhao, Q. Tao, D. Xiong, Y. An and L. Shi, *Langmuir* **25**, 2757 (2009).
34. K. P. Ananthapadmanabhan, E. D. Goddard, N. J. Turro and P. L. Kuo, *Langmuir* **1**, 352 (1985).
35. T. Noda and Y. Morishima, *Macromolecules* **32**, 4631 (1999).
36. M. Wilhelm, C. L. Zhao, Y. Wang, R. Xu and M. A. Winnik, *Macromolecules* **24**, 1033 (1991).

37. I. Astafieva, X. F. Zhong and A. Eisenberg, *Macromolecules* **26**, 7339 (1993).
38. Y. Zhou, K. Jiang, Q. Song and S. Liu, *Langmuir* **23**, 13076 (2007).
39. O. V. Borisov, E. B. Zhulina, F. A. M. Leermakers and A. H. E. Müller, *Adv. Polym. Sci.* **241**, 57 (2011).
40. H. S. Kang, S. R. Yang, J. D. Kim, S. H. Han and I. S. Chang, *Langmuir* **17**, 7501 (2001).
41. T. Kawata, A. Hashidzume and T. Sato, *Macromolecules* **40**, 1174 (2007).
42. R. C. W. Liu, A. Pallier, M. Brestaz, N. Pantoustier and C. Tribet, *Macromolecules* **40**, 4276 (2007).
43. J. G. Ryu, Y. I. Jeong, I. S. Kim, J. H. Lee, J. W. Nah, S. H. Kim, *Int. J. Pharm.* **2**, 231 (2000).
44. Y. Zhang, Q. Zhang, L. Zha, W. Yang, C. Wang, X. Jiang and S. Fu, *Colloid Polym. Sci.* **282**, 1323 (2004).

## *Chapter 2*

### **Structure analysis of $\gamma$ -PGA-Phe unimer nanoparticles**

#### **2.1. Introduction**

The synthesis of polymeric nanoparticles with controlled characteristics has become an appealing research topic lately. Nano-medicine, especially, drug delivery and imaging, are fields that required particles with controlled size and a tailored arrangement of functional groups. Polymeric amphiphiles such as amphiphilic diblock or triblock copolymers, hydrophobically modified water-soluble polymers and graft copolymers are able to spontaneously form micelles/nanoparticles through inter- or intra-molecular associations during which drug molecules are incorporated.<sup>1-4</sup> Due to the fact that self-assembled polymeric nanoparticles have many advantages as highly-efficient drug delivery vehicles, including their nanoscale size, controlled composition and capacity to encapsulate a wide range of drug molecules.

The unique physical properties of amphiphilic random polymers result in a myriad of potential applications. Recently, linear polymers were grafted with non-covalent interacting groups under selected conditions, and resulted in folding of single the polymeric chains in terms of single chain polymeric nanoparticles.<sup>1, 5-8</sup> Furthermore, there has been growing research on the methods to control the single chain state, which are mainly performed under dilute conditions, for example, the photo-induced folding of polymer chain<sup>9, 10</sup> as well as collapse via heating on thermo-responsive polymers.<sup>11</sup> However, those methods required complex synthesis approaches to achieve single polymeric nanoparticles. In contrast, simpler methods to control the folding, such as via

hydrophobic interactions, have been investigated over the past decade.<sup>12, 13</sup> Among them, a few studies have focused on their application as carriers in drug delivery systems.

In a previous study, nanoparticles composed of hydrophobically modified poly( $\gamma$ -glutamic acid) ( $\gamma$ -PGA) by intra-/inter-molecular association in aqueous solution were prepared.<sup>14</sup> By employing hydrophobic moieties of L-phenylalanine (L-Phe) grafted onto  $\gamma$ -PGA main chains, nanoparticles can be easily prepared, and the size can be controlled by altering the preparative conditions. And, a single polymer of  $\gamma$ -PGA-*graft*-L-Phe ( $\gamma$ -PGA-Phe) formed 10-nm sized nanoparticles driven by the intra-molecular associations of the hydrophobic groups of L-Phe by controlling the hydrophobicity/hydrophilicity of the polymer chain as mentioned in Chapter 1. By changing the particle size, it is possible to control the degradation and release behavior after loading with cargo. Furthermore, the large surface area per volume ratio means that smaller nanoparticles are capable of conjugating with drugs on their surface more efficiently than large-sized nanoparticles, and hence these unimer nanoparticles are promising biomaterials for drug delivery.<sup>15</sup> However, the physical structure of these nanoparticles may affect their utility and applications.<sup>16-18</sup> Moreover, it is noted that the release pharmacokinetics of drugs from polymeric systems are dependent on the drug loading contents and the chain length of the hydrophobic/hydrophilic part of the copolymers and inner structures.<sup>19</sup> Therefore, in this chapter, the size and shape of the obtained  $\gamma$ -PGA-Phe unimer nanoparticles formed in aqueous solution were further investigated by scanning electron microscope (SEM), transmission electron microscope (TEM), and small-angle neutron scattering (SANS) measurement. An estimation of the number of hydrophobic domains in one particle and the flexibility/rigidity of their internal structures was also performed by steady-state

fluorescent measurement using cetylpyridinium chloride (CPC) and dipyrene as the quencher and fluorescent probe, respectively. In addition, the effects of pH on the size of unimer nanoparticle as well as their inner structure were also examined (**Figure 2.1**).

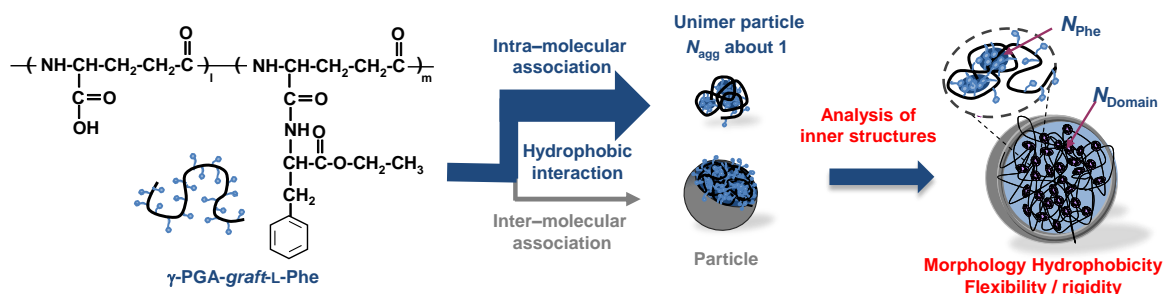


**Figure 2.1.** Illustration of structural analysis of unimer nanoparticles

## 2.2. Experimental section

### *Materials*

Pyrene served as a fluorescence probe, and Cetylpyridinium chloride monohydrate (CPC) as a quencher, were both from Wako Pure. Chemical, Ltd. (Japan). 1,3-bis-(1-pyrenyl)propane (dipyrene) was purchased from Molecular Probes (Invitrogen®) (Eugene, OR, USA). Water was purified with a Direct-Q system (Millipore, Co.). All other chemicals used were of analytical grade.

### *Synthesis of $\gamma$ -PGA-graft-L-Phe copolymers and preparation of unimer nanoparticles*

The obtained  $\gamma$ -PGA-Phe unimer nanoparticles were employed according to synthesis of  $\gamma$ -PGA-graft-L-Phe copolymers and preparation of unimer nanoparticles in Chapter 1.

### ***Scanning electron microscope (SEM)***

The morphology of the  $\gamma$ -PGA-Phe unimer nanoparticles and large-sized nanoparticles were first observed by scanning electron microscopy (SEM). Sample was prepared by dropping a dispersion of the unimer nanoparticles;  $\gamma$ -PGA-Phe-42,  $\gamma$ -PGA-Phe-42 (10-0) and  $\gamma$ -PGA-Phe-46 (10-0) and large-sized nanoparticles;  $\gamma$ -PGA-Phe-58 (10-0) and  $\gamma$ -PGA-Phe-65 (10-0) on SEM state (all samples used polymer concentration at 0.25 mg/ml of PBS). The sample was coated by osmium ( $O_4$ ) before SEM observation. SEM was performed using JEOL JSM-6701F.

### ***Transmission electron microscopy (TEM)***

The morphology of the  $\gamma$ -PGA-Phe unimer nanoparticles was observed by transmission electron microscopy (TEM) (JEOL JES-100CX-S1) at 100 kV. A drop of the nanoparticle suspension was placed on a copper grid coated with formvar. After drying, the unimer samples  $\gamma$ -PGA140k-Phe-42(10-0) were stained with  $RuO_4$  vapor.

### ***Structural analysis of unimer nanoparticles by Small-angle neutron scattering (SANS)***

Unimer nanoparticles  $\gamma$ -PGA140k-Phe-42(10-0) prepared by the dialysis method were dispersed in deuterated PBS before SANS measurements. The SANS measurements were performed by SANS-U of Institute for Solid State Physics, The University of Tokyo, Tokai, Japan. The neutron wavelength was 7.0 Å. Sample solutions (2 mg/mL) were measured in quartz cells (Nippon Silica Glass Co., Tokyo) with a pass length of 4

mm. The sample to detector distance was chose to be 2 and 8. The data were transformed to absolute intensities using a Lupolen standard. From all scattering data of samples, the scattering of solvent and the calculated incoherent scattering of the polymer were subtracted. The SANS data were described by the theoretical form factor of a core-shell model.<sup>20, 21</sup>

### ***Steady-state fluorescence quenching techniques***

First, steady-state fluorescence measurements using pyrene as a probe were carried out to monitor the formation of hydrophobic domains in nanoparticles. Unimer nanoparticles dispersed in PBS were added to a pyrene film formed by drying a pyrene solution ( $1 \times 10^{-4}$  M in ethanol), and the fluorescence intensity of pyrene containing unimer nanoparticles was detected after incubation for 24 h. By varying the concentration of the polymer in PBS, the formation of hydrophobic domains could be observed from their concentration-dependence.<sup>22</sup> Next, a CPC solution which served as a quencher for the fluorescence quenching techniques was added into the nanoparticles solution at the desired concentration before fluorescence measurement using excitation at 339 nm. The decrease in the fluorescence intensities ( $I_1$ ) correlated to the fluorescence intensity before quenching ( $I_0$ ) can be plotted against the CPC concentrations. The plot gives a straight line where the number of L-Phe in one hydrophobic domain ( $N_{\text{Phe}}$ ) and the number of hydrophobic domains in one particle ( $N_{\text{Domain}}$ ) can be calculated from the slope using quenching kinetic equations. The detail of experiment is mentioned as follow.<sup>23, 24</sup>

The sample solutions were prepared by dissolving a certain amount of polymer in a vial which pyrene thin film was in existence. Next, the sample solutions were allowed to stand for 1 day before measurement. Emission spectra of pyrene were measured at room temperature with excitation at 339 nm. An aqueous solution of CPC was prepared at a certain concentration. Then, the CPC solution was added just before measurement. From the quenching kinetics (equation 1), the plots of  $\ln(I_0/I)$  against the CPC concentration [Q] gives a straight line, the slope of the plot corresponds to  $[M]^{-1}$  and thus the total number of L-Phe ( $N_{\text{Phe}}$ ) and the total number of domains ( $N_{\text{Domain}}$ ) can be calculated by equation 2 and 3 respectively.

$$\ln\left(\frac{I_0}{I}\right) = \left(\frac{Q}{M}\right) \quad \text{Equation (1)}$$

$$N_{\text{Phe}} = \left(\frac{\text{Phe}}{M}\right) \quad \text{Equation (2)}$$

$$N_{\text{domain}} = \frac{\sum N_{\text{Phe}}}{N_{\text{Phe}}} \quad \text{Equation (3)}$$

Where;  $I_0$  and  $I$  = fluorescence intensity in the absence and presence of CPC respectively.

[Q] = concentration of CPC (M)

[M] = concentration of hydrophobic domains (M)

[Phe] = concentration of Phenylalanine (M)



The total number of Phe (unit) could be calculated from grafting degree of L-Phe per one polymer chain. Therefore,  $\Sigma N_{\text{Phe}}$  could be calculated from multiple of the total number of Phe (unit/chain) and the total number of polymer chain assembly in one nanoparticle. And thus,  $N_{\text{Domain}}$  and  $N_{\text{Phe}}$  could be obtained from equation 3 and equation 2, respectively.

### *Evaluation of inner core flexibility/rigidity of unimer nanoparticles by fluorescence measurement*

The flexibility/rigidity of the inner structure of the nanoparticles was evaluated by the fluorescence spectroscopy of 1,3-bis(1-pyrenyl)propane (dipyrene).<sup>25</sup> A dipyrene solution dispersed in acetone was prepared ( $2.2 \times 10^{-7}$  M). Next, a thin dipyrene film was prepared and added into a solution of unimer nanoparticles dispersed in PBS. The samples were incubated for 24 h before measurement. For the fluorescent measurements with dipyrene, the wavelength of excitation was fixed at 333 nm. From the emission spectra, the fluorescent intensity ratios between 480 nm (excimer complex) and 398 nm (pyrene monomer) were measured and calculated when the polymer concentration was 0.5 mg/mL. The value of the fluorescent intensity ratio ( $I_{480}/I_{398}$ ) of all unimer nanoparticles with different  $M_w$  as well as differing preparative method are shown in **Table 2.3**.

### *The effect of pH on the stability of unimer nanoparticles*

Unimer nanoparticles ( $\gamma$ -PGA140k-Phe-46(10-0)) were dispersed separately into 100 mM buffer solutions of pH 3-10 (pH 3-5: citrate; pH 6-8: phosphate; pH 9-10:

carbonate) at 1 mg/mL to test the pH stability of the particle size, as well as the changes in their inner structures. The particle size of the sample at different pH values was measured by DLS. To monitor the formation of hydrophobic domains in the unimer nanoparticles at various buffer solutions, unimer nanoparticles at each pH step were added into a pyrene film solution (the nanoparticle concentrations varied in the range 0.001-1 mg/mL) to observe the formation of the hydrophobic domains. In addition, the fluorescence quenching technique using CPC as the quencher was performed in order to detect the changes in the inner structures upon changing the pH conditions. In the experiment, nanoparticles (1 mg/mL) were first suspended in a buffer (pH 7), and the buffer was adjusted to pH 10 by NaOH, followed by adding HCl in order to lower the pH from pH 10 to pH 7 again. At each step, a sample was collected to monitor the fluorescence intensities. Furthermore, the effects of salt concentration, temperature and with or without serum on the size of the  $\gamma$ -PGA-Phe-46(10-0) unimer nanoparticles were investigated with various dispersion media. The nanoparticles (1 mg/mL) were suspended in 1 ml of NaCl concentrations (0 and 0.15M) at 4, 37 or 60°C and culture medium containing 10% fetal bovine serum (FBS). After 1 day incubation, the size of the nanoparticles was measured by DLS.

### **2.3. Results and Discussion**

#### *Scanning electron microscope (SEM)*

SEM images in **Figure 2.2** showed nanoparticles at various grafting degree. Average particle size of  $\gamma$ -PGA140k-Phe-58 (10-0) and  $\gamma$ -PGA140k-Phe-65 (10-0) observed by

SEM were about 25 nm and 55 nm respectively, which agree well with particle size measured by DLS. However, in case of unimer samples;  $\gamma$ -PGA140k-Phe-42,  $\gamma$ -PGA140k-Phe-42 (10-0) and  $\gamma$ -PGA140k-Phe-46 (10-0), average particle size around 10 nm could not be observed by SEM. The smallest particle sizes which could be observed by SEM with width of 3 mm (high resolution) were around 25 nm.

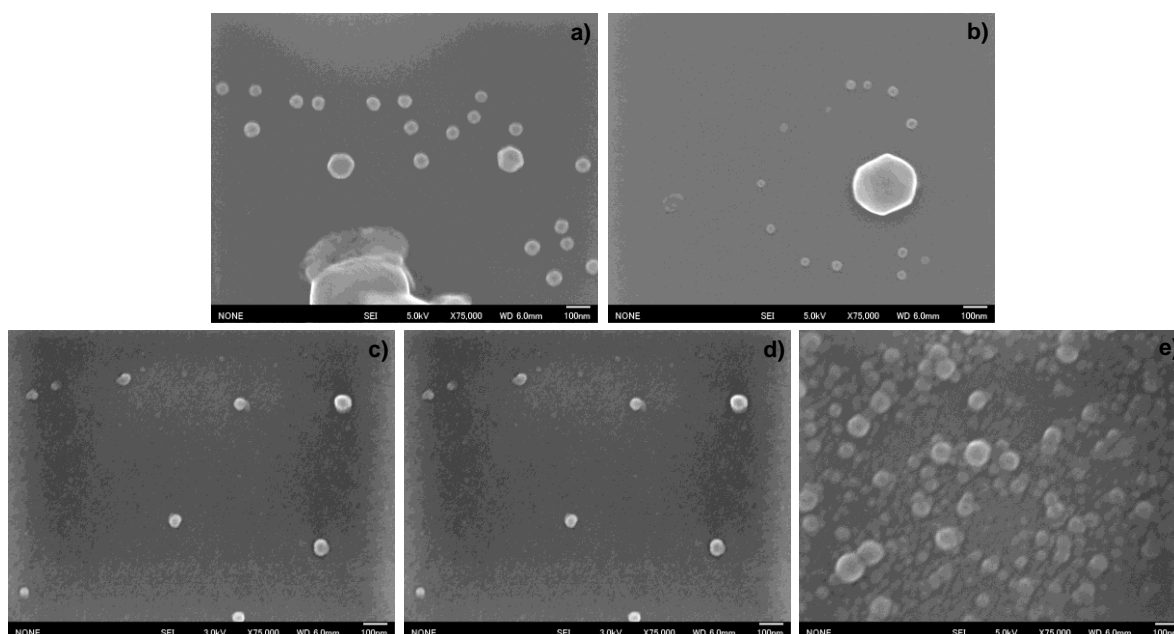


**Figure 2.2.** SEM images of nanoparticles concentration at 0.25 mg/ml of PBS; (a)  $\gamma$ -PGA140k-Phe-42, (b)  $\gamma$ -PGA140k-Phe-42 (10-0), (c)  $\gamma$ -PGA140k-Phe-46 (10-0), (d)  $\gamma$ -PGA140k-Phe-58 (10-0) and (e)  $\gamma$ -PGA140k-Phe-65 (10-0), magnification of 75000 with width length of 6 mm.

### ***Transmission electron microscope (TEM)***

In order to observe the morphology of unimer nanoparticles, TEM observation was performed. TEM observations demonstrated that the unimer nanoparticles were spherical

in shape (**Figure 2.3**). The particle sizes of the nanoparticles observed by TEM (average size:  $7.9 \pm 2.2$  nm) were in agreement with the results of the DLS measurements.

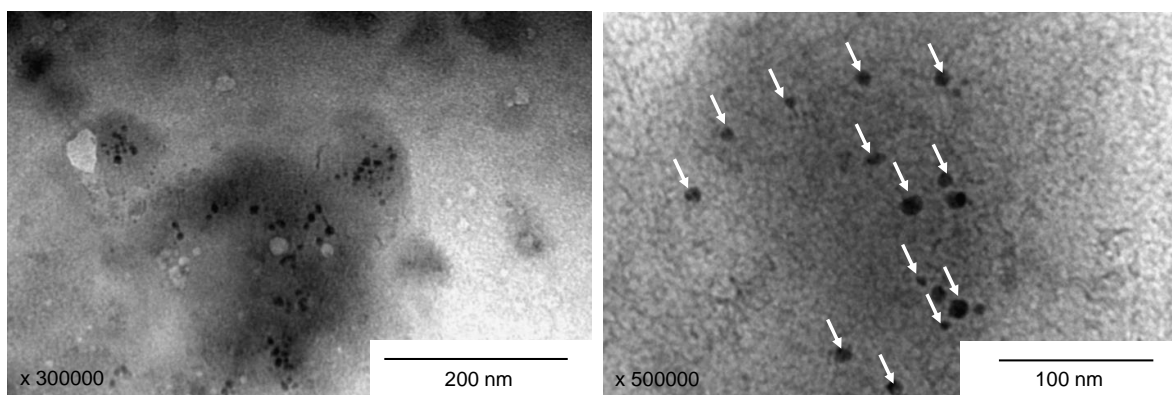


**Figure 2.3.** TEM images of unimer nanoparticles composed of  $\gamma$ -PGA140k-Phe-42. The samples were stained with  $\text{RuO}_4$ .

### *Structural analysis of unimer nanoparticles by small-angle neutron scattering (SANS)*

The molecular weight, the relative block length and the chemical nature of the repeating units in an amphiphilic copolymer constitute the morphology of the self-assembled system. To confirm the formation of unimer nanoparticles and to study their structure, SANS measurements were performed. Unimer nanoparticles  $\gamma$ -PGA140k-Phe-42(10-0) prepared by the dialysis method were dispersed in deuterated PBS. The results of the SANS measurement confirmed the presence of a single polymer chain ( $N_{\text{agg}}$  about 1) with a diameter of about 20 nm, which is consistent with the  $N_{\text{agg}}$  calculated from SLS. Furthermore, the SANS data described by the theoretical form factor of a core-shell model and the Pedersen core-corona model also revealed that the obtained unimer nanoparticles self-assembled into a core-shell structure, where the hydrophobic segments aggregated to form the inner core and the hydrophilic segments oriented towards the

outer aqueous environments. The SANS profiles of  $\gamma$ -PGA140k-Phe-42(10-0) using a PBS-D<sub>2</sub>O solution is shown in **Figure 2.4** (spot ●). The dash line is a fitting curve generated by a simple core-shell model and the Pedersen model.

Moreover,  $\gamma$ -PGA140k-Phe copolymers with high grafting degrees as well as large-sized nanoparticles were measured by SANS as well. The obtained results demonstrated the self-assembly of various sized of nanoparticles into unimer nanoparticles, forming a core-shell structure as shown in **Figure 2.5** and **Figure 2.6**.

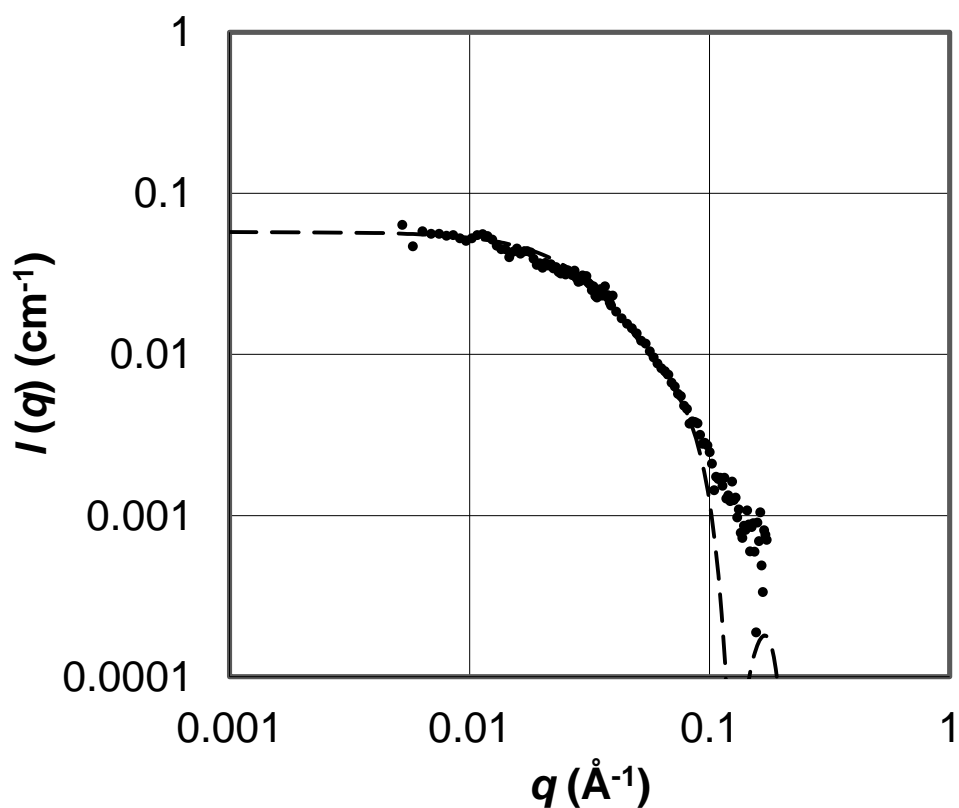


**Figure 2.4.** Small-angle neutron scattering (SANS) profiles for  $\gamma$ -PGA140k-Phe-42(10-0) using a PBS-D<sub>2</sub>O solution (spot ●). The dash line (---) is the fitting curve derived from a simple core-shell model and the Pedersen model.

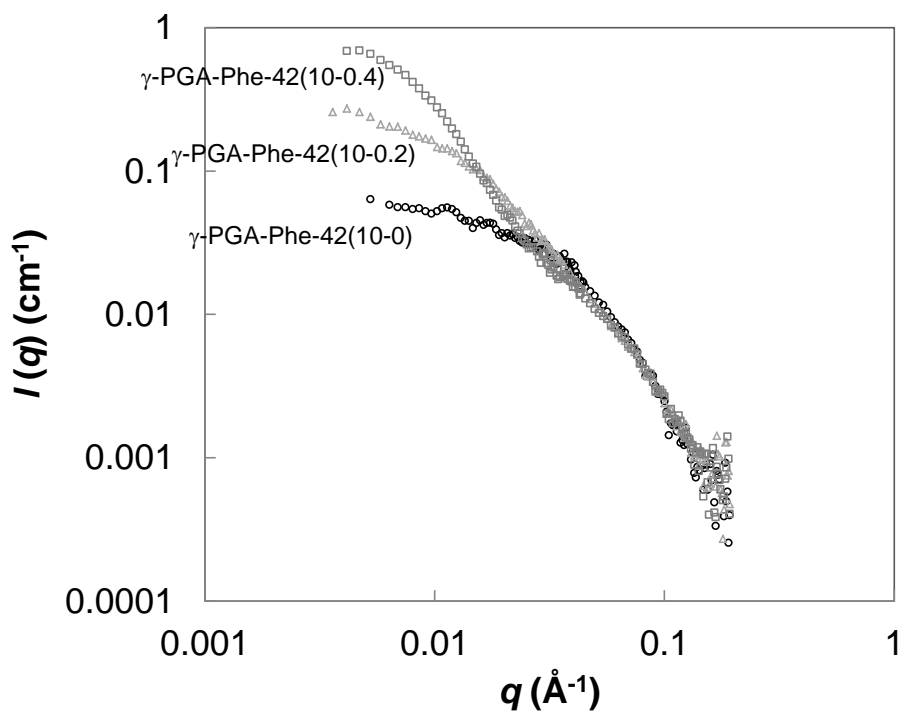


**Figure 2.5.** Small-angle neutron scattering (SANS) profiles for  $\gamma$ -PGA140k-Phe-42, prepared by dialysis method different NaCl concentrations, dissolved in a PBS-D<sub>2</sub>O solution.

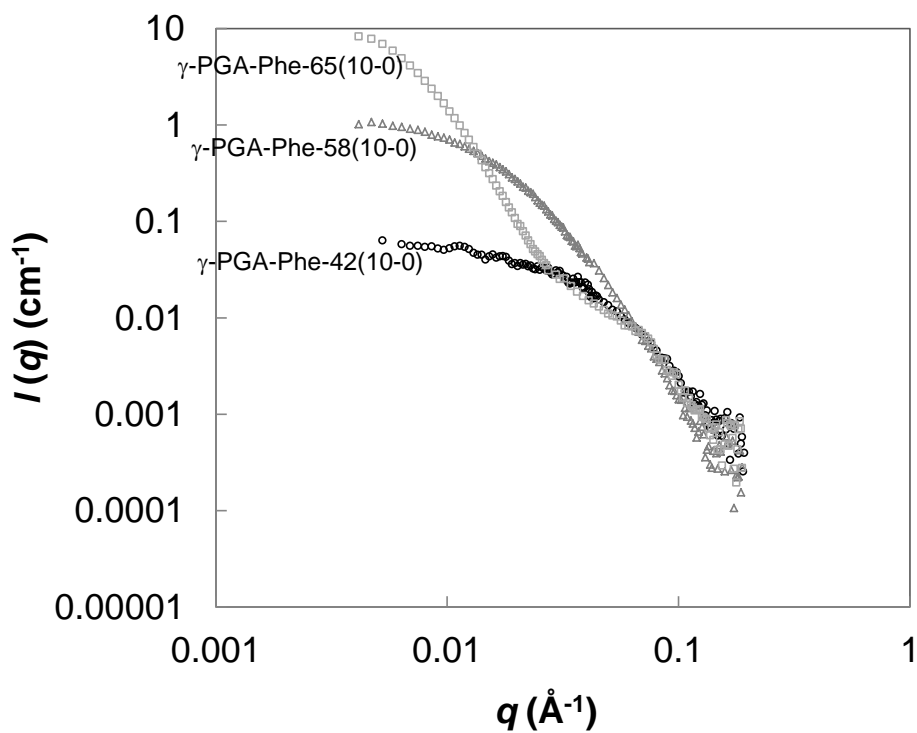


**Figure 2.6.** Small-angle neutron scattering (SANS) profiles for  $\gamma$ -PGA140k-Phe, prepared by dialysis method different grafting degree, dissolved in PBS-D<sub>2</sub>O solution.

## *Evaluation of internal structures of unimer nanoparticles by fluorescence measurements*

### *Hydrophobicity*

The fluorescence quenching technique using CPC as a quencher was performed to evaluate the hydrophobicity of the inner particles represented by the total number of hydrophobic domains in one nanoparticle ( $N_{\text{Domain}}$ ), as well as the number of L-Phe moieties in one domain ( $N_{\text{Phe}}$ ). The plots of the  $\ln(I_0/I)$  against the quencher concentration  $[\text{CPC}] \times 10^{-5}$  M for  $\gamma$ -PGA140k-Phe at various grafting degree, particle size as well as preparative methods, gave a straight line with the intercept at 0, as shown by the example in **Figure 2.7** and summarized in **Figure 2.8**. From the slope, the mean association number of L-Phe in one domain,  $N_{\text{Phe}}$ , could be estimated. The calculated  $N_{\text{Phe}}$  and  $N_{\text{Domain}}$  values for all samples are listed in **Table 2.1**. According to our results, the obtained  $N_{\text{Phe}}$  ranged from 100-200 L-Phe moieties per one hydrophobic domain. Moreover,  $N_{\text{Domain}}$  values ranged from 3 to 7. In the case of unimer nanoparticles with a  $N_{\text{agg}}$  of about 1, it was found that the  $N_{\text{Domain}}$  increased slightly with increasing grafting degree, as well as the particle size by volume. In contrast, large-sized nanoparticles at a grafting degree of 42% prepared by the dialysis method showed that the  $N_{\text{Domain}}$  significantly increased upon increasing the particle size, owing to the higher amount of aggregation in one nanoparticle (**Table 2.2**), implying that unimer nanoparticles having a larger volume tended to show a lower density of L-Phe aggregation. Thus, these results indicated that the  $N_{\text{Domain}}$  depends on the particle size, as well as the grafting degree of L-Phe. Interestingly, in **Table 2.2** it was clearly observed that  $N_{\text{domain}}$  per volume (density) of nanoparticles  $\gamma$ -PGA140k-Phe-42 prepared by dialysis method increased with

decreasing particle size as well as the  $N_{agg}$ . Therefore, 10-nm unimer nanoparticles showed higher in density of  $N_{domain}$  per volume than large-sized nanoparticles.

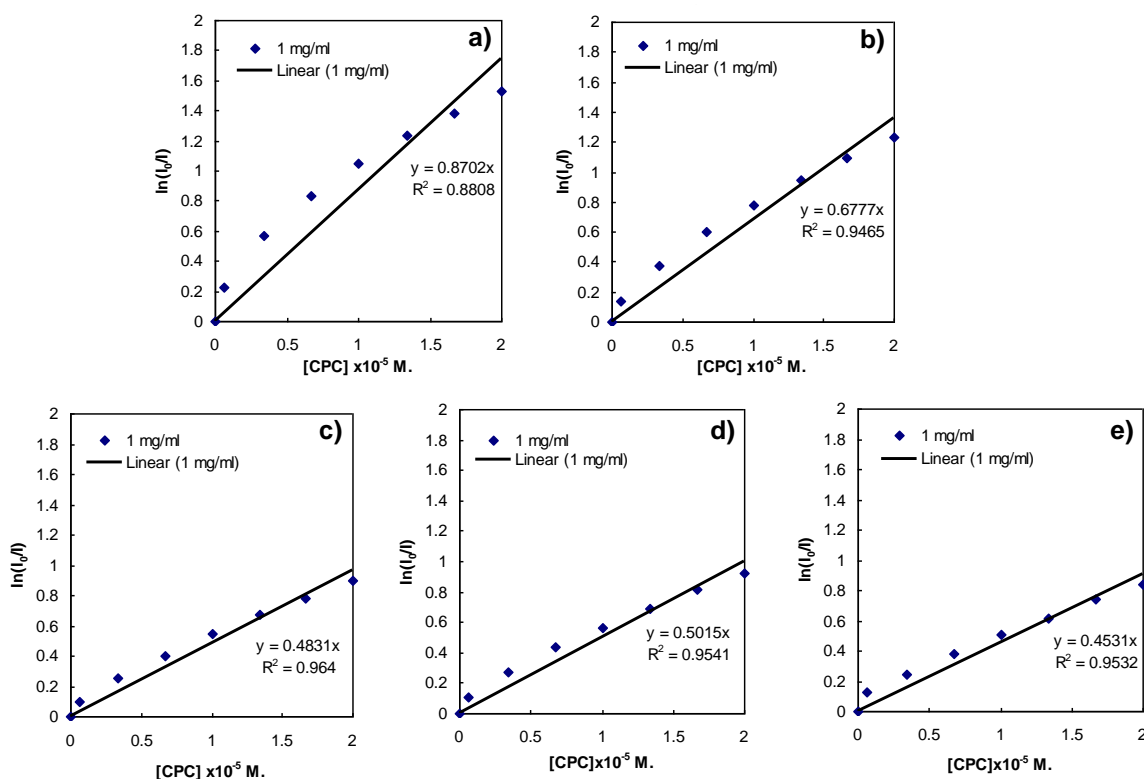


**Figure 2.7.**  $\ln(I_0/I)$  of pyrene fluorescence as a function of the CPC concentration in the presence of (a)  $\gamma$ -PGA140k-Phe-35, (b)  $\gamma$ -PGA140k-Phe-42, (c)  $\gamma$ -PGA140k-Phe-42(10-0), (d)  $\gamma$ -PGA140k-Phe-42(10-0.3), and (e)  $\gamma$ -PGA140k-Phe-42(10-0.5).  $[Py] = 1 \times 10^{-6}$  M. Linear are best fits of equation 2 to the data.

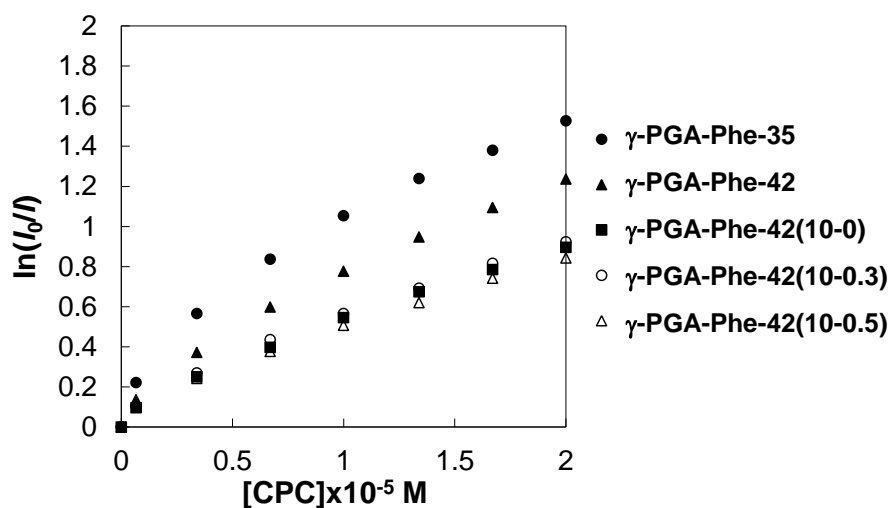


**Figure 2.8.**  $\ln(I_0/I)$  of pyrene fluorescence as a function of the CPC concentration in the presence of  $\gamma$ -PGA140-Phe at various grafting degree, particle size as well as preparative methods,  $[Py] = 1 \times 10^{-6}$  M.



**Table 2.1. Hydrophobicity of unimer nanoparticles measured by fluorescence techniques**

Unimer nanoparticles	$N_{agg}$	Size (nm)	$N_{Phe}^a$	$N_{Domain}^a$	Volume <sup>b</sup> (nm <sup>3</sup> )	$N_{Domain}/Volume$ (nm <sup>3</sup> )
$\gamma$ -PGA140k-Phe-35	1.3	7.9 $\pm$ 1.3	150	3.3	258	1.2 x 10 <sup>-2</sup>
$\gamma$ -PGA140k-Phe-42	1.3	9.7 $\pm$ 0.5	127	4.4	478	9.2 x 10 <sup>-3</sup>
$\gamma$ -PGA140k-Phe-42(10-0)	1.4	9.8 $\pm$ 1.0	96	7	493	1.4 x 10 <sup>-2</sup>
$\gamma$ -PGA220k-Phe-27	1.4	10.2 $\pm$ 1.0	220	2.9	556	5.2 x 10 <sup>-3</sup>
$\gamma$ -PGA220k-Phe-35	1.0	10.0 $\pm$ 2.2	193	2.2	524	4.2 x 10 <sup>-3</sup>
$\gamma$ -PGA220k-Phe-42	1.1	9.5 $\pm$ 0.2	169	4.6	449	1.0 x 10 <sup>-2</sup>
$\gamma$ -PGA220k-Phe-42(10-0)	1.0	10.3 $\pm$ 0.2	139	5	572	8.7 x 10 <sup>-3</sup>

<sup>a</sup> $N_{domain}$  and  $N_{Phe}$  were calculated from quenching kinetic equation. <sup>b</sup>Volume = 4/3 $\pi$ r<sup>3</sup>.

**Table 2.2. Hydrophobicity of nanoparticles measured by fluorescence techniques**

Nanoparticles	$N_{agg}$	Size (nm)	$N_{Phe}^a$	$N_{Domain}^a$	Volume <sup>b</sup> (nm <sup>3</sup> )	$N_{Domain}/Volume$ (nm <sup>3</sup> )
$\gamma$ -PGA140k-Phe-35	1.3	7.9 $\pm$ 1.3	150	3.3	258	1.2 x 10 <sup>-2</sup>
$\gamma$ -PGA140k-Phe-42	1.3	9.7 $\pm$ 0.5	127	4.4	478	9.2 x 10 <sup>-3</sup>
$\gamma$ -PGA140k-Phe-42(10-0)	1.4	9.8 $\pm$ 1.0	96	7	493	1.4 x 10 <sup>-2</sup>
$\gamma$ -PGA140k-Phe-42(10-0.3)	8	30.3 $\pm$ 0.8	99	38	14566	2.6 x 10 <sup>-3</sup>
$\gamma$ -PGA140k-Phe-42(10-0.5)	23	61.4 $\pm$ 2.8	90	122	121200	1.0 x 10 <sup>-3</sup>

<sup>a</sup> $N_{domain}$  and  $N_{Phe}$  were calculated from quenching kinetic equation. <sup>b</sup>Volume = 4/3 $\pi$ r<sup>3</sup>.

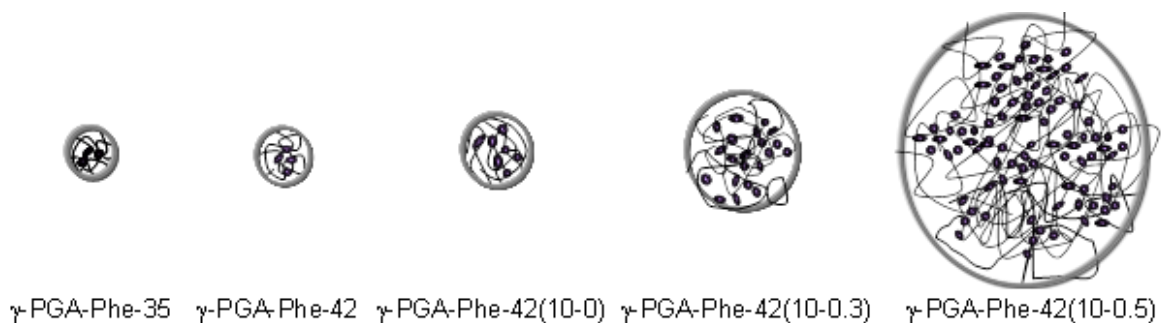


**Figure 2.9.** Illustration of  $N_{\text{domain}}$  and  $N_{\text{Phe}}$  for unimer nanoparticles;  $\gamma$ -PGA140k-Phe-35, 42 and 42(10-0) and large-sized NPs;  $\gamma$ -PGA140k-Phe-42(10-0.3) and 42(10-0.5).

### *Flexibility/Rigidity*

In general, the stability of drug-conjugated nanoparticles can be defined in several ways, for example the number/distribution of hydrophobic domains, as well as the drug release profile. Herein, the inner structure of unimer nanoparticles was studied by considering the flexibility/rigidity of the inner core, since it has been reported that the flexibility/rigidity of the interior is also one of the factors that relate to the stability of drug incorporation. The rigidity of the inner structure of the nanoparticles was evaluated by fluorescence spectroscopy using dipyrrene, which quantifies the flexibility/rigidity by the fluorescent intensity ratio between the excimer complex and the monomer ( $I_{480}/I_{398}$ ) (**Figure 2.10**). This is because dipyrrene forms an intramolecular excimer complex if the environment surrounding the probe has low rigidity. Therefore, when the inner-core rigidity decreases (flexibility increases), the value of the fluorescent intensity ratio between the excimer complex to the monomer increases.<sup>25</sup> **Table 2.3** summarizes the fluorescent intensity ratios at  $I_{480}/I_{398}$ . All measurements were conducted at 0.1 mg/mL polymer concentration. When unimer nanoparticles with the same  $M_w$  of  $\gamma$ -PGA were

compared, it was found that the unimer nanoparticles prepared by the dialysis method ( $\gamma$ -PGA-Phe-42(10-0)) had much more rigid inner cores than unimer nanoparticles prepared by directly dissolving the sample ( $\gamma$ -PGA-Phe-35 and  $\gamma$ -PGA-Phe-42). The same phenomenon was observed for both  $\gamma$ -PGA 140 kDa and 220 kDa. This is due to the fact that the freeze-drying process can completely remove water from a material while leaving the structure and composition intact, thus resulting in close-packed internal structures. According to the results of the flexibility/rigidity tests, the lyophilization-treated samples showed the most rigidity in the inner core, significantly higher than that of the non-lyophilized ones, implying that the stability of drug-conjugated unimer nanoparticles prepared by the dialysis method should be more stable. However, this hypothesis does require further study for confirmation. In addition, the fluorescent intensity ratios at  $I_{480}/I_{398}$  for  $\gamma$ -PGA-Phe nanoparticles diameter of 10, 65, 130 and 200 nm were 0.21, 0.10, 0.05 and 0.02 respectively. Thus, unimer nanoparticles show higher flexibility of inner core over than large-sized nanoparticles. These results suggested that the flexibility/rigidity of the inner core was also strongly affected by the particle size (**Table 2.4**).

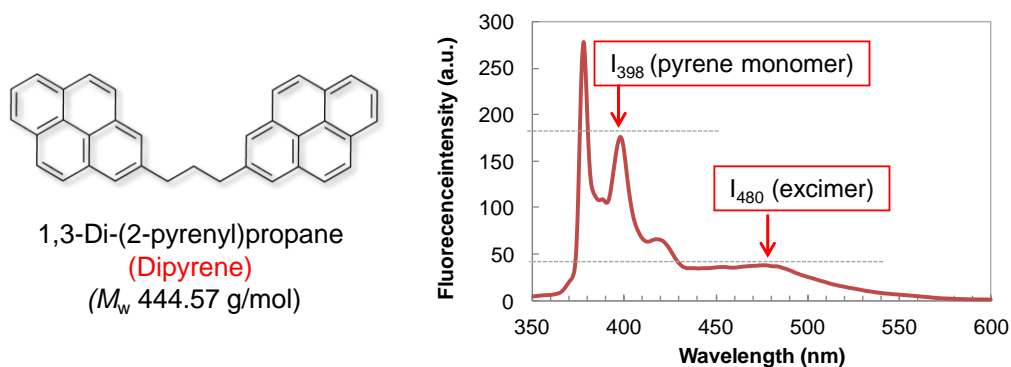


**Figure 2.10.** Chemical structure of dipyrene and the plot of fluorescence intensity of excimer to pyrene monomer ( $I_{480}/I_{398}$  of dipyrene emission).

**Table 2.3. Flexibility/rigidity of unimer nanoparticles**

Unimer nanoparticles	$N_{agg}$	Size (nm)	$I_{480}/I_{398}$ of dipyrene emission <sup>a</sup>
$\gamma$ -PGA140k-Phe-35	1.3	7.9 $\pm$ 1.3	0.44
$\gamma$ -PGA140k-Phe-42	1.3	9.7 $\pm$ 0.5	0.46
$\gamma$ -PGA140k-Phe-42(10-0)	1.4	9.8 $\pm$ 1.0	0.21
$\gamma$ -PGA220k-Phe-27	1.4	10.2 $\pm$ 1.0	0.39
$\gamma$ -PGA220k-Phe-35	1.0	10.0 $\pm$ 2.2	0.46
$\gamma$ -PGA220k-Phe-42	1.1	9.5 $\pm$ 0.2	0.24
$\gamma$ -PGA220k-Phe-42(10-0)	1.0	10.3 $\pm$ 0.2	0.08

<sup>a</sup>  $I_{480}/I_{398}$  represented the inner flexibility/rigidity, samples were conducted at 0.1 mg/mL of PBS.

**Table 2.4. Flexibility/rigidity of  $\gamma$ -PGA-Phe nanoparticles different size**

Particle size of $\gamma$ -PGA-Phe	$I_{480}/I_{398}$ of dipyrene emission <sup>a</sup>
10 nm (Unimer nanoparticles)	0.21
65 nm	0.10
130 nm	0.05
200 nm	0.02

<sup>a</sup>  $I_{480}/I_{398}$  represented the inner flexibility/rigidity, samples were conducted at 0.1 mg/mL of PBS.

### *Effect of pH on the stability of unimer nanoparticles*

To investigate the effect of pH, salt concentration, temperature and with or without serum on the size of the  $\gamma$ -PGA140k-Phe-46(10-0) unimer nanoparticles, the nanoparticles (1 mg/mL) were suspended in buffers of varying pH values (pH 3–10), NaCl concentration (0–0.15M) at 4, 37 or 60°C and culture medium containing 10% FBS. The particle size did not change at pH 5–10 (**Figure 2.11**), NaCl concentration 0–0.15 M at 4, 37 or 60°C, and in the presence of serum (data not shown), but the particles formed aggregates below pH 4. The formation of aggregate was due to the ionization of the carboxyl groups of  $\gamma$ -PGA located near the surfaces. In addition, these  $\gamma$ -PGA-Phe nanoparticles had high stability for the freeze-drying process. The lyophilized nanoparticles were easily re-dispersed, and the size and structure of the nanoparticles showed no change in initial particles as compared to before freeze-drying.

It should be noted that the formation of hydrophobic domains by the intra- or inter-molecular associations of  $\gamma$ -PGA-Phe is important for maintaining the stability of unimer nanoparticles. Therefore, we further examined the effect of pH by focusing on the stability of the internal structure of unimer nanoparticles using fluorescence techniques. To this end, unimer nanoparticles were suspended in buffers at different pH values (pH 5–10). The concentration-dependence was observed for all samples in all buffer solutions (pH 5–10) after detection of hydrophobic domains by steady-state fluorescence measurements (**Figure 2.12**), indicating that unimer nanoparticles could form hydrophobic domains over pH 5–10. Interestingly, as shown in **Figure 2.13**, a decrease in the fluorescence intensities of the unimer samples (1 mg/mL in PBS) upon increasing the pH was observed, implying a change in the internal structures under these pH

conditions. This was attributed to salinity of the solution can trigger abrupt structural rearrangements of the copolymer aggregates.<sup>26</sup> However, in order to clarify the changes in the inner structure, the number of hydrophobic domains ( $N_{\text{Domain}}$ ) was further investigated by steady-state quenching techniques. It revealed that the  $N_{\text{Domain}}$  at pH was about 7, but the  $N_{\text{Domain}}$  at pH 7 and pH 9 were 4 and 2, respectively. As a result, the gradual decrease in the  $N_{\text{Domain}}$  upon increasing the pH supported and correlated well with the reduction in the fluorescence intensities in **Figure 2.13**.

For further clarification, the change in the inner structure upon changing the pH was detected by monitoring the  $N_{\text{Domain}}$  while adjusting the pH using NaOH and HCl. It was observed that the fluorescent intensity at pH 7 only decreased after adjusting and returning to pH 10 again, implying that the inner hydrophobic domains were changed under alkaline condition. In a previous study, the cleavage of the ester bond in L-Phe (ethyl ester part) occurred under pH 9-10 with longer incubation times have been reported.<sup>27</sup> In the manner, therefore after adjusting the sample to a basic pH, the hydrolysis of the ester bonds occurred, resulting in a loose packing of the inner structures and change in the fluorescent intensity features of the sample (**Figure 2.14**).

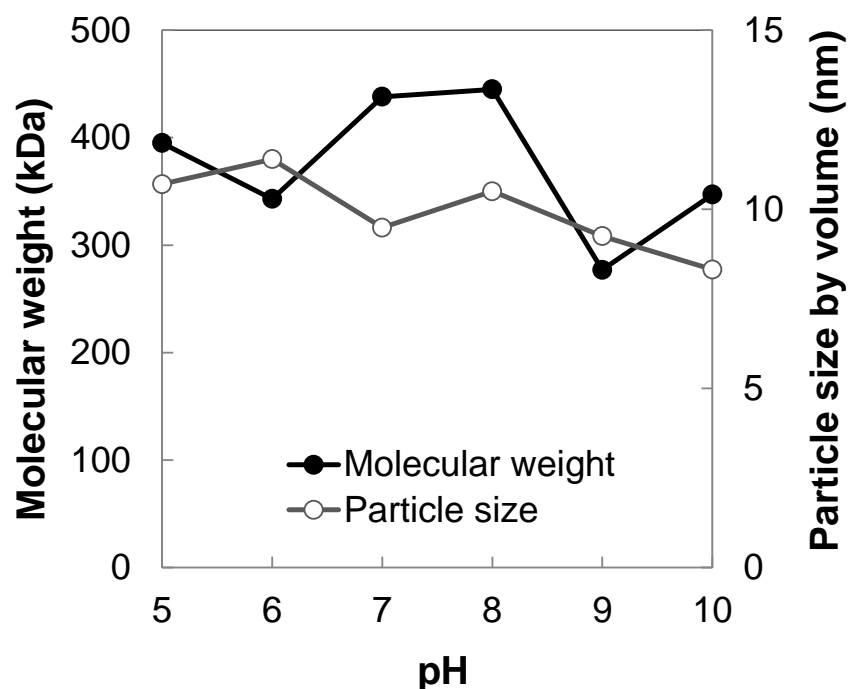


**Figure 2.11.** Plots of pH against  $M_w$  and particle size by volume of unimer nanoparticles  $\gamma$ -PGA140k-Phe-46 (10-0).

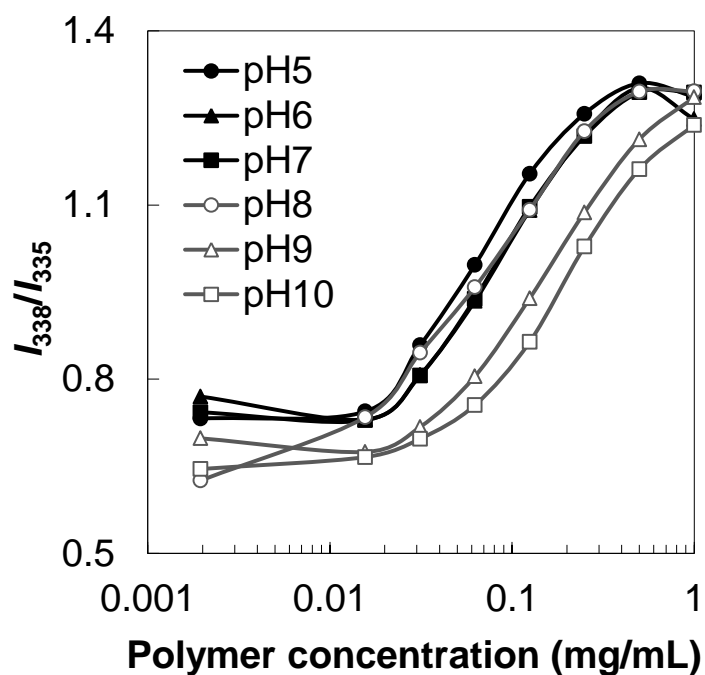


**Figure 2.12.** Intensity ratio  $I_{338}/I_{335}$  obtained from the fluorescence excitation spectra of pyrene plotted versus the  $\gamma$ -PGA-Phe unimer nanoparticles concentration (0.015-1 mg/mL) at different pH values (pH 5-10).

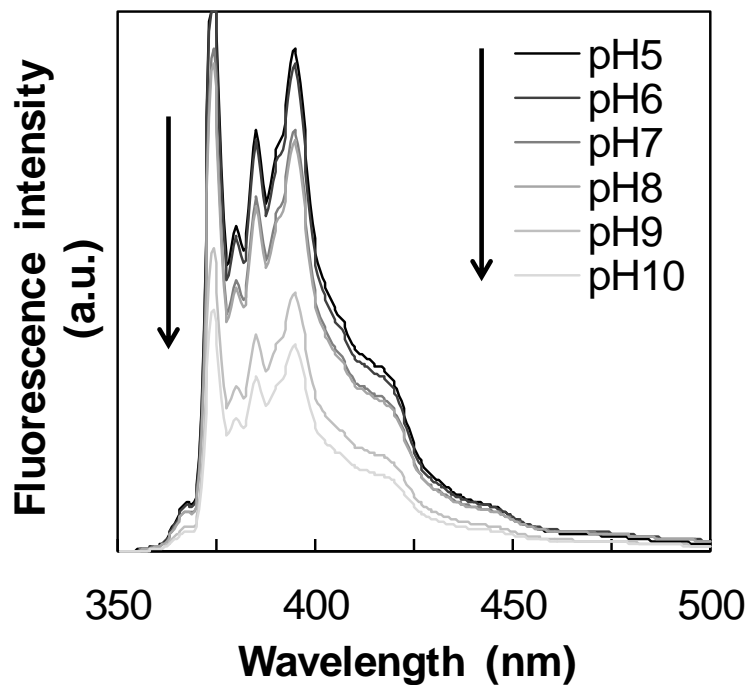


**Figure 2.13.** Steady-state fluorescence emission spectra monitored at 372 nm for pyrene ( $1.4 \times 10^{-7}$  M) with unimer nanoparticles at various pH values.

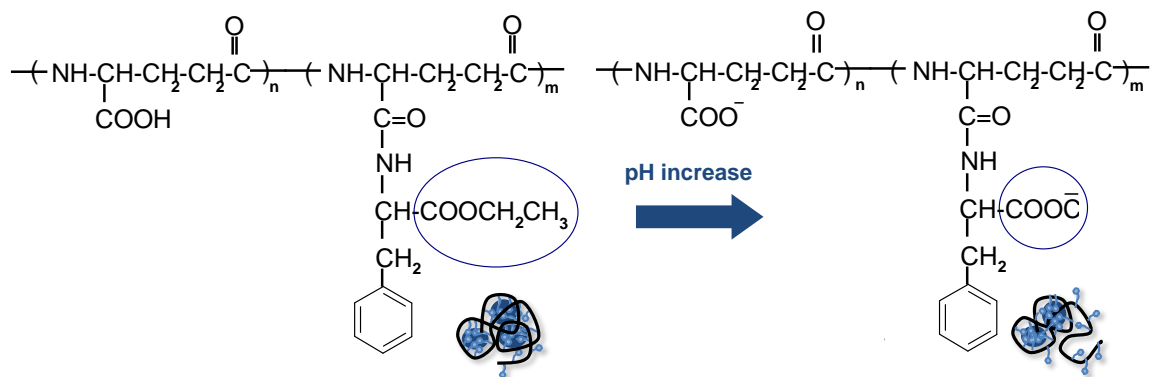


**Figure 2.14.** Illustration of the loose packing of the inner structures under alkaline condition.



## 2.4. Conclusion

10 nm-sized particles with spherical shape were observed by TEM for unimer sample. Besides, a structural analysis of unimer nanoparticles measured by SANS confirmed the existence of this unimer state forming spherical core-shell structures. Further investigation of their inner structures such as  $N_{\text{Domain}}$  examined by steady-state fluorescence quenching techniques indicated that the  $N_{\text{Domain}}$  depended on the particle size, as well as the grafting degree of L-Phe. Moreover, the stability of the unimer nanoparticles against pH revealed that the hydrophobic domains of the Phe groups were formed at pH values ranging from pH 3-10. However, a reduction of the  $N_{\text{Domain}}$  was observed in alkaline conditions due to the cleavage of the ester bonds. Interestingly, inner core of 10 nm unimer nanoparticles is more flexible and show higher in the density of  $N_{\text{Domain}}$  per volume over than large-sized nanoparticles. These differences in the inner structures of  $\gamma$ -PGA-Phe unimer nanoparticles are expected to show various great potential for applications as small drug carriers, for example, providing the opportunity for hydrophobic drugs to easily penetrate and absorb into the inner core of the unimer nanoparticles. In addition, recent research from our group has reported that  $\gamma$ -PGA-based nanoparticles are suitable for the intracellular delivery of protein-based drugs as well as tumor vaccines.<sup>26</sup> Besides, the effectiveness of small particles over larger particles and vice versa plays a critical role in controlling the immune response.<sup>27, 28</sup> Therefore, the obtained unimer nanoparticles are expected to offer the possibility of enhanced biomedical applications, such as drug or gene carriers for cancer therapy. In particular, the advantage of its large surface area may lead to the possibility of surface modification of unimer nanoparticles for site specific delivery.

## References

1. C. Wang, G. Li and R. Guo, *Chem. Comm.* **28**, 3591 (2005).
2. D. Sutton, N. Nasongkla, E. Blanco and J. Gao, *Pharm. Res.* **24**, 1029 (2007).
3. N. Nasongkla, X. Shuai, H. Ai, B. D. Weinberg, J. Pink, D. A. Boothman and J. Gao, *Angew. Chem. Int. Ed.* **43**, 6323 (2004).
4. V. P. Torchilin, A. N. Lukyanov, Z. Gao and S. P. Sternberg, *Proc. Natl. Acad. Sci. USA.* **100**, 6039 (2003).
5. M. Seo, J. B. Beck, J. M. J. Paulusse, C. J. Hawker, S. Y. Kim, *Macromolecules* **41**, 6413 (2008).
6. E. J. Foster, E. B. Berda and E. W. Meijer, *J. Am. Chem. Soc.* **131**, 6964 (2009).
7. B. S. Murray and D. A. Fulton, *Macromolecules* **44**, 7242 (2011).
8. O. Altintas and C. B. Kowollik, *Macromol. Rapid Commun.* **33**, 958 (2012).
9. T. Mes, R. V. D. Weegen, A. R. A. Palmans and E. W. Meijer, *Angew. Chem. Int. Ed.* **50**, 5085 (2011).
10. J. He, L. Tremblay, S. Lacelle and Y. Zhao, *Soft Matter* **7**, 2380 (2011).
11. E. Harth, B. V. Horn, V. Y. Lee, D. S. Germack, C. P. Gonzales, R. D. Miller and C. J. Hawker, *J. Am. Chem. Soc.* **124**, 8653 (2002).
12. Y. Morishima, S. Nomura, T. Ikeda, M. Seki and M. Kamachi, *Macromolecules* **28**, 2874 (1995).

13. S. Yusa, A. Sakakibara, T. Yamamoto and Y. Morishima, *Macromolecules* **35**, 5243 (2002).
14. H. Kim, T. Akagi and M. Akashi, *Macromol. Biosci.* **9**, 842 (2009).
15. T. Akagi, P. Piyapakorn and M. Akashi, *Langmuir* **28**, 5249 (2012).
16. H. Maeda, *Adv. Drug Deliv. Revs.* **46**, 169 (2001).
17. H. Maeda, T. Sawa and T. Konno, *J. Controlled Release* **74**, 47 (2001).
18. Y. Song, Z. Zhang, E. Ali, E. Hani, H. Wang, L. L. Henry, Q. Wang, *Nanoscale* **3**, 31 (2011).
19. R. Semwal, D. K. Semwal, R. Badoni, S. Gupta and A. K. Madan, *J. Med. Sci.* **10**, 130 (2010).
20. P. Kaewsaiha, K. Matsumoto and H. Matsuoka, *Langmuir* **21**, 9938 (2005).
21. P. Kaewsaiha, K. Matsumoto and H. Matsuoka, *Langmuir* **23**, 9162 (2007).
22. H. Morinaga, H. Morikawa, Y. Wang, A. Sudo and T. Endo, *Macromolecules* **42**, 2229 (2009).
23. Y. Ozawa, S. Sawada, N. Morimoto and K. Akiyoshi, *Macromol. Biosci.* **9**, 694 (2009).
24. H. Takahashi, S. Sawada and K. Akiyoshi, *ACS Nano* **5**, 337 (2011).
25. T. Yamamoto, M. Yokoyama, P. Opanasopit, A. Hayama, K. Kawano and Y. Maitani, *J. Controlled Release* **123**, 11 (2007).

26. T. Yoshikawa, N. Okada, A. Oda, K. Matsuo, K. Matsuo, Y. Mukai, Y. Yoshioka, T. Akagi, M. Akashi and S. Nakagawa, *Biochem. Biophys. Res. Commun.* **366**, 408 (2008).
27. H. Kim, T. Uto, T. Akagi, M. Baba and M. Akashi, *Adv. Funct. Mater.* **20**, 3925 (2010).
28. I. Gutierrez, R. M. Hernández, M. Igartua, A. R. Gascón, J. L. Pedraz, *Vaccine* **22**, 67 (2002).

## *Chapter 3*

### **Stimuli-responsive unimer nanoparticles and their potential applications for cancer therapy**

#### **3.1. Introduction**

Carriers used as anti-cancer agents with the capability for the controlled release and targeting of drugs are now being continuously developed and fabricated for cancer treatment. Recently, the particle size of carriers has become an important parameter because it not only controls the enhanced permeability and retention (EPR) effect<sup>1-3</sup>, which can provide a great opportunity for more selective targeting into tumors, but also efficient penetration into poorly-permeable tissues, leading to increased tumor accumulation of drug-conjugated carriers.<sup>4</sup> Therefore, the precise size-control of drug carriers is a challenging issue, especially for the small-sized range.

There has been growing research on the construction of polymeric unimolecular micelles/nanoparticles, for example, star-shaped polymers<sup>5-6</sup> and dendritic polymers.<sup>7</sup> Such polymeric systems have their own hydrophobic domains formed by only intramolecular associations, which are capable of encapsulating hydrophobic molecules, while not displaying any critical micelle concentration (CMC). However, these polymeric systems often require complex synthesis and preparation. Their characterization cannot be easily carried out because of the highly branched structures with a large number of functional end groups, and this increases the possibility of structural defects of the polymer causing complexity and heterogeneity within its final structure.<sup>8</sup>

Our research group has recently demonstrated the effectiveness of smaller particles in playing a critical role to control the immune response.<sup>9</sup> By taking advantage of a single chain component forming very small nanoparticles, which would be expected to control both release and degradation due to their high surface area, we have recently reported the formation of biodegradable unimer nanoparticles composed of hydrophobically-modified poly ( $\gamma$ -glutamic acid) ( $\gamma$ -PGA) by employing facile synthesis and preparative methods.<sup>10</sup> Furthermore, the most current structural analysis studies have revealed that unimer nanoparticles have a large number of hydrophobic domains in their core. Therefore, the obtained 10-nm sized biodegradable unimer nanoparticles are expected to be useful as drug carries.<sup>11</sup> Interestingly, the structure of our prepared unimer nanoparticles achieved by controlling the aggregation number is likely to be similar to a single polypeptide chain, and thus it can be considered an artificial protein.

In general, proteins such as human serum albumin have been used as carriers in order to improve the solubility of drugs, for example conjugation with paclitaxel (trade name Abraxane), an anti-cancer drug.<sup>12-13</sup> However, protein albumin does not possess the capability of controlled release such as stimuli-sensitive systems, which represent one of the most outstanding achievements in the drug delivery field. Additionally, the tertiary structure of a protein is stabilized by various types of interactions (hydrogen bonds, disulfide bonds, hydrophobic interactions, and ionic interactions), which play important roles in controlling the basic functions of the protein. Among them, disulfide bonds have received increased interest, especially in the field of controlled release. There have been several reports on the formation of micelles/nanoparticles with the help of disulfide bonds; for example, Kataoka's group has reported that the assembly of iminothiolane-modified poly(ethylene glycol)-*block*-poly(L-lysine) [PEG-*b*-(PLL-IM)] and siRNA

could form a core-shell-type polyion complex (PIC) micelle with a disulfide cross-linked core.<sup>14</sup> Furthermore, drug-loaded redox-responsive nanoparticles assembled from the single disulfide bond-bridged block polymer of poly( $\epsilon$ -caprolactone) and poly(ethylene phosphate) (PCL-SS-PEEP) have also been demonstrated.<sup>15</sup> By employing disulfide bonds, the formation-dissociation of cargo-conjugated nanocarriers could be triggered under oxidative-reductive conditions.<sup>16-17</sup>

In order to enhance the capability of controlling the intra-molecular associations of our unimer nanoparticles, the current study aimed to fabricate stimuli-responsive unimer nanoparticles composed of hydrophobized  $\gamma$ -PGA. For this purpose, disulfide bonds were introduced into hydrophobized  $\gamma$ -PGA. **Figure 3.1** shows the fabrication strategy of these stimuli-responsive unimer nanoparticles, which consist of a single polymer chain forming unimer nanoparticles achieved by the combination of hydrophobic interactions and disulfide bonds. Their characteristic behaviors as well as their potential applications as drug carriers were studied. It is expected that by introducing cysteine residues onto the side chain of the amphiphilic copolymer, it is possible to not only obtain protein-mimetic unimer nanoparticles through disulfide bond formation, but also to control its release behavior efficiently in response to a reducing stimulus.

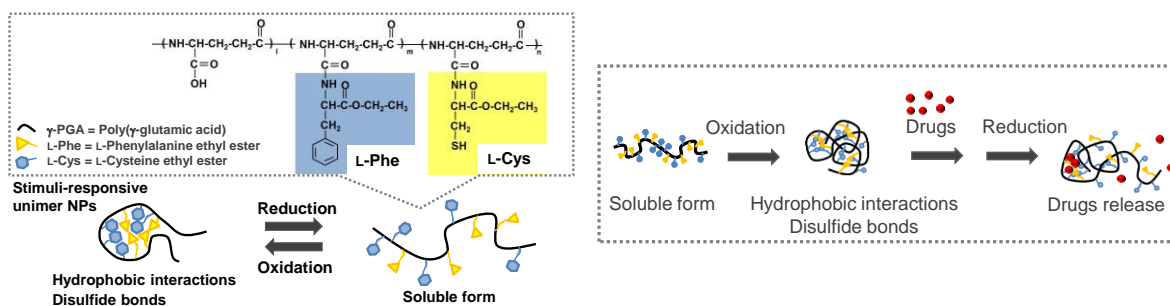


**Figure 3.1.** Fabrication strategy of stimuli-responsive unimer nanoparticles composed of  $\gamma$ -PGA conjugated with L-phenylalanine and L-cysteine.

## 3.2. Experimental section

### *Materials*

$\gamma$ -PGA with molecular weights ( $M_w$ ) of 140 kDa as determined by static light scattering (SLS) were purchased from Wako Pure Chemical, Ltd. (Japan). The size and PDI of  $\gamma$ -PGA determined by dynamic light scattering (DLS) were  $12.0 \pm 0.4$  nm and  $0.22 \pm 0.02$ , respectively. The results are presented as means  $\pm$  SD ( $n=3$ ). L-phenylalanine ethyl ester (L-Phe) and L-cysteine ethyl ester (L-Cys) were purchased from Sigma-Aldrich Chem. Co., and 1-ethyl-3-[3-dimethylaminopropyl]carbodiimide hydrochloride (EDC) was from Dojindo Laboratories (Japan). Coomassie Brilliant Blue G-250 (CBB) served as a probe was purchased from Wako Pure. Chemical, Ltd. (Japan). Water was purified with a Direct-Q system (Millipore, Co.). All other chemicals used were of analytical grade. Capsaicin ( $M_w$  305.4 g/mol) a model drug, as well as irinotecan ( $M_w$  586.7 g/mol) and cisplatin ( $M_w$  301.1 g/mol) anti-cancer drugs were purchased from Wako Pure Chemical Industries, Japan. Dithiothreitol (DTT), a reducing agent commonly used for the cleavage of disulfide bonds, was purchased from Wako Pure. Chemical, Ltd. (Japan).

### *Synthesis of $\gamma$ -PGA-Phe graft copolymers*

$\gamma$ -PGA (4.7 unit mmol) was dissolved into 100 mM NaHCO<sub>3</sub>. Subsequently, a specific amount of coupling agent (EDC) (from 1.2 to 3.5 mmol) and L-Phe (4.7 unit mmol) were added into the solution. After incubation for 24 h, the mixtures were dialyzed against distilled water and freeze-dried for several days. The chemical structures



of the obtained copolymers were confirmed by  $^1\text{H}$  NMR and FT-IR, and the grafting degree of L-Phe was evaluated by  $^1\text{H}$  NMR using integral intensity ratio of the methylene peaks of  $\gamma$ -PGA to the phenyl group peaks of Phe.

### ***Synthesis of $\gamma$ -PGA-Phe-Cys graft copolymers***

The obtained  $\gamma$ -PGA-Phe copolymers with grafting degree of L-Phe 12-35% (2.4 unit mmol) were dissolved into 100 mM  $\text{NaHCO}_3$ . In order to achieve only intra-molecular associations, therefore  $\gamma$ -PGA-Phe-Cys copolymers with low grafting degree of L-Cys were controlled by the addition of small amounts of coupling agent (EDC) (0.6 mmol) and L-Cys (0.6 mmol) into the solution. After incubation for 24 h, the mixtures were dialyzed against distilled water and freeze-dried for several days in the same way as the synthesis of  $\gamma$ -PGA-Phe copolymers. The chemical structures of the obtained copolymers were confirmed by  $^1\text{H}$  NMR and FT-IR, and the grafting degree of L-Cys was evaluated by elemental analysis for sulfur atom.

### ***Preparation and characterization of $\gamma$ -PGA-Phe-Cys nanoparticles***

The obtained  $\gamma$ -PGA-Phe-Cys copolymers were prepared by direct dispersion into PBS method. The particle size,  $M_w$ , and zeta potential were determined by means of dynamic and static light scattering (DLS and SLS) methods taking the average of at least 3 measurements ( $n = 3$ ), respectively. Furthermore, the number of aggregates ( $N_{\text{agg}}$ ) can be calculated by the ratio of the measured  $M_w$  /calculated  $M_w$ .

### ***The formation of hydrophobic associations***

To monitor the formation of hydrophobic associations due to the hydrophobic moieties of L-Phe, UV measurement was performed using CBB as a probe. The packed CBB dye acts as a probe for nanoparticles, and offers a sensitive method for determining the formation of hydrophobic associations. The single chain state samples obtained in the presence and absence of the L-Cys moieties;  $\gamma$ -PGA-Phe and  $\gamma$ -PGA-Phe-Cys (0-2 mg/mL in PBS) were mixed with dye solution (0.05 mM CBB in PBS) in the ratio 1:1. After incubation for 1 h, the absorbances of various nanoparticles concentrations were measured by UV measurement as shown in **Figure 3.5**. The shift of the maximum wavelength of CBB upon increasing the nanoparticles concentration indicated the formation of hydrophobic domains.

### ***The effect of the cleavage of disulfide bonds on the formation of hydrophobic domains***

The existence of disulfide bonds as well as the cleavage of disulfide bonds was confirmed by measuring the change in the maximum wavelength of CBB. In this experiment, only the unimer nanoparticles samples containing L-Cys moieties (single chain state forming hydrophobic domains of Phe) were selected. Firstly, DTT was dissolved in PBS (pH 8.4) at a desired concentration. Next, DTT solution was added into the sample solution, following by adding CBB dye solution (final concentrations were 1 mg/mL for unimer nanoparticles sample, and 0 and 0.2 mM for DTT). After incubation for 1 h, the absorbance was detected by UV measurement.

### ***Large-size nanoparticles composed of $\gamma$ -PGA-Phe27-Cys copolymers and their stimuli-responsive properties***

$\gamma$ -PGA-Phe27 copolymers were firstly synthesized by controlling the grafting degree of L-Phe about 27%. In the next step,  $\gamma$ -PGA-Phe27-Cys copolymers different in grafting degree of L-Cys were synthesized by adjusting the amount of EDC which served as a coupling agent in the reaction. In the experiment, the feeding amount of EDC was increased in order to increase the grafting degree of L-Cys as shown in **Table 3.4**. Then, the chemical structures of copolymers were confirmed by  $^1\text{H}$  NMR, FTIR and elemental analysis. The obtained copolymer was prepared nanoparticles by dispersed in water/PBS. The results were shown in **Table 3.5**. The samples (single chain state) were then monitored the formation of hydrophobic domains by UV measurement using CBB. Furthermore, the existing of disulfide bonds was studied by DLS via observation the change of particle size upon the incubation time after treatment with DTT.

### ***Stimuli-responsive nanoparticles composed of $\gamma$ -PGA-Cys graft copolymers and their stimuli-responsive properties***

Not only  $\gamma$ -PGA-Phe-Cys, the stimuli-responsive unimer nanoparticles composed of  $\gamma$ -PGA-Cys were also try to synthesize by introducing only L-Cys onto carboxylic groups of  $\gamma$ -PGA to obtain  $\gamma$ -PGA-Cys copolymers. Due to inter-molecular associations are easy to occur for disulfide bonds, thus the grafting degree of L-Cys was controlled in order to obtain at low grafting degree. The chemical structures of copolymers were confirmed by  $^1\text{H}$  NMR, FTIR and elemental analysis. The grafting degree of L-Cys was determined by

$^1\text{H}$  NMR. Next, nanoparticles were prepared by direct dispersion into PBS method, and observed their morphology by SEM (for large-sized nanoparticles). The effect of L-Cys grafting degree for the formation of nanoparticles, and the effect of cleavage of disulfide bonds were studied in the same manner as  $\gamma$ -PGA-Phe-Cys copolymers.

### *Potential applications as drug carriers*

#### *Model drug-loaded $\gamma$ -PGA-Phe unimer nanoparticles and their release behavior*

The potential applications as hydrophobic carriers for unimer  $\gamma$ -PGA-Phe nanoparticles (10 nm) were first studied using capsaicin as a model drug. In order to study the drug absorption of unimer nanoparticles prepared by direct dispersion into PBS method for  $\gamma$ -PGA140k-Phe at grafting degree lower than 42, thus  $\gamma$ -PGA140k,  $\gamma$ -PGA140k-Phe-12,  $\gamma$ -PGA140k-Phe-27,  $\gamma$ -PGA140k-Phe-35 and  $\gamma$ -PGA140k-Phe-42 were dispersed into PBS at various concentrations. Capsaicin solution was prepared by dissolving capsaicin in ethanol. Next, each sample was mixed with capsaicin solution at various concentrations. The final concentrations of the mixture were 10, 5, 2.5 and 1.25 mg/mL and final concentration of capsaicin was 0.5 mg/mL. The change in solubility of the resulting mixtures was then observed.

To evaluate the potential of unimer nanoparticles for encapsulation and release of hydrophobic drugs (capsaicin). **Unimer nanoparticles**;  $\gamma$ -PGA140k-Phe-42 (prepared by direct dispersion into PBS method),  $\gamma$ -PGA-Phe140k-42(10-0) and  $\gamma$ -PGA140k-Phe-46(10-0) (prepared by dialysis method) as well as **large-size nanoparticles**;  $\gamma$ -PGA140k-Phe-46(10-0.3) and  $\gamma$ -PGA140k-Phe-65(10-0) (prepared by dialysis method) were

dissolved in PBS at certain concentration. Capsaicin solution was prepared by dissolving capsaicin in ethanol. The solutions were mixed with capsaicin. The final concentrations of capsaicin and nanoparticles in the mixtures were 0.5 and 10 mg/mL respectively. The mixtures were then sealed in dialysis bags (molecular weight cut-off 10000 kDa). Capsaicin was released into 50 mL of distilled water at room temperature. The medium was withdrawn at determined time intervals to monitor its fluorescence intensity (excitation at 312 nm). Released capsaicin concentration was obtained from standard curve plotted between capsaicin concentration and fluorescence intensity.

***Preparation of anti-cancer drug-loaded  $\gamma$ -PGA-Phe unimer nanoparticles and their release behavior***

The potential applications as hydrophobic carriers for unimer  $\gamma$ -PGA-Phe nanoparticles (10 nm) to absorb irinotecan and cisplatin as compared to large-sized  $\gamma$ -PGA-Phe nanoparticles (200 nm) were first studied. The drug-loaded  $\gamma$ -PGA-Phe nanoparticles were prepared by mixing the drugs solution (in ultrapure water/PBS) with nanoparticles solutions at the desired concentrations at the same volume. The resultant nanoparticles were incubated, and collected by ultrafiltration before measurement by UV. The amount of drug loading into unimer nanoparticles could be calculated from unconjugated irinotecan after subtraction from reference sample without nanoparticles.

In addition to further study on the release behavior, irinotecan was mixed with unimer nanoparticles and large-sized nanoparticles. The final concentrations of irinotecan and nanoparticles in the mixtures were 0.5 and 0.1 mg/mL respectively. The mixtures were then sealed in dialysis bags (molecular weight cut-off 2000 kDa). The amount of

irinotecan release into medium was detected by UV measurement (absorbance at 364 nm) comparison to standard curve.

### ***Preparation of drug-loaded $\gamma$ -PGA-Phe-Cys unimer nanoparticles***

The potential applications as drug carriers were studied using irinotecan as a model anti-cancer drug. The drug-loaded unimer nanoparticles were prepared by mixing the irinotecan solution (2 mg/mL in ultrapure water) with unimer nanoparticles solutions both  $\gamma$ -PGA-Phe and  $\gamma$ -PGA-Phe-Cys (2-10 mg/mL in PBS) at the same volume. The resultant nanoparticles were incubated 24 hours, and collected by ultrafiltration (molecular weight cut-off 3000 kDa) before measurement of unconjugated irinotecan by UV spectroscopy absorbance at 364 nm. The drug-absorbed efficiency of unimer nanoparticles could be calculated from unconjugated irinotecan after subtraction from reference sample without nanoparticles. The results are presented as means  $\pm$  SD (n = 3).

### ***The cleavage of disulfide bonds for drug-loaded unimer nanoparticles***

To determine the cleavage of disulfide bonds for 10-nm size unimer nanoparticles, irinotecan was employed to absorb and penetrate into the hydrophobic domains of the unimer nanoparticles. The release of irinotecan was then observed in response to oxidation-reduction conditions. The obtained drug-loaded unimer nanoparticles (irinotecan 160  $\mu$ g/nanoparticles 1 mg) were tested by treatment with DTT in comparison to the control sample. After the drug-loaded unimer nanoparticles were prepared as mentioned before, DTT was then added into the mixture (final concentration

DTT 20 mM, pH 8.4). The resultant nanoparticles were incubated 24 h, and collected by ultrafiltration (molecular weight cut-off 3000 kDa) before measurement of the released-irinotecan by UV (absorbance at 364 nm). The release (%) of irinotecan was calculated in comparison to the control sample. The results are presented as means  $\pm$  SD (n = 3).

### 3.3. Results and Discussion

#### *Synthesis of $\gamma$ -PGA-Phe-Cys graft copolymers*

Stimuli-responsive, single polymer chain based nanoparticles were synthesized via the chemical modification of  $\gamma$ -PGA by a two-step grafting of L-Phe and L-Cys. First,  $\gamma$ -PGA-Phe were prepared by the conjugation of L-Phe to  $\gamma$ -PGA ( $M_w$  of 140 kDa). The substitution degree of the L-Phe moieties was varied by changing the amount of carbodiimide (**Table 3.1**). Next, L-Cys was introduced onto the  $\gamma$ -PGA-Phe copolymers by adjusting the preparative conditions (**Table 3.2**). Thereby, stimuli-responsive unimer nanoparticles composed of  $\gamma$ -PGA-Phe-Cys could be synthesized by the combination of hydrophobic interactions driven by the hydrophobic moieties of L-Phe, and disulfide bonds obtained from the thiol groups in L-Cys. The chemical structures of these copolymers were confirmed by  $^1\text{H}$  NMR (**Figure 3.2**), FT-IR (**Figure 3.3**), and elemental analyses. The substitution degrees of L-Phe and L-Cys were evaluated by  $^1\text{H}$  NMR in DMSO- $d_6$  using the integral intensity ratio of the methylene peaks of  $\gamma$ -PGA to the phenyl group peaks of L-Phe, and by elemental analysis for sulfur atoms, respectively (**Table 3.2**). To simplify the notations, the samples were abbreviated as  $\gamma$ -PGA-PheX-

CysY, where X and Y refer to substitution degree of L-Phe and L-Cys on the  $\gamma$ -PGA main chain, respectively (**Table 3.3**).

### ***Preparation and characterization of $\gamma$ -PGA-Phe-Cys nanoparticles***

As a result,  $\gamma$ -PGA-Phe-Cys copolymers at a grafting degree of L-Phe lower than 42% could be easily soluble in aqueous solutions, and moreover, the phenyl peaks of the  $\gamma$ -PGA-Phe-Cys copolymers were not observed in their  $^1\text{H}$  NMR spectra when  $\text{D}_2\text{O}$  was employed as the solvent (**Figure 3.4**), and thus particle formation in water could be confirmed. Furthermore,  $^1\text{H}$  NMR spectra in  $\text{D}_2\text{O}$  (**Figure 3.5**) showed the evidence of the increase of the formation of hydrophobic domains with increasing grafting degree of L-Phe.

As shown in **Table 3.3**, protein-mimetic single chain polymers composed of  $\gamma$ -PGA-Phe-Cys with substitution degrees of L-Phe of 12%, 27% and 35%, and substitution degrees of L-Cys around 7-10%, could be obtained in the same fashion as the  $\gamma$ -PGA-Phe samples. The unique side chain provides for the self-assembly of unimer nanoparticles by hydrophobic interactions and disulfide bonds in aqueous solution.

**Table 3.1. Synthesis of  $\gamma$ -PGA-Phe**

Sample	$\gamma$ -PGA (unit mmol)	EDC (mmol)	L-Phe (mmol)	Yield (%)	Grafting degree of L-Phe <sup>a</sup> (%)
$\gamma$ -PGA-Phe12	4.7	1.2	4.7	56	12
$\gamma$ -PGA-Phe27	4.7	2.4	4.7	46	27
$\gamma$ -PGA-Phe35	4.7	3.5	4.7	58	35

<sup>a</sup>The grafting degree of L-Phe was measured by  $^1\text{H}$  NMR.



**Table 3.2. Synthesis of  $\gamma$ -PGA-Phe-Cys**

Sample	$\gamma$ -PGA-Phe (unit mmol)	EDC (mmol)	L-Cys (mmol)	Yield (%)	Grafting degree of L-Cys <sup>a</sup> (%)
$\gamma$ -PGA-Phe12-Cys7	2.4	0.6	0.6	75	7
$\gamma$ -PGA-Phe27-Cys10	2.4	0.6	0.6	78	10
$\gamma$ -PGA-Phe35-Cys7	2.4	0.6	0.6	71	7

<sup>a</sup>The grafting degree of L-Cys was determined by elemental analysis for sulfur atom.

**Table 3.3. Characterization of  $\gamma$ -PGA-Phe and  $\gamma$ -PGA-Phe-Cys nanoparticles.**

Sample	Calculated $M_w$ (kDa) <sup>a</sup>	Particle size (nm) <sup>b</sup>	PDI <sup>c</sup>	Zetapotential (mV) <sup>b</sup>	Measured $M_w$ (kDa) <sup>d</sup>	$N_{agg}$ <sup>e</sup>
$\gamma$ -PGA-Phe12	168	13.6 $\pm$ 2.4	0.32 $\pm$ 0.06	- 23.0 $\pm$ 2.2	246	1.5
$\gamma$ -PGA-Phe27	202	11.0 $\pm$ 1.6	0.31 $\pm$ 0.03	- 23.1 $\pm$ 1.3	276	1.4
$\gamma$ -PGA-Phe35	220	7.9 $\pm$ 1.3	0.33 $\pm$ 0.06	- 26.7 $\pm$ 3.5	296	1.3
$\gamma$ -PGA-Phe12-Cys7	179	11.0 $\pm$ 0.8	0.47 $\pm$ 0.06	- 25.5 $\pm$ 2.5	236	1.3
$\gamma$ -PGA-Phe27-Cys10	218	11.4 $\pm$ 1.2	0.54 $\pm$ 0.16	- 29.9 $\pm$ 0.7	257	1.2
$\gamma$ -PGA-Phe35-Cys7	232	9.3 $\pm$ 0.1	0.33 $\pm$ 0.04	- 26.0 $\pm$ 0.3	289	1.2

<sup>a</sup> The  $M_w$  of  $\gamma$ -PGA-Phe and  $\gamma$ -PGA-Phe-Cys were calculated from the  $M_w$  of  $\gamma$ -PGA measured by SLS; the grafting degree of L-Phe (%) was measured by <sup>1</sup>H NMR; and the grafting degree of L-Cys (%) measured by elemental analysis. <sup>b</sup> The particle diameter and zeta potential were measured in PBS (1 mg/mL) by DLS and laser doppler velocimetry using a Zetasizer nano ZS. <sup>c</sup> PDI represents the polydispersity index. The results are presented as means  $\pm$  SD (n = 3). <sup>d</sup> The  $M_w$  of the samples in PBS were measured by SLS. <sup>e</sup> The number of aggregates ( $N_{agg}$ ) was calculated by the ratio of the Measured  $M_w$  / Calculated  $M_w$ .

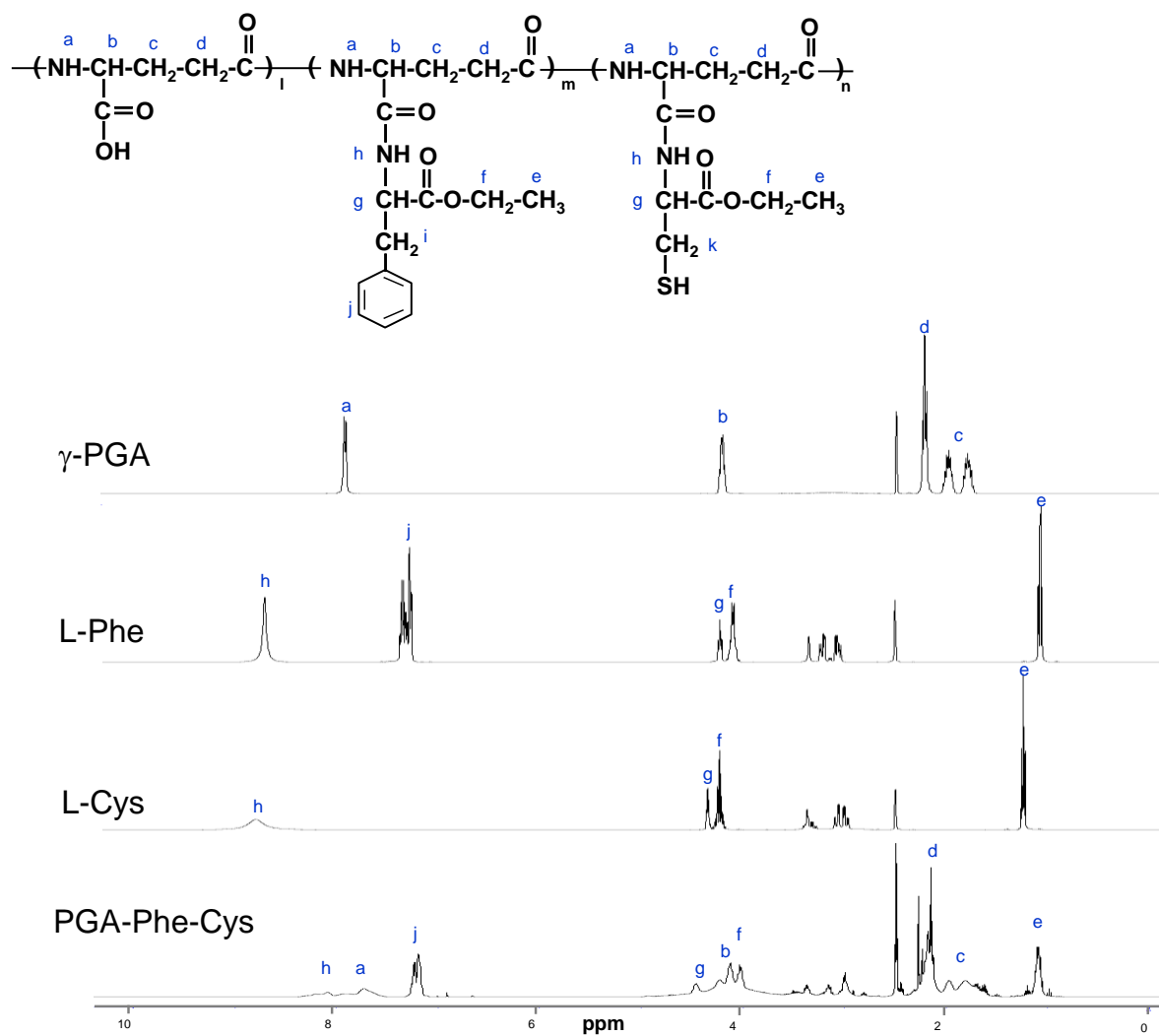


**Figure 3.2.**  $^1\text{H}$  NMR was performed to confirm the modified structure and to determine the grafting degree of L-Phe moieties (%).

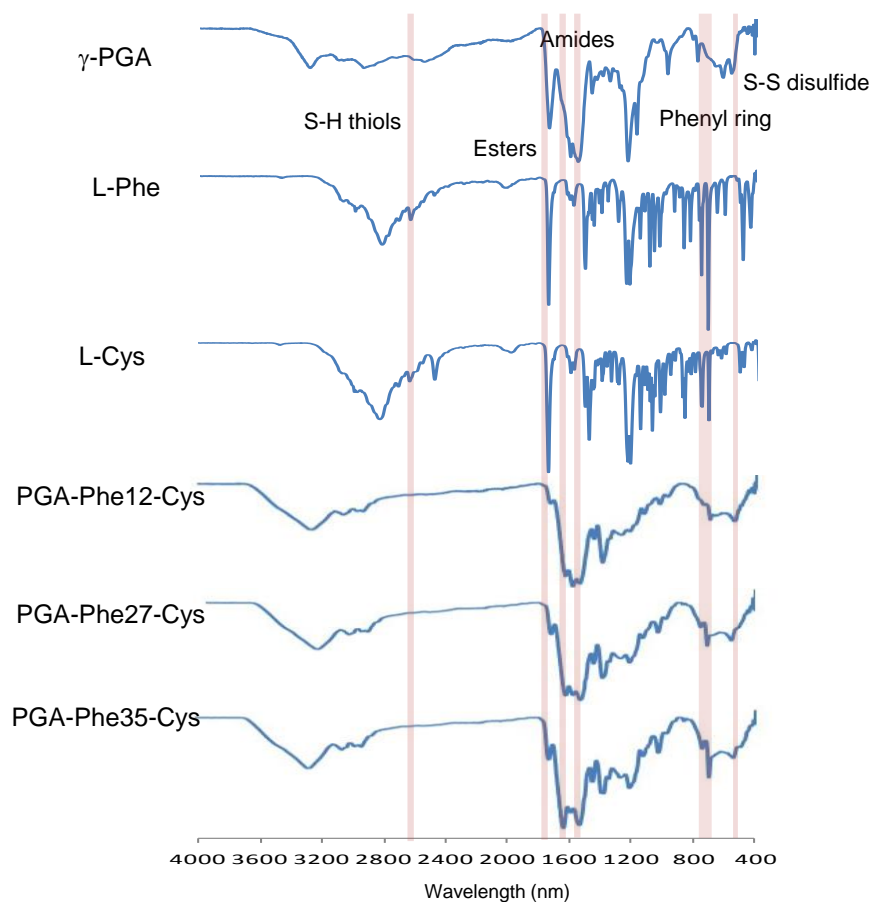


**Figure 3.3.** FT-IR was performed to confirm the chemical structure of  $\gamma$ -PGA-Phe-Cys copolymers.

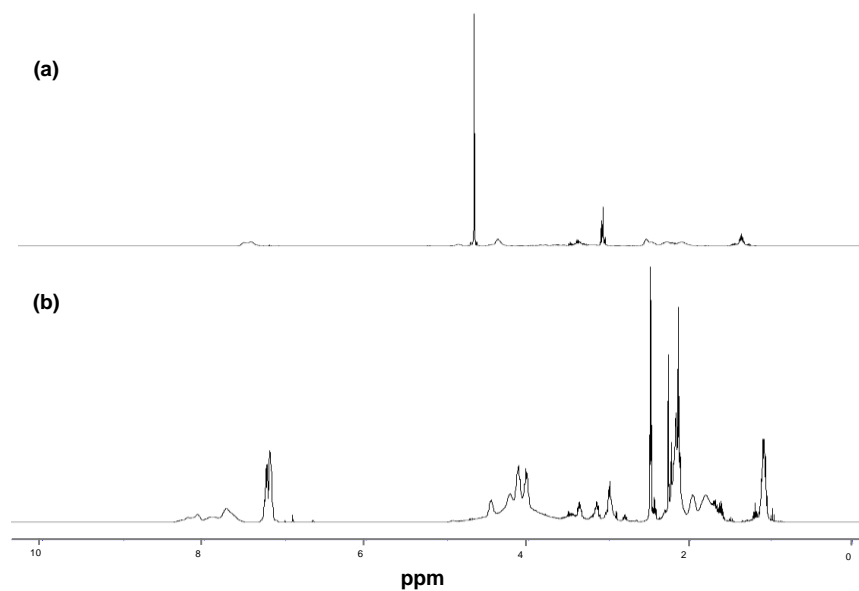


**Figure 3.4.**  $^1\text{H}$  NMR spectra of  $\gamma$ -PGA-Phe27-Cys10 copolymers in  $\text{D}_2\text{O}$  (a) and in  $\text{DMSO-d}_6$  (b).

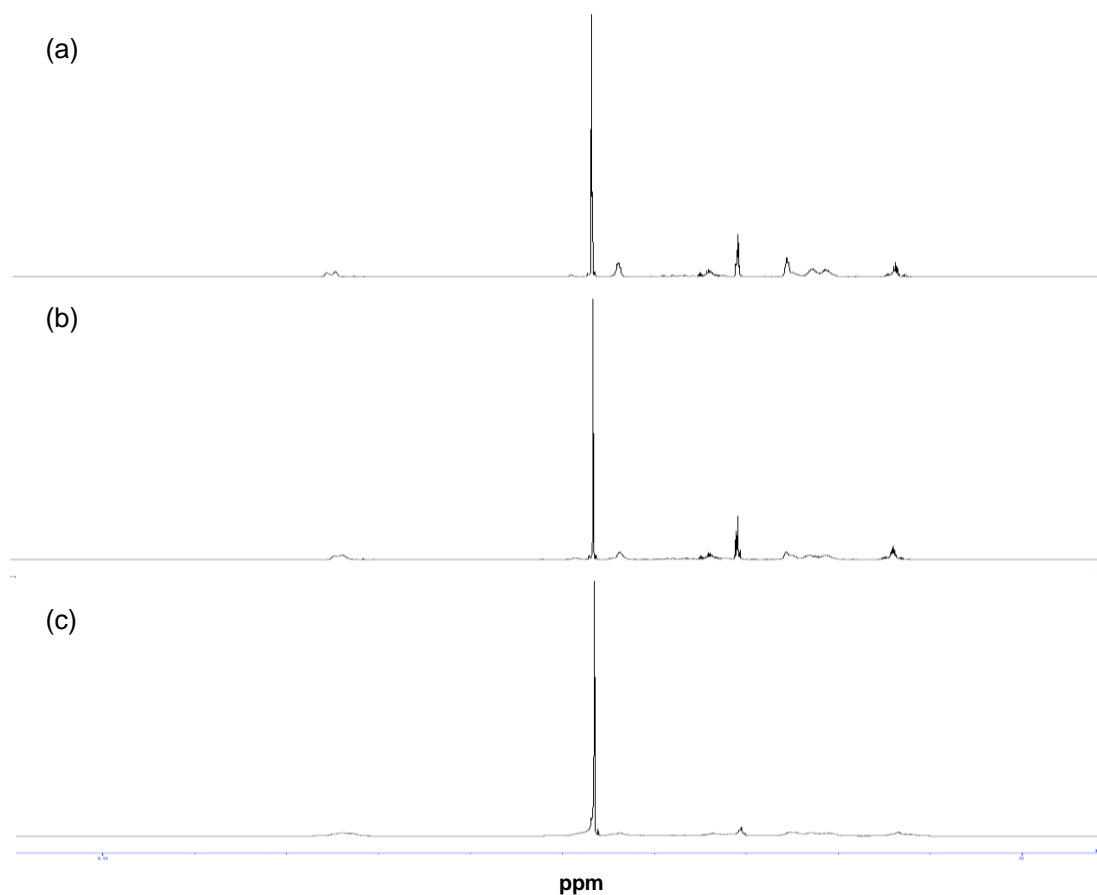


**Figure 3.5.**  $^1\text{H}$  NMR spectra of  $\gamma$ -PGA-Phe12-Cys7 (a),  $\gamma$ -PGA-Phe27-Cys10 (b) and  $\gamma$ -PGA-Phe35-Cys7 (c) in  $\text{D}_2\text{O}$ .

### *The formation of hydrophobic associations*

To monitor the formation of hydrophobic associations due to the hydrophobic moieties of L-Phe, UV measurements were performed using CBB as a probe.<sup>18-19</sup> The packed CBB dye acts as a probe for nanoparticles, and offers a sensitive method for determining the formation of hydrophobic associations. The absorbances of various nanoparticles concentrations were measured for all of the single chain state samples obtained in the presence and absence of the L-Cys moieties as shown in **Figure 3.6**. The shift of the maximum wavelength of CBB upon increasing the nanoparticles

concentration indicated the formation of hydrophobic domains. The plot of the maximum wavelength of CBB against the nanoparticles concentration in **Figure 3.7** revealed that unimer nanoparticles composed of  $\gamma$ -PGA-Phe-Cys containing more than 27% L-Phe moieties, could form hydrophobic domains.

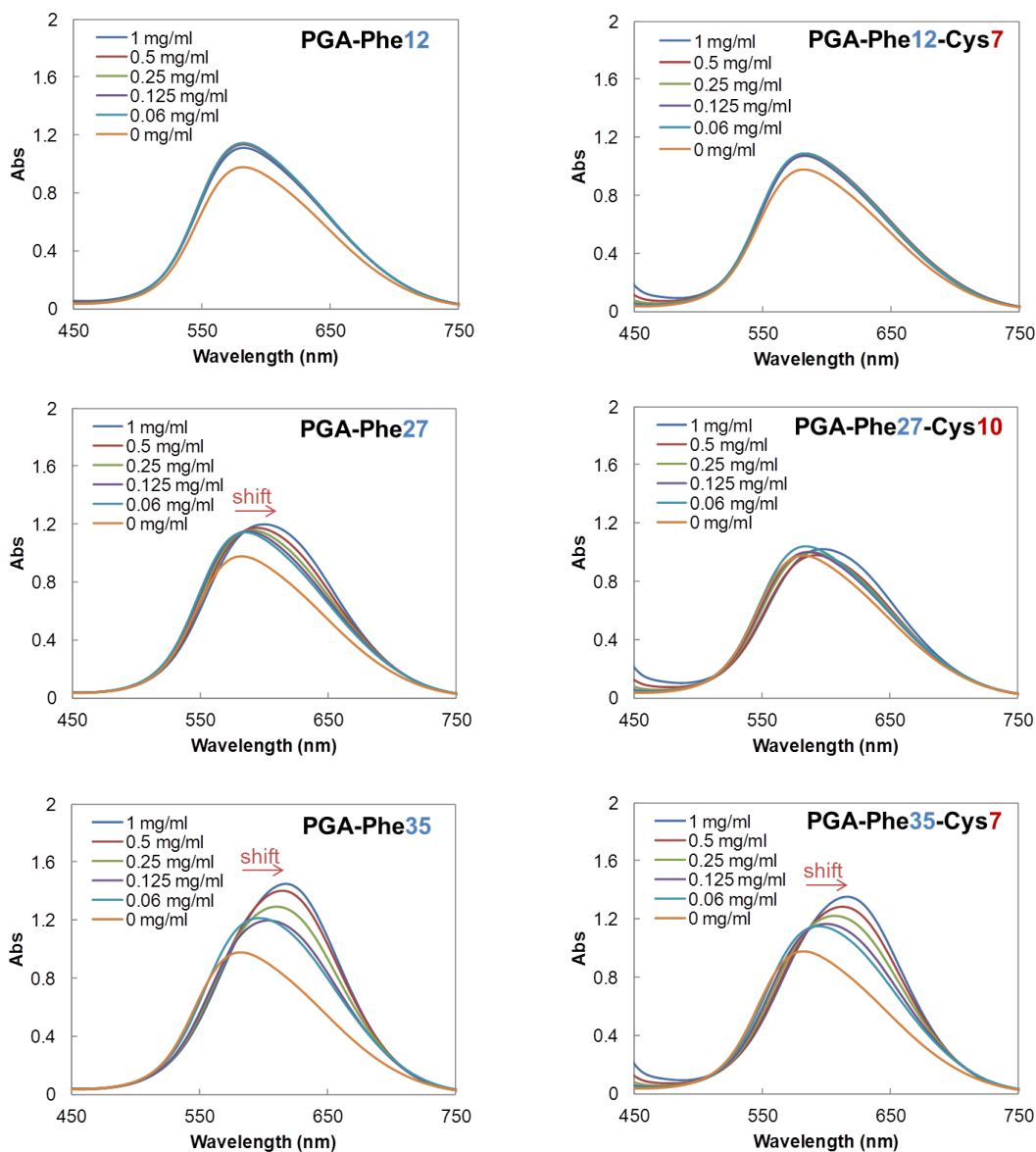


**Figure 3.6.** The plots of absorbance versus wavelength for  $\gamma$ -PGA-Phe (left) and  $\gamma$ -PGA-Phe-Cys (right) various grafting degree and concentrations.

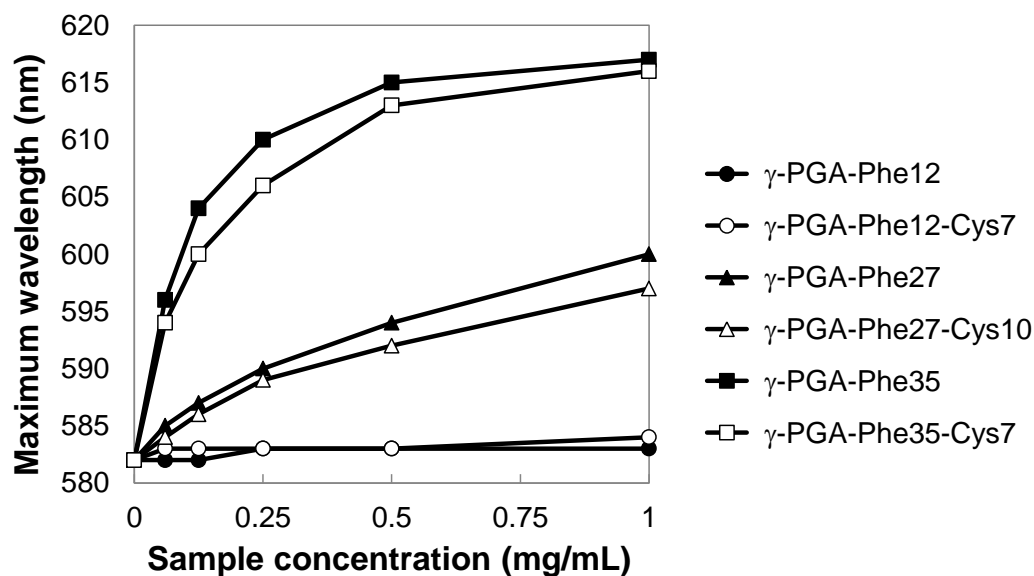


**Figure 3.7.** The plot of the maximum wavelength of CBB against the sample concentration.

*The effect of the cleavage of disulfide bonds on the formation of hydrophobic domains*

To further confirm the existence of disulfide bonds, the change in the maximum wavelength of CBB was measured only in the unimer samples containing L-Cys moieties ( $\gamma$ -PGA-Phe27-Cys10 and  $\gamma$ -PGA-Phe35-Cys7) which was performed by treatment with DTT, a reducing agent commonly used for the cleavage of disulfide bonds. As shown in **Figure 3.8a and 3.8b**, the decrease in the maximum wavelength of CBB was observed after treatment with DTT only in  $\gamma$ -PGA-Phe27-Cys10, supporting a decrease in the number of hydrophobic domains induced by the cleavage of disulfide bonds, and therefore the formation of hydrophobic domains affected disulfide bond formation. In contrast, in  $\gamma$ -PGA-Phe35-Cys7, the maximum wavelength of CBB did not show any change.

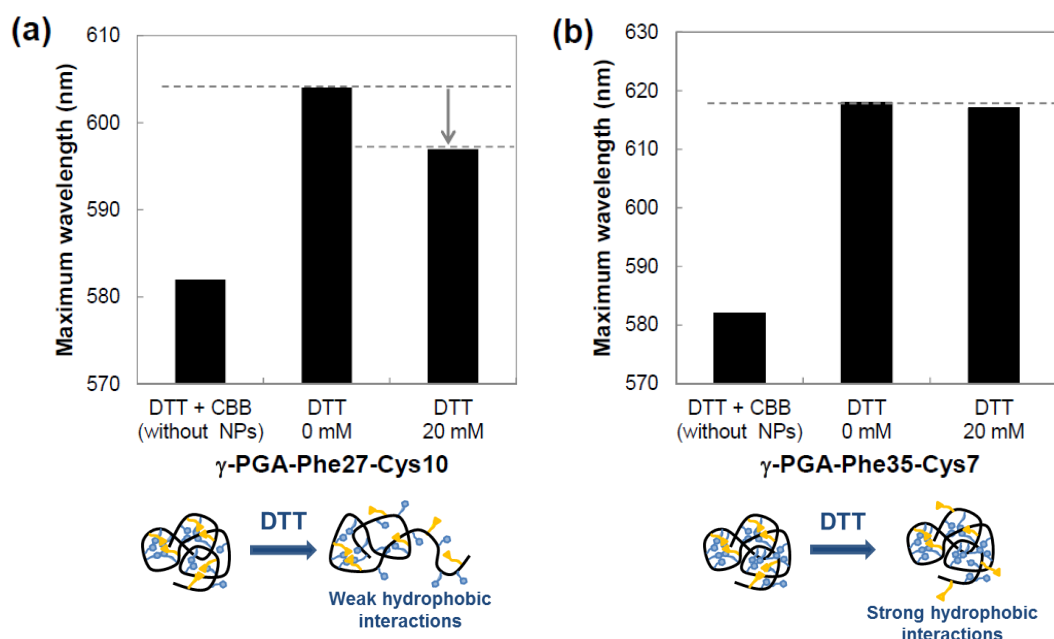


**Figure 3.8.** The change in the maximum wavelength after treatment with 20 mM dithiothreitol (DTT) for  $\gamma$ -PGA-Phe27-Cys10 (1 mg/mL) (a) and  $\gamma$ -PGA-Phe35-Cys7 (1 mg/mL) (b).

### *Large-size nanoparticles composed of $\gamma$ -PGA-Phe27-Cys copolymers and their stimuli-responsive properties*

By increasing the amount of both EDC and L-Cys (mmol), the grafting degree of L-Cys were increased as shown in **Table 3.4**. The obtained copolymers were then prepared nanoparticles by direct dispersion method and characterized in the same way as other samples (**Table 3.5**). As expected, unimer nanoparticles showing single chain could not be obtained from  $\gamma$ -PGA-Phe27-Cys copolymers having high grafting degree of L-Cys. Next, large-sized nanoparticles obtained from  $\gamma$ -PGA-Phe27-Cys copolymers were monitored the formation of hydrophobic domains. As shown the results in **Figure 3.9**, it was clearly observed the formation of hydrophobic domain for  $\gamma$ -PGA-Phe27-Cys27 and  $\gamma$ -PGA-Phe27-Cys34 copolymers.

**Table 3.4. Synthesis of  $\gamma$ -PGA-Phe27-Cys copolymers**

Sample	$\gamma$ -PGA-Phe (unit mmol)	EDC (mmol)	L-Cys (mmol)	Yield (%)	Grafting Degree of L-Phe (%) <sup>a</sup>	Grafting Degree of L-Cys (%) <sup>b</sup>
$\gamma$ -PGA-Phe-27-Cys-27	2.4	1.2	1.2	63	27	27
$\gamma$ -PGA-Phe-27-Cys-34	2.4	2.4	2.4	47	27	34

<sup>a</sup> The grafting degree of L-Phe was measured by <sup>1</sup>H NMR.

<sup>b</sup> The grafting degree of L-Cys was determined by elemental analysis.

**Table 3.5. Characterization of  $\gamma$ -PGA-Phe-Cys prepared by the direct dispersion method in PBS**

Sample	Size (nm) <sup>b</sup>	PDI <sup>c</sup>	Zeta potential (mV) <sup>b</sup>	Measured $M_w$ (kDa) <sup>d</sup>	$N_{agg}$ <sup>e</sup>	Domain formation <sup>e</sup>
$\gamma$ -PGA-Phe-27-Cys-27	159±1	0.08±0.01	-29.5±1.3	3390	15	○
$\gamma$ -PGA-Phe-27-Cys-34	449±23	0.39±0.10	-32.8±2.1	3610	17	○

<sup>a</sup> The  $M_w$  of  $\gamma$ -PGA-Phe was calculated from the  $M_w$  of  $\gamma$ -PGA measured by static light scattering (SLS) and the grafting degree of L-Phe (%) and L-Cys determined by <sup>1</sup>H NMR and elemental analysis, respectively. <sup>b</sup> The particle diameter and zeta potential was measured in PBS (1 mg/ml) by DLS and laser doppler velocimetry using a Zetasizer nano ZS. <sup>c</sup> PDI represents polydispersity index.

<sup>d</sup> The  $M_w$  of  $\gamma$ -PGA-Phe-Cys in PBS was measured by SLS. <sup>e</sup> The number of  $\gamma$ -PGA-Phe-Cys aggregates ( $N_{agg}$ ) was calculated by the Measured  $M_w$  / Calculated  $M_w$ . <sup>e</sup> The formation of hydrophobic domains was monitored by UV using CBB as a probe (O = Domain, X = No domain).



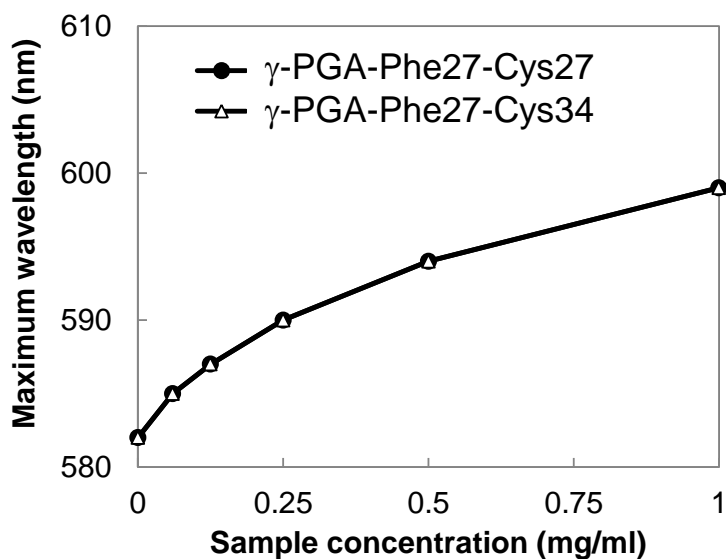


**Figure 3.9.** The plots of maximum wavelength against sample concentration for  $\gamma$ -PGA-Phe27-Cys27 and  $\gamma$ -PGA-Phe27-Cys34.

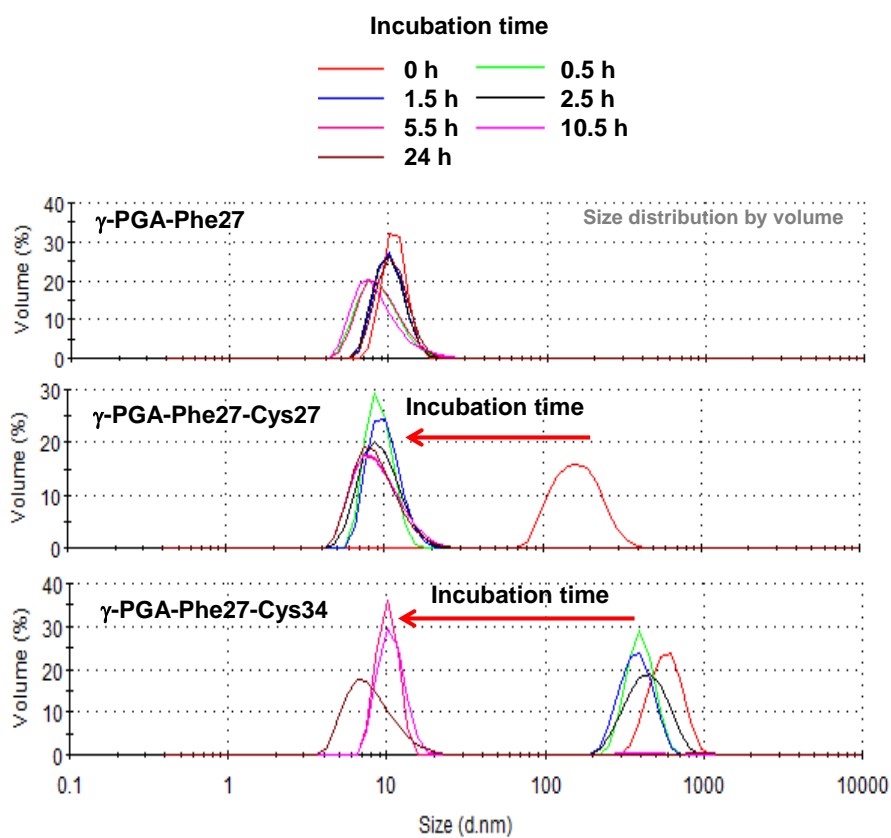


**Figure 3.10.** The change in size distribution by volume upon incubation time of  $\gamma$ -PGA-Phe27-Cys and  $\gamma$ -PGA-Phe27 after treatment with DTT.

Furthermore, the cleavage of disulfide bonds (under reductive condition using DTT) was studied and confirmed by observation of the change of particle size upon the incubation time using DLS. The result is shown in **Figure 3.10**. For  $\gamma$ -PGA-Phe27 unimer nanoparticles, the change of particle size could not be observed in reductive condition due to their original particle sizes were 10 nm. However, by employing DTT as reducing agent for cleavage disulfide linkage of large-size  $\gamma$ -PGA-Phe27-Cys27 and  $\gamma$ -PGA-Phe27-Cys34, the decreases of particle size upon incubation time were observed, implying the cleavage of disulfide bonds. According to the results, it suggested that large-sized nanoparticles composed of  $\gamma$ -PGA-Phe27-Cys show the evidence of stimuli-responsive polymers after treatment with DTT.

*Stimuli-responsive nanoparticles composed of  $\gamma$ -PGA-Cys graft copolymers and their stimuli-responsive properties*

The proposed concept of stimuli-responsive nanoparticles composed of  $\gamma$ -PGA-Cys graft copolymers is shown in **Figure 3.11**.  $\gamma$ -PGA-Cys having different grafting degree of L-Cys was successfully synthesized by introducing only L-Cys onto carboxylic groups of  $\gamma$ -PGA (**Figure 3.12**). The obtained grafting degree of L-Cys was around 10-20 %. Next, nanoparticles were prepared by direct dispersion into PBS method as shown in **Table 3.6**.

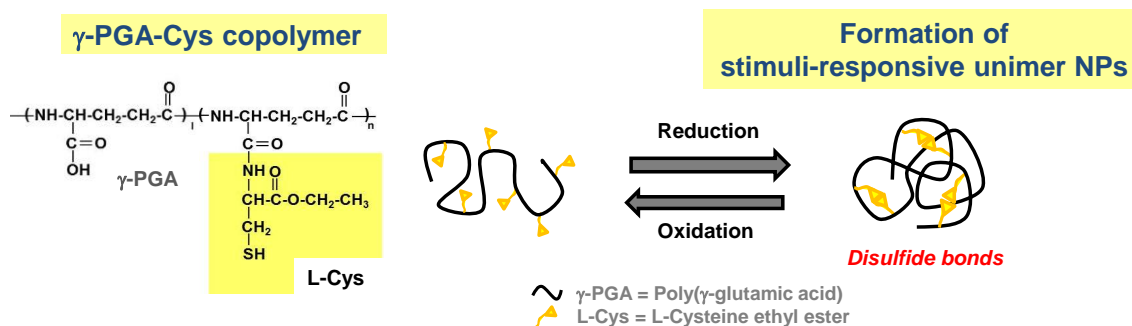


**Figure 3.11.** The concept of stimuli-responsive unimer nanoparticles forming by only disulfide bonds.

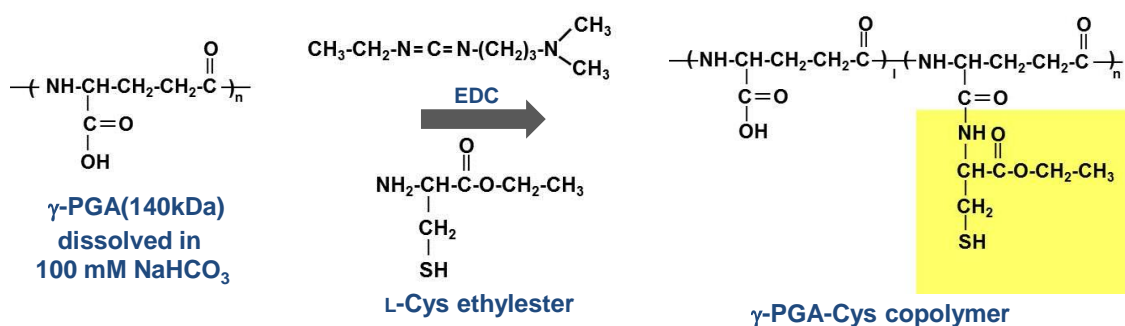


**Figure 3.12.** Synthesis scheme of stimuli-responsive nanoparticles composed of  $\gamma$ -PGA-Cys copolymer.

**Table 3.6. Characterization of  $\gamma$ -PGA-Cys copolymer**

Sample	Calculated $M_w^a$ (kDa)	Particle size <sup>b</sup>		Zeta potential <sup>b</sup> (mV)	Measured $M_w^c$ (kDa)	$N_{agg}^d$
		by vol (nm)	PDI			
$\gamma$ -PGA-Cys13 (Run 1)	161	15.4±2.5	0.36±0.04	-29.3±2.7	271	1.7
$\gamma$ -PGA-Cys18 (Run 2)	170	192.8±6.0	0.08±0.03	-35.2±2.1	3850	23

<sup>a)</sup> Calculated from  $M_w$  of  $\gamma$ -PGA measured by SLS ( $M_w$  of 140 kDa), and grafting degree (%) of L-Cys determined by <sup>1</sup>H NMR. <sup>b)</sup> Particle size diameter and zeta potential were measured in PBS (1 mg/mL) by DLS and Zetasizer nano ZS. <sup>c)</sup>  $M_w$  of  $\gamma$ -PGA-Cys in PBS was measured by SLS. <sup>d)</sup> The aggregation number ( $N_{agg}$ ) was calculated by the measured  $M_w$ /calculated  $M_w$ .

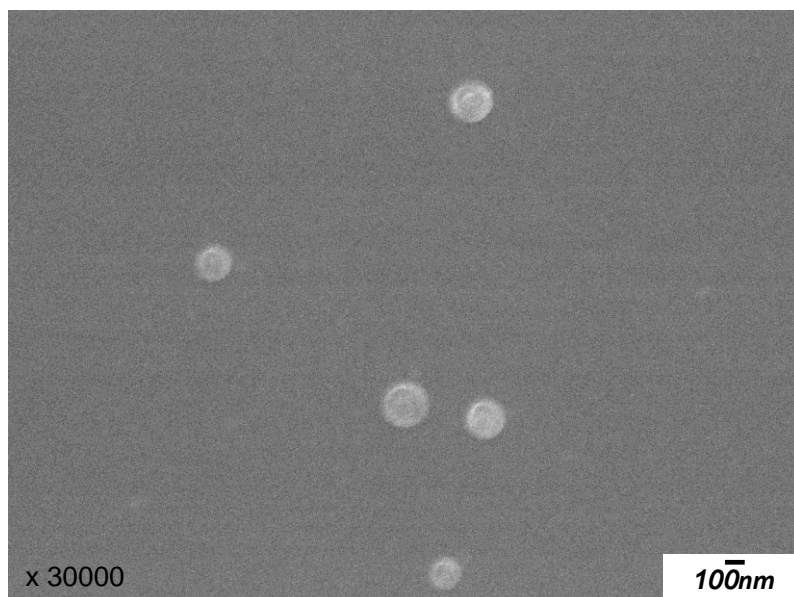


**Figure 3.13.** SEM observation for  $\gamma$ -PGA-Cys18 (Run 2, 200 nm)

The particle size of  $\gamma$ -PGA-Cys13 (**Run 1**) and  $\gamma$ -PGA-Cys18 (**Run 2**) measured by DLS were 15 nm and 200 nm, respectively. The aggregation number around 1 was observed for Run 1 which consists of grafting degree of L-Cys about 13%. Besides, the morphology of  $\gamma$ -PGA-Cys copolymer in pure water was observed by SEM for large-sized nanoparticles (200 nm) as shown in **Figure 3.13**. SEM image shows spherical particles, suggesting that  $\gamma$ -PGA-Cys copolymer (Run 2) could form particles driven by only disulfide bonds. However, Run 1 which is about 15 nm in size was difficult to observe its morphology by SEM.

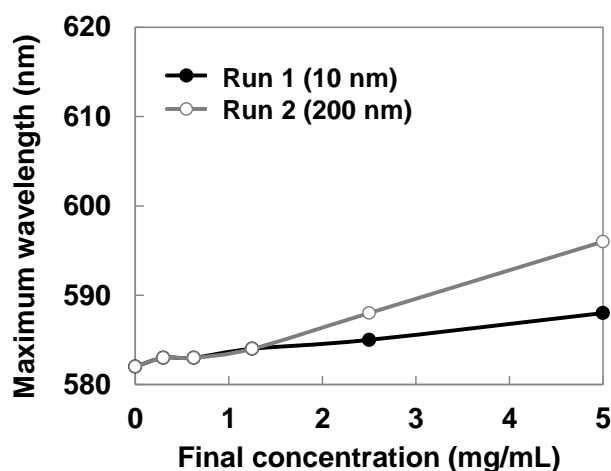


**Figure 3.14.** The change of maximum wavelength (nm) upon increasing concentration detected by UV for observation of hydrophobic associations.

The formation of hydrophobic domain was detected by UV measurement using CBB Dye as probe. As shown in **Figure 3.14**, it was observed that both samples at concentration lower than 1 mg/mL showed no domain formation. The maximum wavelength slightly increased with increasing copolymers concentration, especially in Run 2 which grafting degree of L-Cys is higher. This suggested that concentration and grafting degree affected the formation of hydrophobic domain.

According to Run 2 (particle size around 200 nm) could be detected the formation of hydrophobic domains, thus the cleavage of disulfide bonds under reductive conditions using DTT as reducing agent was studied using Run 2 by monitoring the change of particle size by volume measured by DLS. In the experiment, two concentrations of DTT (40 and 400 mM) were employed for detection of the effect of the cleavage of disulfide bonds. After sample dispersed in PBS was mixed at the same volume with DTT dispersed in PBS (pH 8), the sample was then measured their size on time. Size distributions by volume were shown in **Figure 3.15 and 3.16**. From the results, the

decrease in particle size was detected which indicated that disulfide bonds were reduced with DTT upon incubation time. Besides, the ability for reduction of disulfide bonds depends on the concentration of DTT as observed that after 2 h and after 10 min, the particle size changed from 200 nm to about 15 nm when employing DTT at concentration 40 and 400 mM, respectively.

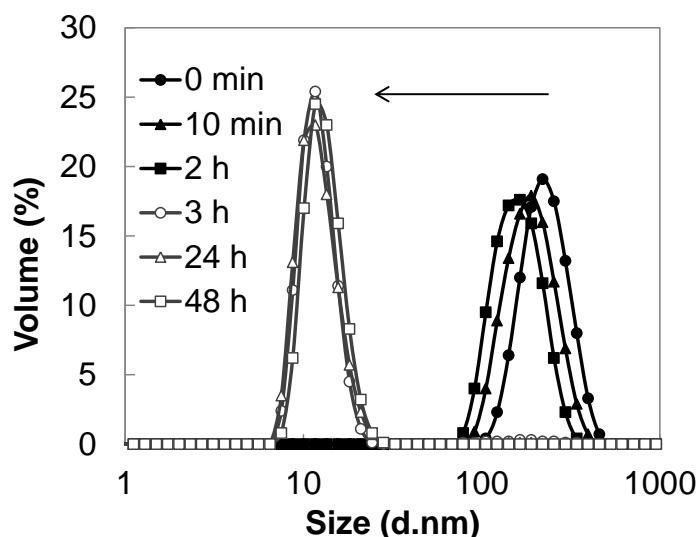


**Figure 3.15.** Size distribution by volume for large-sized nanoparticles composed of  $\gamma$ -PGA-Cys-18 (Run 2) after treatment with DTT 40 mM. After 2 hours the particle size changed to 15 nm.

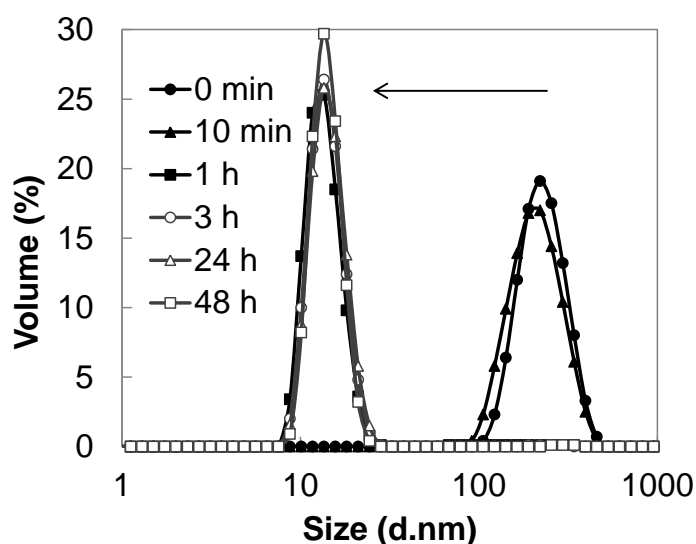


**Figure 3.16.** Size distribution by volume for large-sized nanoparticles composed of  $\gamma$ -PGA-Cys-18 (Run 2) after treatment with DTT 400 mM. After 10 minutes the particle size changed to 15 nm.

### *Potential applications as drug carriers*

#### *Model drug-loaded $\gamma$ -PGA-Phe unimer nanoparticles and their release behavior*

$\gamma$ -PGA140k-Phe samples were mixed with capsaicin solution at various concentrations. The final concentrations of the mixture were 10, 5, 2.5 and 1.25 mg/mL and final concentration of capsaicin was 0.5 mg/mL. The solubility of the resulting mixtures was observed (**Figure 3.17**) and summarized in **Table 3.7**. It found that  $\gamma$ -PGA140k-Phe at high grafting degree with high concentration of polymer showed clear solutions. While, at low grafting degree and polymer concentration, turbid solutions were observed. This observation suggested that the absorption of capsaicin for nanoparticles depends strongly on hydrophobicity of nanoparticles.

**Table 3.7. Solubility of samples after mixing with capsaicin**

Sample	Solubility <sup>b</sup> of samples after mixing with capsaicin at final concentration of nanoparticles (mg/ml)			
	10	5	2.5	1.25
$\gamma$ -PGA	●	●	●	●
$\gamma$ -PGA-Phe-12	●	●	●	●
$\gamma$ -PGA-Phe-27	●	●	●	●
$\gamma$ -PGA-Phe-35	○	●	●	●
$\gamma$ -PGA-Phe-42	○	○	●	●

<sup>a</sup> ○ represented clear solution, ● represented turbid solution

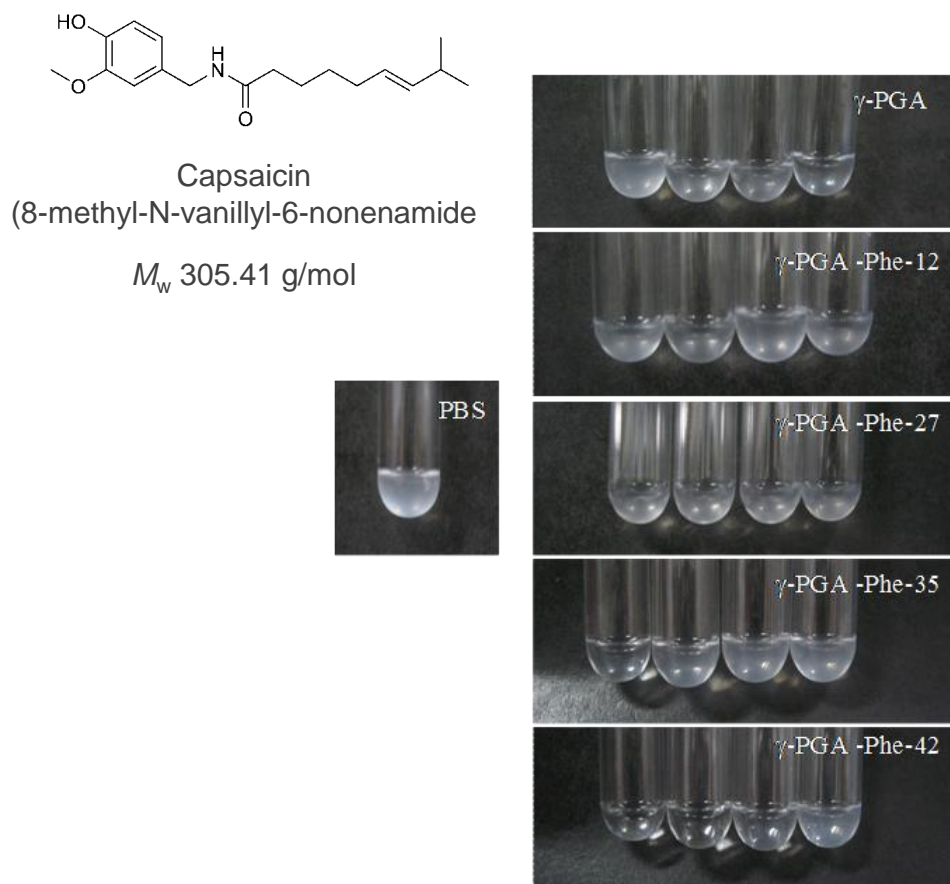


**Figure 3.17.** Photo images of capsaicin encapsulated  $\gamma$ -PGA140k-Phe at various grafting degree. From left final concentration of nanoparticles are 10, 5, 2.5 and 1.25 mg/ml respectively. Final concentration of capsaicin is 0.5 mg/mL.

Further study on the release of capsaicin, the samples were mixed with capsaicin. The final concentrations of capsaicin and nanoparticles in the mixtures were 0.5 and 10 mg/mL respectively. Capsaicin was released into medium. Released capsaicin concentration was obtained from standard curve plotted between capsaicin concentration and fluorescence intensity as shown in **Figure 3.18**.



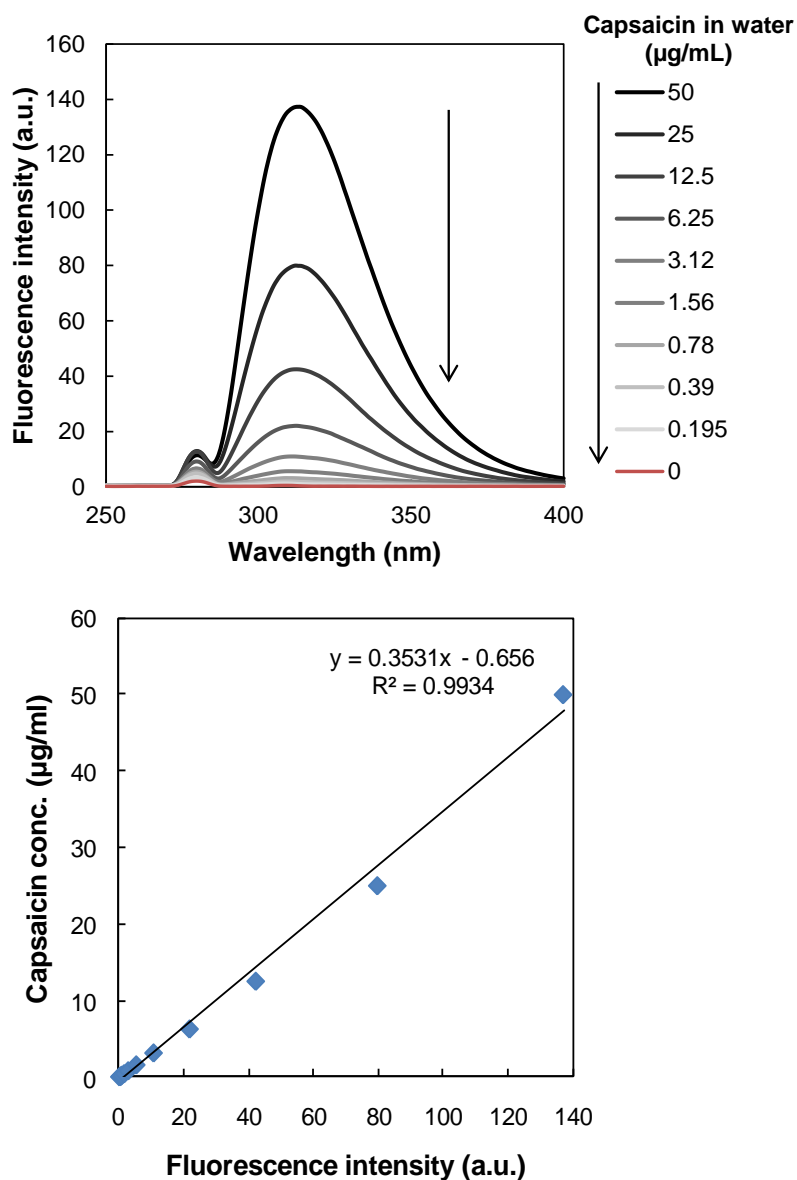


**Figure 3.18.** Standard curve derived from fluorescence intensities of capsaicin at different concentration.

In **Figure 3.18**, the plots of capsaicin concentration against intensity gave a straight line which was then used for calculation of capsaicin concentration of the withdrawn samples via the obtained equation. The calculated release (%) values were then plotted in **Figure 3.19** against time for 24 hours.

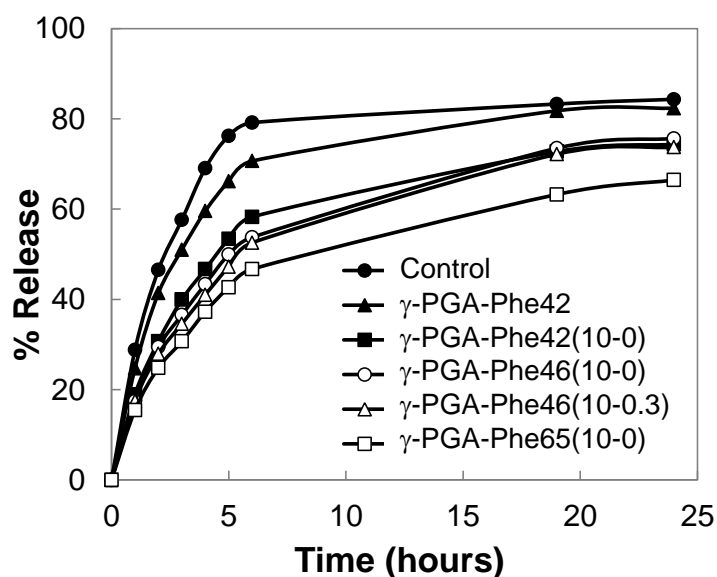


**Figure 3.19.** % Release of capsaicin-conjugated nanoparticles on time. Unimer samples are  $\gamma$ -PGA-Phe-42,  $\gamma$ -PGA-Phe-42(10-0) and  $\gamma$ -PGA-Phe-46(10-0) different in the number of hydrophobic domain ( $N_{\text{domain}}$ ).

As shown in **Figure 3.19**, sustained release was obtained from these nanoparticles. Moreover, it was observed that the release rate and % release depend strongly on grafting degree. Moreover, when compare  $\gamma$ -PGA-Phe-42 prepared by directly dissolved into PBS and  $\gamma$ -PGA-Phe-42 (10-0) prepared by dialysis method, the results showed that unimer nanoparticles prepared by dialysis method could retard the release of hydrophobic drugs more than that of prepared by directly dissolved into PBS. This is probably due to the number of hydrophobic domains ( $N_{\text{domain}}$ ) of  $\gamma$ -PGA-Phe-42 less than  $\gamma$ -PGA-Phe-42 (10-0) as reported in **Table 2.2, Chapter 2**.

In addition, the particle sizes of capsaicin-conjugated nanoparticles before and after conjugation were measured by DLS as shown in **Table 3.8** which showed that particle size of nanoparticles increased after nanoparticles were conjugated with capsaicin. This

suggested that unimer nanoparticles as well as large-sized nanoparticles could conjugate with hydrophobic drugs, capsaicin.

**Table 3.8. Particle size of nanoparticles before and after conjugation with capsaicin**

Sample	Particle size by volume (nm)		PDI	
	before	after	before	after
$\gamma$ -PGA-Phe-42	8.3	15.5	0.393	0.578
$\gamma$ -PGA-Phe-42 (10-0)	9.2	21.5	0.436	0.501
$\gamma$ -PGA-Phe-65 (10-0)	65.6	91.0	0.143	0.175

#### *Anti-cancer drug-loaded $\gamma$ -PGA-Phe unimer nanoparticles*

The potential applications as drug carriers for cancer therapy were studied using irinotecan and cisplatin as model anti-cancer drugs for  $\gamma$ -PGA-Phe unimer nanoparticles. Irinotecan was employed to absorb and penetrate into the hydrophobic domains of the unimer nanoparticles, while, cisplatin can conjugate to carboxylic group of  $\gamma$ -PGA main chain **Figure 3.20**. As shown the results in **Figure 3.21**, 10-nm unimer nanoparticles composed of  $\gamma$ -PGA-Phe showed higher absorption of irinotecan and cisplatin over large-sized  $\gamma$ -PGA-Phe nanoparticles (200 nm), indicating the higher potential applications due to the advantages on their particle size and large surface per volume ratio. This is due to unimer nanoparticles have larger surface per volume, and higher density of  $N_{\text{domain}}$  per volume over than 20- nm nanoparticles.

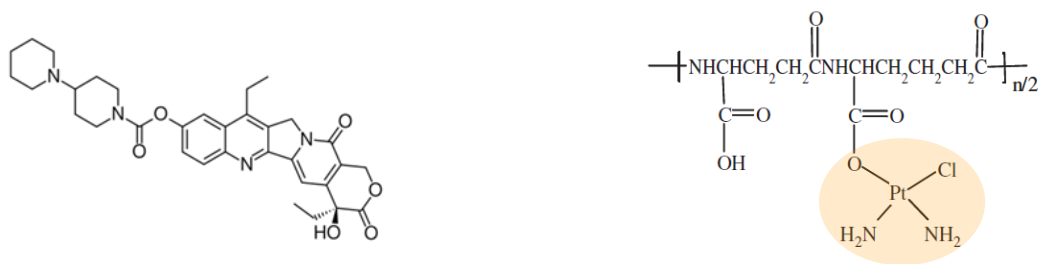


**Figure 3.20.** Chemical structure of irinotecan (left) and cisplatin-conjugated to carboxylic group (right).

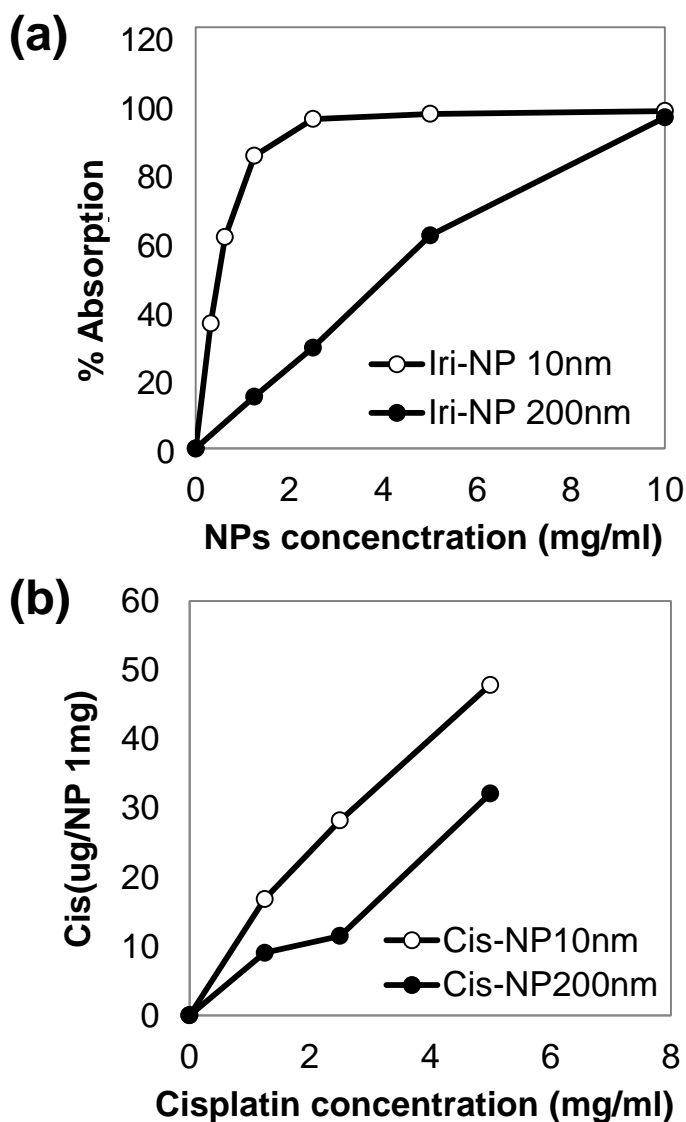


**Figure 3.21.** Absorption of anti-cancer drugs incorporated into  $\gamma$ -PGA-Phe 10-nm unimer nanoparticles compared to 200-nm nanoparticles. Irinotecan incorporation into nanoparticles at various nanoparticles concentration, fixing irinotecan concentration at 2 mg/mL (a), and cisplatin conjugated-nanoparticles at various cisplatin concentration, fixing nanoparticles concentration at 10 mg/mL (b).

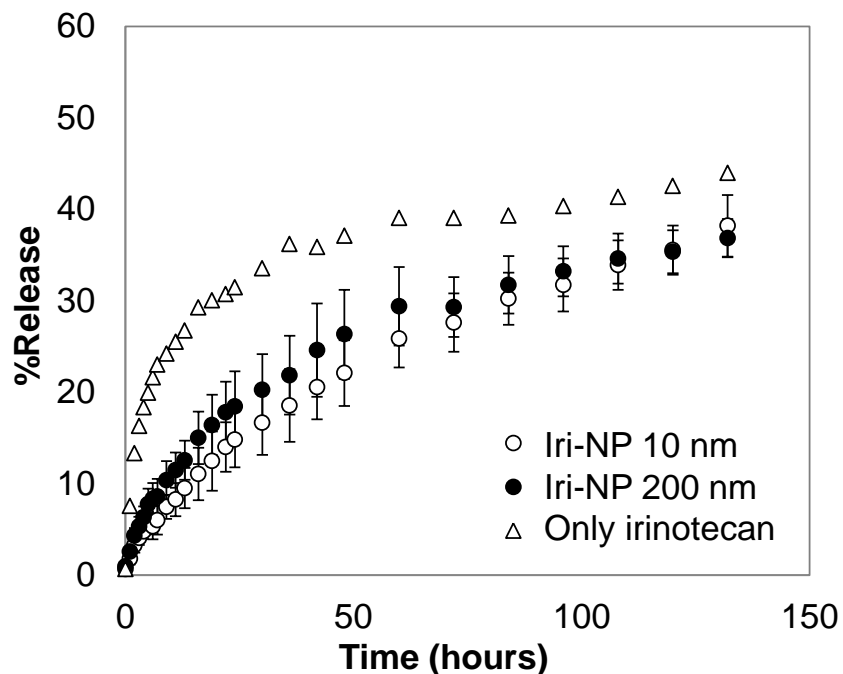


**Figure 3.22.** Release of irinotecan on time of 10 nm unimer nanoparticles compared to 200 nm  $\gamma$ -PGA-Phe nanoparticles.

The release behavior of irinotecan was then studied by comparison 10 nm unimer nanoparticles to 200 nm sized nanoparticles. After drug-loaded nanoparticles were prepared, the amount of irinotecan release into medium was then detected by UV measurement (absorbance at 364 nm). The release of irinotecan on time is shown in **Figure 3.22** which sustained release was observed. However, the release rate of unimer nanoparticles was a bit slower than large-sized nanoparticles at the beginning. This is probably due to the inner core density of 10 nm unimer nanoparticles is higher than 200 nm nanoparticles, resulting in retard release of drugs. Besides, it was observed that the release (%) of irinotecan was low even after 120 hours owing to strong interaction between irinotecan and hydrophobic core of nanoparticles ( $M_w$  of irinotecan is 586.7 g/mol).

### *Drug-loaded $\gamma$ -PGA-Phe-Cys unimer nanoparticles*

The capacity of  $\gamma$ -PGA-Phe-Cys stimulus-responsive unimer nanoparticles to absorb irinotecan as compared to  $\gamma$ -PGA-Phe unimer nanoparticles was studied. It was postulated that the stimulus-responsive unimer nanoparticles would encapsulate the drugs in a manner similar to that of non-stimulus nanoparticles ( $\gamma$ -PGA-Phe). To this end, drug-loaded unimer nanoparticles were prepared by mixing the irinotecan solution (2 mg/mL in ultrapure water) with unimer nanoparticles solutions at the desired concentrations at the same volume. The resultant nanoparticles were incubated 24 hours, and collected by ultrafiltration before measurement by UV. **Figure 3.23** shows the drug-absorbed efficiency of unimer nanoparticles with different substitution degrees of L-Phe and/or L-Cys. It was observed that both types of unimer nanoparticles could efficiently absorb irinotecan. The absorption increased with increasing nanoparticles concentration. Furthermore, the amount of drug loaded into unimer nanoparticles both types were comparable, as expected.

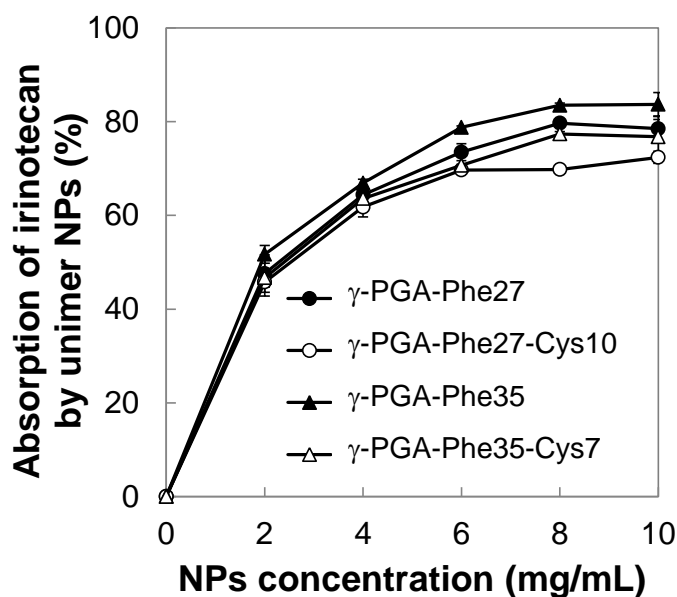


**Figure 3.23.** Absorption of irinotecan at various concentrations of unimer nanoparticles.

### ***The cleavage of disulfide bonds for drug-loaded unimer nanoparticles***

To determine the cleavage of disulfide bonds for 10-nm size unimer nanoparticles, irinotecan was employed to absorb and penetrate into the hydrophobic domains of the unimer nanoparticles. The release of irinotecan was then observed in response to oxidation-reduction conditions. The following experiment was then designed to determine the effect of a reducing agent on the release of irinotecan to further confirm the potential applications of these stimuli-responsive unimer nanoparticles. According to the maximum drug absorptions demonstrated in **Figure 3.23**, the obtained drug-loaded unimer nanoparticles (irinotecan 160  $\mu\text{g}$ /nanoparticles 1 mg) were tested by treatment with DTT in comparison to the control sample. As shown in **Figure 3.24**, the release of drugs in response to a reducing agent could be observed only in unimer nanoparticles composed of  $\gamma$ -PGA-Phe-Cys. This result indicated that the presence of disulfide cross-links at the side chain of the unimer nanoparticles would stabilize the formation of hydrophobic associations between the L-Phe moieties, as well as providing a unique drug release strategy. After treatment with DTT, the release of irinotecan from unimer nanoparticles composed of  $\gamma$ -PGA-Phe<sub>27</sub>-Cys<sub>10</sub> occurred due to the cleavage of the disulfide bonds collapsing the hydrophobic domains. In the case of  $\gamma$ -PGA-Phe<sub>35</sub>-Cys<sub>7</sub>, which showed no evidence of changes in the number of hydrophobic domains after treatment with DTT (**Figure 3.8**), the release of irinotecan was probably due to the cleavage of the disulfide bonds, which affected the packing density of the hydrophobic associations. This in turn might reduce the interactions between the drugs and the hydrophobic domains, resulting in the release of drugs in response to the stimulus as well.

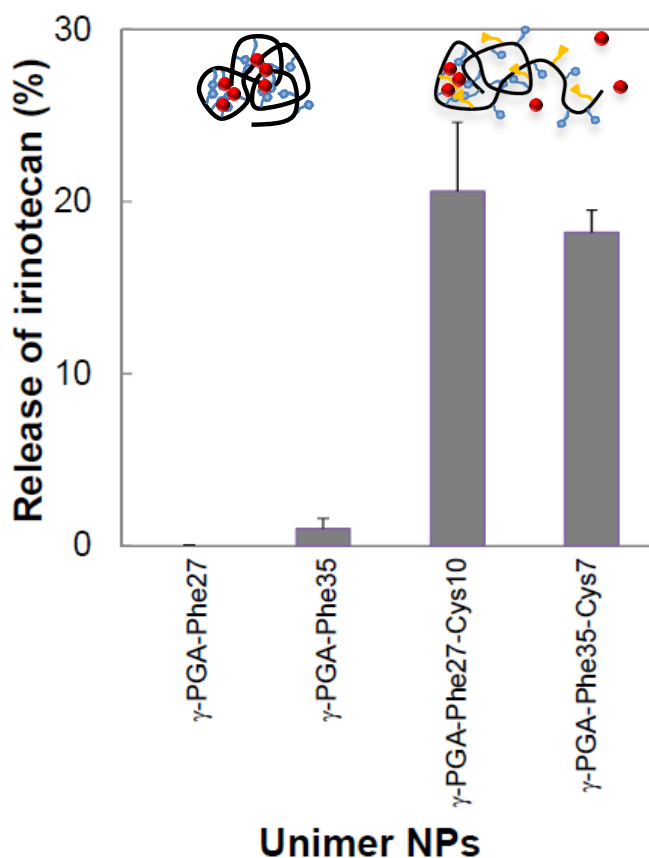


**Figure 3.24.** The release (%) of irinotecan from irinotecan-loaded unimer nanoparticles (irinotecan 160  $\mu\text{g}$ /nanoparticles 1 mg) after treatment with 20 mM dithiothreitol (DTT).

### 3.4. Conclusion

In conclusion, by introducing disulfide bonds into hydrophobized  $\gamma$ -PGA, stimuli-responsive unimer nanoparticles consisting of a single polymer chain could be fabricated. According to the optimal hydrophobicity of these polymers, the unique side chains could provide for the self-assembly of unimer nanoparticles by hydrophobic interactions and disulfide bond interactions in aqueous solution. The resulting unimer nanoparticles could efficiently absorb irinotecan in the same way as non-stimulus unimer nanoparticles. However, the release of this drug was demonstrated in response to a reducing agent in



the former nanoparticles. Besides, the stimuli-responsive properties were clearly observed from large-sized  $\gamma$ -PGA-Phe-Cys nanoparticles as well as  $\gamma$ -PGA-Cys nanoparticles. Depending on the desired applications, it is expected that this new type of unimer nanoparticles with stimuli-responsive properties, which allows the drug carrier to liberate a therapeutic drug when it is required in response to a specific stimulus, can be an interesting candidate as a solubilizer and carrier for hydrophobic drugs, especially targeted cancer therapies. Further studies, including intracellular drug release, cytotoxicity and in vivo study with drug-loaded unimer nanoparticles, are in progress for the development of unimer NP-based drug delivery systems.

## References

1. H. Maeda, J. Wu, T. Sawa, Y. Matsumura and K. Hori, *J. Control. Release* **65**, 271 (2000).
2. S. Acharya and S. K. Sahoo, *Adv. Drug Deliver. Rev.* **63**, 170 (2011).
3. N. Patankar and D. Waterhouse, *Cancer Therapy* **8**, 90 (2012).
4. H. Cabral, Y. Matsumoto, K. Mizuno, Q. Chen, M. Murakami, M. Kimura, Y. Terada, M. R. Kano, K. Miyazono, M. Uesaka, N. Nishiyama and K. Kataoka, *Nat. Nanotechnol.* **23**, 815 (2011).
5. M. C. Jones, M. Ranger and J. C. Leroux, *Bioconjugate Chem.* **14**, 774 (2003).
6. K. Knop, G. M. Pavlov, T. Rudolph, K. Martin, D. Pretzel, B. O. Jahn, D. H. Scharf, A. A. Brakhage, V. Makarov, U. Möllmann, F. H. Schacher and U. S. Schubert, *Soft Matter* **9**, 715 (2013).

7. S. Gupta, R. Tyagi, V. S. Parmar, S. K. Sharma and R. Haag, *Polymer* **53**, 3053 (2012).
8. Karak, Niranjana. *Fundamentals of Polymers: Raw Materials to. Finish Products*, PHI Learning Pvt. Ltd., 2009.
9. H. Kim, T. Uto, T. Akagi, M. Baba and M. Akashi, *Adv. Funct. Mater.* **20**, 3925 (2010).
10. T. Akagi, P. Piyapakorn and M. Akashi, *Langmuir* **28**, 5249 (2012).
11. P. Piyapakorn, T. Akagi and M. Akashi, *Macromolecules* **46**, 6187 (2013).
12. F. Dosio, S. Arpicco, P. Brusa, B. Stella and L. Cattel, *J. Control. Release* **76**, 107 (2001).
13. M. Skwarczynski, Y. Hayashi, Y. Kiso, *J. Med. Chem.* **49**, 7253 (2006).
14. S. Matsumoto, R. J. Christie, N. Nishiyama, K. Miyata, A. Ishii, M. Oba, H. Koyama, Y. Yamasaki and K. Kataoka, *Biomacromolecules* **10**, 119 (2009).
15. Y. C. Wang, F. Wang, T. M. Sun and J. Wang, *Bioconjugate Chem.* **22**, 1939 (2011).
16. Y. Bae and K. Kataoka, *Adv. Drug Deliver. Rev.* **61**, 768 (2009).
17. O. Hayashida and K. Ichimura, *Chem. Lett.* **41**, 1650 (2012).
18. C. Duval-Terrie, J. Huguet and G. Muller, *Colloids Surf. A* **220**, 105 (2003).
19. T. Akagi, M. Baba and M. Akashi, *Polymer* **48**, 6729 (2007).

## Concluding Remarks

The objective of the present studies was to fabricate unimer nanoparticles of amphiphilic copolymers by controlling the association number of polymer chain.

In **Chapter 1**, amphiphilic  $\gamma$ -PGA-Phe copolymers with various lengths of  $\gamma$ -PGA main chains ( $M_w$  of 70, 140 and 220 kDa) and various grafting degree of L-Phe (12-60%) self-assembled in aqueous media to form nanoparticles. The aggregation number of polymer chain in one nanoparticle ( $N_{agg}$ ) could be adjusted according to their molecular structures as well as the preparative methods/conditions. The obtained  $\gamma$ -PGA-Phe nanoparticles were further characterized by means of dynamic and static light scattering, small-angle neutron scattering, as well as steady-state fluorescence measurements/quenching techniques. Unimer nanoparticles (single chain state forming hydrophobic domains of L-Phe) were obtained by using  $M_w$  of  $\gamma$ -PGA higher than 140kDa conjugated with L-Phe at 27-42% due to the balance of hydrophobicity/hydrophilicity along the polymer chain.

In **Chapter 2**, the morphologies of unimer nanoparticles were observed by TEM, SANS. The number of hydrophobic domains in one NP ( $N_{domain}$ ), estimated by means of fluorescence quenching techniques, and the flexibility/rigidity of the inner particles detected by dipyranyl fluorescence demonstrated that the  $N_{domain}$  and the flexibility/rigidity were affected by the particle size and the method of preparation. In addition, the effect of pH on the stability of the unimer nanoparticles indicated a reduction of  $N_{domain}$  with increasing pH, supporting loose packing due to hydrophobic

association under alkaline conditions. Interestingly, the inner core of 10 nm unimer nanoparticles is more flexible and shows their density ( $N_{\text{Domain}}$  per volume) higher than large-sized nanoparticles. These differences in the inner structure of  $\gamma$ -PGA-Phe unimer nanoparticles are expected to provide the great opportunity for hydrophobic drugs to easily penetrate and absorb into the inner core of the unimer nanoparticles.

In **Chapter 3**, by introducing L-Cys onto hydrophobized  $\gamma$ -PGA copolymers ( $\gamma$ -PGA-Phe) having different grafting degree of L-Phe (12-42%),  $\gamma$ -PGA-Phe-Cys copolymers could be successfully synthesized. The unique side chains provide self-assembly of unimer nanoparticles by hydrophobic interactions and disulfide bonds in aqueous solution. The formation of hydrophobic domains was observed when employing copolymers having grafting degrees of L-Phe higher than 27%. The stimuli-responsive properties were clearly observed from large-sized  $\gamma$ -PGA-Phe-Cys nanoparticles and  $\gamma$ -PGA-Cys nanoparticles. Therefore, the presence of disulfide bonds at the side chain of unimer nanoparticles would stabilize the formation of hydrophobic domains, providing a new release strategy.

For the potential application as drug carriers for cancer treatment using anti-cancer drug, two types of anti-cancer drugs; cisplatin and irinotecan were employed as model drugs. It was observed that 10-nm  $\gamma$ -PGA-Phe unimer nanoparticles show higher drug absorption than large-sized  $\gamma$ -PGA-Phe nanoparticles due to the higher surface per volume ratio and the optimized range of hydrophobicity and flexibility/rigidity of inner particles. Moreover, the amount of drug (irinotecan)-loading for stimuli-responsive unimer nanoparticles composed of  $\gamma$ -PGA-Phe-Cys was comparable to non-stimuli-responsive  $\gamma$ -PGA-Phe unimer nanoparticles. However, after treatment with reducing

agent, the release of irinotecan was observed only from stimuli-responsive  $\gamma$ -PGA-Phe-Cys unimer nanoparticles due to the reduction of disulfide bonds affected the formation of hydrophobic domains formed by low grafting degree of L-Phe.

It is expected that  $\gamma$ -PGA-Phe unimer nanoparticles and the one incorporated with stimuli-responsive property can be one of interesting candidates as small-sized drug carriers which would be amenable to address some of the systemic and intracellular delivery barriers, especially for cancer therapeutics.

## List of Publications

### Chapter 1:

T. Akagi, **P. Piyapakorn**, M. Akashi, “Formation of unimer nanoparticles by controlling the self-association of hydrophobically modified poly(amino acid)s “, *Langmuir* **28**, 5249 (2012).

### Chapter 2:

**P. Piyapakorn**, T. Akagi, M. Hachisuka, T. Onishi, H. Matsuoka, M. Akashi, “Structural analysis of unimer nanoparticles composed of hydrophobized poly(amino acid)s”, *Macromolecules* **46**, 6187 (2013).

### Chapter 3:

**P. Piyapakorn**, T. Akagi, M. Akashi, “Stimuli-responsiveness unimer nanoparticles composed of poly(amino acid) derivatives as promising protein-mimetic drug carriers” *Chem. Lett.* **42**, 1534 (2013).

**P. Piyapakorn**, T. Akagi, M. Akashi, “Application of Redox-responsive nanoparticles composed of poly(amino acid) derivatives as anti-cancer drug carriers, *in preparation*.”

## International Conferences

1. Phassamon Piyapakorn, Takami Akagi, Mitsuru Akashi, “Preparation and characterization of unimer nanoparticles composed of hydrophobized poly(amino acid)”, 9<sup>th</sup> World Biomaterial Congress (WBC), Chengdu, China, June 1-6, 2012.
2. Phassamon Piyapakorn, Takami Akagi, Mitsuru Akashi, “Structural analysis of unimer nanoparticles composed of hydrophobized poly(amino acid)s and their potential application as drug carriers”, Society For Biomaterials 2013 Annual Meeting and Exposition, Boston, Massachusetts, USA, April 10-13, 2013.
3. Phassamon Piyapakorn, Takami Akagi, Mitsuru Akashi, “Stimuli-responsive unimer nanoparticles composed of poly(amino acid)s as drug carriers”, The 12<sup>th</sup> US-Japan symposium on drug delivery systems, Lahaina, Maui, Hawaii, December 16-20, 2013.

## Acknowledgement

This study was performed at Akashi Laboratory, Department of Applied Chemistry, Graduate School of Engineering, Osaka University, from 2009 to 2014. This work was supported by CREST from the Japan Science and Technology Agency (JST).

First of all, I would like to express my deepest gratitude to my supervisor, Professor Mitsuru Akashi, who gave me a valuable opportunity to study Master degree and Doctoral degree in his laboratory, continue giving generous guidance, great kindness, support and invaluable encouragement.

I would like to express his sincere gratitude to my advisor, Associate Professor Takami Akagi, for his support and generous guidance throughout the research.

I would like to express his guidance to Associate Professor Toshiyuki Kida, Assistant Professor Michiya Matsusaki, Associate Professor Hiroharu Ajiro of Osaka University for their kind help and valuable discussions.

I am greatly indebted to Professor Yoshihisa Inoue, Professor Yoshio Aso, Professor Shu Seki, Professor Masahiro Miura, Professor Naoto Chatani, Professor Sensuke Ogoshi, Professor Nobuaki Kambe, and all Professor as well as Associate/Assistant Professor of Department of Applied Chemistry, Osaka University for their helpful comments and suggestions.

I would like to gratefully acknowledgments to Associate Professor Hideki Matsuoka, Mr. Masahiro Hachisuka and Mr. Tomoyuki Onishi, Graduate School of Engineering,



Kyoto University, and Tomofumi uto, University of Miyazaki, for his helpful advices and assistances.

I would like express appreciate and thank to Dr. Wanpen Techaboonyakiat, Senior project advisor of Department of Materials Science, Faculty of Science, Chulalongkorn University, for her continuous support and encouragement.

I also express appreciate to Associate Professor Junji Watanabe of Konan University, Dr. Mitsuhiro Ebara, Assistant Professor Taka-aki Asoh of Tokyo University of Science, Dr. Chizuru Hongo, Dr. Dongjian Shi, Dr. Tomonori Waku, Dr. Hyuang Jin Kim, Dr. Tran Hang Thi, Dr. Masaaki Omichi, Dr. He-Yun Shen, Dr. Hiroaki Yoshida, Dr. Koji Kadowaki, Dr. Daisuke Kamei, Mr. Takayuki Imoto, Mr. Yoshinori Fujino, Mr. Nakano Sugura, Mr. Ryotaro Amekawa, Ms. Suzuka Amemori, Mr. Yasuhiro Marui, Ms. Yukie Takemoto, Mr. Kenta Kondo, Ms. Kayo Sakaue, Mr. Takashi Miura, Mr. Kazuki Watanabe, Ms. Tomoko Sato(Tsukuda) for their kind advices and assistances during my master degree.

I also thanks to Research Professor Takeshi Nakano, Ms. Natsuko Hashimoto, Dr. Haruyasu Asahara, Dr. Shintaro Kawano, Dr. Tomoaki Hinoue, Mr. Masahiro Matsumoto, Ms. Ye Zhu, Mr. Fumiaki Shima, Mr. Akihiro Nishiguchi, Ms. Paninee Chetprayoon, Mr. Chunyen Liu, Mr. Takuya Iwamoto, Mr. Masumi Maegawa, Mr. Shinichiro Sato, Mr. Yoshikazu Takahashi, Mr. Ryota Fukumoto, Ms. Kumiko Fujimoto, Ms. Manami Shudo, Mr. Kazuya Takemura, Ms. Mitsuyo Hamada, Mr. Takashi Yoshikai, Mr. Koki Azuma, Mr. Tatsuaki Ueyama, Mr. Shun Takahama, Mr. Daichi Hikimoto and Ms. Chizuru Kogame and all members of the Akashi laboratory for their kind help, encouragement and useful advices.

Finally, I would like to express appreciation and big thank to my parents Mr. Paitoon Piyapakorn and Ms. Vilaiwan Piyapakorn, and my relatives in Thailand, for their continuous support and invaluable encouragement.

January 2014

PHASSAMON PIYAPAKORN (OB)